# “STRESS DISTRIBUTION IN THE MAXILLOFACIAL SKELETON AND THE TEMPOROMANDIBULAR JOINT FOLLOWING BONE ANCHORED MAXILLARY PROTRACTION: A THREE-DIMENSIONAL FINITE ELEMENT METHOD STUDY”

## THESIS

**Submitted to**

**All India Institute of Medical Sciences, Jodhpur**

**In partial fulfilment of the requirement for the degree of**

**MASTER OF DENTAL SURGERY (MDS)**

**ORTHODONTICS & DENTOFACIAL ORTHOPAEDICS**

**JULY 2020**

**AIIMS, JODHPUR** **DR. SUPRATIM KUNDU**

# ALL INDIA INSTITUTE OF MEDICAL SCIENCES
# JODHPUR

## CERTIFICATE

This is to certify that thesis entitled **"STRESS DISTRIBUTION IN THE MAXILLOFACIAL SKELETON AND THE TEMPOROMANDIBULAR JOINT FOLLOWING BONE ANCHORED MAXILLARY PROTRACTION: A THREE-DIMENSIONAL FINITE ELEMENT METHOD STUDY"** is an original work of **DR. SUPRATIM KUNDU** and has been carried out under our direct supervision and guidance, at All India Institute of Medical Sciences, Jodhpur.

**GUIDE**


**Dr. Vinay Kumar Chugh**
Additional Professor
Orthodontics and Dentofacial Orthopaedics
Department of Dentistry
AIIMS Jodhpur


**CO-GUIDE**


**Dr. Ankur Gupta**
Assistant Professor
Department of Mechanical Engineering
IIT Jodhpur


**CO-GUIDE**


**Dr. Pravin Kumar**
Professor & Head
Department of Dentistry
AIIMS Jodhpur

## ALL INDIA INSTITUTE OF MEDICAL SCIENCES, JODHPUR

## DECLARATION

I, hereby declare that the work reported in the thesis entitled **"Stress distribution in the maxillofacial skeleton and the temporomandibular joint following bone anchored maxillary protraction: A three-dimensional finite element method study"** embodies the result of original research work carried out by me in the Department of Dentistry – Orthodontics and Dentofacial Orthopaedics, All India Institute of Medical Sciences, Jodhpur.

I further state that no part of the thesis has been submitted either in part or in full for any other degree of All India Institute of Medical Sciences or any other Institution/ University.

Supratim Kundu

**Dr. Supratim Kundu**
Junior Resident,
Orthodontics and Dentofacial Orthopaedics,
Department of Dentistry,
All India Institute of Medical Sciences, Jodhpur.

## *ACKNOWLEDGEMENT*

*I would like to express my heartfelt gratitude to the Almighty God who has given me a life full of opportunities to learn and to upgrade myself to a better person. This research study is one of those opportunities which might not be possible without the proficient guidance of my mentor and guide* ***Dr. Vinay Kumar Chugh,*** *M.D.S, MOrth RCS (Edin), Additional Professor, Orthodontics and Dentofacial Orthopaedics, AIIMS Jodhpur. I am greatly thankful to his invaluable teachings and blessings. He has always been a source of inspiration and motivation for me. I consider myself extremely fortunate to have had the opportunity to get trained under his knowledgeable guidance. I thank him for continuously encouraging me to finish this thesis work successfully.*

*With sincere regards, I express thanks to my esteemed teacher and co-guide,* ***Dr. Ankur Gupta****, PhD, Assistant Professor, Department of Mechanical Engineering, Indian Institute of Technology (IIT) Jodhpur, for providing me the necessary guidance, infrastructure, resources and invaluable suggestions throughout my research period. His enthusiasm, positive and challenging attitude inspires me each day. I thank him for his selfless guidance throughout my study.*

*My sincere regards to Head of Department and Professor* ***Dr. Pravin Kumar****, M.D.S, Conservative Dentistry and Endodontics, AIIMS Jodhpur, for his encouragement and support throughout my post-graduation period.*

*I find myself lucky to have a colleague like* ***Dr. Himani*** *in whom I find my friend, and a well-wisher at the same time. I cannot thank her enough for her suggestions, constant support and inspiration not just during the study but also in my Jodhpur life, where I've learnt a lot from her. She has always inspired me with the way she caring her surrounding people.*

*My heartfelt gratitude to* ***Dr. Priyawati****, M.D.S, Senior Resident,* ***Dr. Navleen****, M.D.S, Senior Resident,* ***Dr. Rinkle****, M.D.S, Senior Resident,* ***Dr. Baskar****, M.D.S Senior Resident,* ***Dr. Niraj****, M.D.S, Senior Resident, Orthodontics and Dentofacial Orthopedics, for their immense support and guidance for this study.*

*I would like to extend my gratitude to my dear juniors* ***Dr. Akanksha****,* ***Dr. Ayush****,* ***Dr. Pooja****, and* ***Dr. Nikita*** *for motivating me and keeping my spirits high throughout.*

*Specially I want to thank to **Er. Prince**, PhD scholar, **Er. Gulshan**, PhD scholar, **Er. Vinay**, PhD scholar, for their constant help and support during my IIT days.*

*I would like to thank **Mr. Dinesh Vishal**, **Mr. Mukesh**, **Mr. Hanuman, Miss. Kavita** for all the assistance, co-operation and help they offer in smooth functioning of the department.*

*The study would never have been possible without the co-operation of **MY PATIENTS**, who form the backbone of this study. I pay my sincere tribute to them and always pray for their well-being.*

*My deepest gratitude goes to my family for their love and support throughout my life; this dissertation is simply impossible without them. No words of gratitude can ever repay the great debt that I owe to my **PARENTS, SISTER & FRIENDS** for their love, support and inspiration.*

**DR. SUPRATIM KUNDU**

***Dedicated***

***to***

***My Guide***

***and***

***Mentor***

***Dr. Vinay Kumar Chugh***

# TABLE OF CONTENTS

# LIST OF ABBREVIATIONS

| ABBREVIATIONS | FULL FORM |
|---|---|
| TAD | Temporary anchorage devices |
| ZAS | Zygoma anchorage system |
| BAMP | Bone anchored maxillary protraction |
| FEA | Finite element analysis |
| TMJ | Temporomandibular joint |
| CT | Computed tomography |
| MRI | Magnetic resonance imaging |
| ANS | Anterior nasal spine |
| PNS | Posterior nasal spine |
| FEM | Finite element model |
| RME/FM | Rapid maxillary expander with facemask |
| CBCT | Cone beam computed tomography |
| GF | Glenoid fossa |
| UCLP | Unilateral complete cleft lip and palate |
| CG | Cleft group |
| NCG | Non-cleft group |
| ACF | Anterior cranial fossa |
| RME | Rapid maxillary expansion |
| FM | Facemask |
| 3D | Three dimensional |
| I-SAMP | Intra-oral mechanics for skeletally anchored maxillary protraction |
| IEC | Institutional ethics committee |
| DICOM | Digital Imaging and Communications in Medicine |
| MIMICS | Materialise interactive medical image control system |
| HU | Hounsfield unit |
| STL | Stereolithography |
| CAD | Computer aided design |
| MPa | Megapascals |

# LIST OF TABLES

# LIST OF FIGURES

# INTRODUCTION

Class III skeletal malocclusion, also known as "underbite" can be due to maxillary deficiency or mandibular excess or combination of both. Prevalence rate of Class III malocclusion ranges from 0-26.7% depending upon the racial group. It affects nearly 4.8% in Europeans and 15.80% in Southeast Asians (1). It is one of the most common facial deformities seen in Asian population (2). Indian population shows relatively low prevalence rate compared to other populations- 2.5% in North Indian population (3), 2.1%- 4.1% in South Indian population (4,5). Maxillary hypoplasia is the primary etiological factor in most of the Class III skeletal malocclusion cases (6, 7, 8).

Conventional treatment options in growing patients with skeletal Class III malocclusion involves extraoral devices like facemask to protract maxilla, chin cup to restrain mandibular growth, Frankel functional regulator III, reverse twin block depending on the skeletal deformity present. Maxillary protraction facemask has shown 4 mm of advancement of maxilla within 8-12 months (9). However, such appliances often have unwanted dento-alveolar changes which includes proclination of the maxillary incisors, lingual tipping of the mandibular incisors, extrusion and mesial tipping of the maxillary molars and clockwise rotation of mandible (10,11). Moreover, successful facemask therapy has been shown to be limited to the primary or early mixed dentition stage (12). Success through conventional orthopedic treatment approach is more dependent on patient compliance. Long term follow-up has shown evidence of 25%-33% relapse of negative overjet after growth completion when patients were treated by conventional facemask therapy (13, 14, 15).

With the introduction of temporary anchorage devices (TAD) in orthodontics, different approaches have been developed to treat Class III skeletal malocclusion such as placement of miniplates on the lateral nasal wall followed by maxillary protraction through modified facemask; hybrid hyrax approach and intraoral traction through zygomatic miniplates.

De Clerck et al. (16) proposed innovative treatment option for growing Class III patients with maxillary deficiency using miniplates, together with intermaxillary Class III elastics for promoting more orthopaedic effects. This technique is referred to as ZAS (Zygoma anchorage system) or BAMP (bone anchored maxillary protraction). It involves placement of four orthodontic miniplates (two on each side): Upper plates are inserted at first and second molar level (infra-zygomatic crest), while the lower plates are inserted between the lateral incisor and canine.150gm, 250gm and 400gm of Class III force is applied sequentially.

Heymann et al. (17) observed significant forward displacement of orbitale, upper lip, nasal region and posterior repositioning of mandible after the BAMP procedure. The reason for forward displacement is thought to be significant opening of the craniomaxillary sutures. Hino et al. (18) found one sixth of BAMP patients shows a predominantly vertical maxillary displacement. Clerck et al. (19) found remodelling of the glenoid fossa at the anterior eminence and bone resorption at the posterior wall during bone anchored maxillary protraction.

Yan et al. (20) reported significant amount of stress generation around circum-maxillary sutures during bone anchored maxillary protraction as compared to dental anchorage. Lee et al. (21) found that stress distribution pattern depends on the site of placement of miniplates. Stress values in frontonasal, fronto-maxillary, zygomaticomaxillary and pterygomaxillary sutures are greater when implants are placed in the infrazygomatic crest than on the lateral nasal wall in a finite element model. But stress pattern generated during this procedure in the mandible and temporomandibular joint components was not reported in these studies. (20,21)

Bhad et al. (22) found more restraining effect of the mandible contributing in the skeletal changes rather than forward displacement of maxilla from a finite element analysis (FEA). However, biomechanical reaction of soft tissue of temporomandibular joint (TMJ) was not studied and anchor plates were not assembled in the computed tomography (CT) scan mesh model. Tanaka et al. (23) studied the stress distribution pattern in the temporomandibular joint of a normal subject on a finite element model constructed from magnetic resonance imaging (MRI) slices and indicated that during jaw opening relatively high stresses are produced in the anterior and posterior regions of articular disc. However, there is no study evaluating the effects of BAMP protocol on soft tissue and hard tissue structures of TMJ. Therefore, the aim of the present study was to evaluate stress distribution among various circum-maxillary sutures, condyle and articular disc during bone anchored maxillary protraction.

# AIMS AND OBJECTIVES

**Aims:**

To analyze stress distribution pattern in the circum-maxillary sutures, mandibular condyle and articular disc and displacement of various surface landmarks during bone anchored maxillary protraction procedure.

**Objectives:**

1. To measure maximum Von Mises stress values at circum-maxillary sutures, condylar head and articular disc during application of intermaxillary Class III protraction force of 150, 250, and 400 gm force at an angle of 10°,20°, and 30° to the occlusal plane.
2. To measure the displacement of anterior nasal spine (ANS), posterior nasal spine (PNS), pogonion and condylion in anteroposterior and vertical dimension during application of intermaxillary Class III protraction force of 150, 250, and 400 gm at an angle of 10°,20° and 30° to the occlusal plane.

**Research Question:**

1. How are the stresses distributed in the circummaxillary sutures, mandibular condyle and articular disc of the temporomandibular joint during application of Class III protraction force of 150, 250, and 400 gm force at an angle of 10°, 20°, and 30° to the occlusal plane?
2. How does anterior nasal spine (ANS), posterior nasal spine (PNS), pogonion and condylion displace in anteroposterior and vertical dimension during application of Class III protraction force of 150, 250, and 400 gm at an angle of 10°,20°, and 30° to the occlusal plane?

# REVIEW OF LITERATURE

- ***Tanne et al.*** (24) in 1989, investigated the biomechanical effect of protractive maxillary orthopedic forces on the craniofacial complex using three-dimensional finite element method (FEM). The three-dimensional FEM model of dry skull was developed on the of a young human being. Eighteen cranial and facial sutural systems were integrated in the model. An anteriorly directed 1-kg force was applied on the buccal surfaces of the maxillary first molars in both a horizontal direction and a 30° downward direction to the functional occlusal plane.

  The nasomaxillary complex showed a forward displacement with upward and forward rotation in a horizontal protraction case, whereas a downward force produced almost translatory repositioning of the complex in an anterior direction. High stress levels were observed in the nasomaxillary complex and its surrounding structures. However, the pattern of stress distributions within the complex was different in two force systems. A downward protraction force produced relatively uniform stress distributions, indicating the importance of the force direction in determining the stress distributions from various orthopedic forces.

- ***Gautam et al.*** (25) in 2009, evaluated biomechanical effect of two treatment modalities: maxillary protraction alone and in combination with maxillary expansion, by comparing the displacement of various craniofacial structures using finite element method. Two three-dimensional analytical models were developed from sequential computed tomography scan images taken at 2.5-mm intervals of a dry young skull. AutoCAD and ANSYS software were used to generate the mesh model and solution of problem. In the first model, maxillary protraction forces were simulated by applying one kg of anterior force 30° downward to the palatal plane. In the second model, a 4-mm midpalatal suture opening and maxillary protraction were simulated.

  Forward displacement of the nasomaxillary complex with upward and forward rotation was observed with maxillary protraction alone. No rotational tendency was noted when protraction was carried out with 4 mm of transverse expansion. The amounts of displacement in the frontal, vertical, and lateral directions with midpalatal suture opening were greater compared with no opening of the midpalatal suture. The forward and downward displacements of the nasomaxillary complex with maxillary protraction and maxillary expansion more closely approximated the natural growth direction of the maxilla. Displacements of craniofacial structures were more favourable for the treatment of skeletal Class III maxillary retrognathia when maxillary protraction was used with maxillary expansion.

- ***De Clerck et al.*** (16) in 2009, treated three girls of 10-11 years age having skeletal Class III malocclusion with retrognathic maxilla, by placing four bollard type titanium miniplates at the infrazygomatic region of the upper jaw and between lower lateral incisor and canine bilaterally. 100 gm of Class III intermaxillary force was applied twenty hours a day for one year. lateral cephalograms were taken at the pre-treatment stage, end of orthopaedic correction and at follow up period. Cephalometric evaluation showed a marked increase of ANB angle, Wits, and facial convexity values in all three cases. No rotation of the mandible was observed in two cases, whereas a slight clockwise rotation was seen in one case; there was a slight counter-clockwise rotation of the maxilla in all patients. No major changes were found in the upper incisor inclination, whereas the lower incisors were proclined. During the follow-up period (from end of treatment to 11 to 38 months later), the Class III correction was maintained. Cone-beam computed tomography scans from one case were superimposed on the anterior cranial base. Significant forward movement of the maxilla and the infraorbital border was observed, whereas the horizontal growth of the mandible was restricted.

- ***De Clerck et al.*** (26) in 2010, analyzed the treatment effects of bone-anchored maxillary protraction (BAMP) with miniplates in the maxilla and mandible in a treated sample consisted of twenty-one Class III patients. Records were taken before the pubertal growth spurt (mean age, 11.10 ± 1.8 years) and re-evaluated one year after BAMP therapy. The treated group was compared with a matched control group of eighteen untreated Class III subjects.

  Sagittal measurements of the maxilla showed significant improvements during active treatment (about 4 mm more than the untreated controls), with protraction effects at orbitale and pterygomaxillare. Significant improvements of overjet and molar relationship were recorded, as well as in the mandibular skeletal measures at Point B and pogonion. Vertical skeletal changes and modifications in incisor inclination were negligible, except for a significant proclination of the mandibular incisors in the treated group. Significant soft-tissue changes also reflected the underlying skeletal modifications.

- ***Cevidanes et al.*** (27) in 2010, compared two protocols for maxillary protraction-bone anchors versus face mask with rapid maxillary expansion. Changes in dentoskeletal cephalometric variables from start of treatment (T1) to end of active treatment (T2) with an average T1–T2 interval of about 1 year were contrasted in a BAMP sample of twenty-one subjects with RME/FM (rapid maxillary expander with facemask) sample of thirty-four patients. They observed that the BAMP protocol produced significantly larger maxillary advancement than the RME/ FM therapy (with a difference of 2 mm to 3 mm). Mandibular sagittal changes were similar, while vertical changes were better controlled with BAMP. The sagittal intermaxillary relationships improved 2.5 mm more in the BAMP patients. Additional favourable outcomes of BAMP treatment were the lack of clockwise rotation of the mandible as well as a lack of retroclination of the lower incisors. The BAMP protocol produced significantly larger maxillary advancement than the RME/FM therapy.

- ***Heymann et al.*** (17) in 2010, analyzed three dimensional effects of maxillary protraction with intermaxillary elastics to miniplates. Six patients with Class III occlusion and maxillary deficiency were treated by using intermaxillary elastics to titanium miniplates. Cone-beam computed tomography scans taken before and after treatment were used to create 3-dimensional volumetric models that were superimposed on nongrowing structures in the anterior cranial base to determine anatomic changes during treatment. They found that the effect of the intermaxillary elastic forces was throughout the nasomaxillary structures. All six patients showed improvements in the skeletal relationship, primarily through maxillary advancement with little effect on the dentoalveolar units or change in mandibular position. The changes in the anterior mandibular region were more variable in both magnitude and direction. There were small individual differences in surface distances between the left and right condyles, but all patients showed a positive change on the posterior surfaces and a negative (inward) change on the anterior surfaces.

- ***Nguyen et al.*** (28) in 2011, assessed three-dimensional changes associated with bone anchored maxillary protraction in the maxilla, the surrounding hard and soft tissues, and the circum-maxillary sutures. Twenty-five consecutive skeletal Class III patients between the ages of nine and thirteen years (mean, 11.10±1.1 years) were treated with Class III intermaxillary elastics and bilateral miniplates (two in the infra-zygomatic crests of the maxilla and two in the anterior mandible). Cone-beam computed tomographs were taken before initial loading and 1 year out. Three-dimensional models were generated from the tomographs, registered on the anterior cranial base, superimposed, and analyzed by using colour maps. The maxilla showed a mean forward displacement of 3.7 mm, and the zygomas and the maxillary incisors came forward 3.7 and 4.3 mm, respectively. This treatment approach produced significant orthopedic changes in the maxilla and the zygomas in growing Class III patients.

- ***Lee and Beak*** (21) in 2012, in a finite element analysis, compared the pattern and amount of stress and displacement between maxillary protraction with miniplates placed at the infra-zygomatic crest and the lateral nasal wall from two separate finite element model. After a protraction force (500 g/side) was applied to the distal end of the miniplate with a forward and 30° downward vector to the maxillary occlusal plane, stress distributions in the circum-maxillary sutures and displacements of the surface landmarks were analyzed. They found difference in the maximum stress distribution area according to the site of the miniplate: infra-zygomatic crest and middle part of the maxilla in the infra-zygomatic crest and paranasal area adjacent to the pyriform aperture in the lateral nasal wall. Stress values of the frontonasal, frontomaxillary, zygomaticomaxillary, and pterygomaxillary sutures were greater in the infra-zygomatic crest than in the lateral nasal wall. The lateral nasal wall exhibited forward, downward, and outward displacements of ANS, Point A, and prosthion. However, the infra-zygomatic crest showed forward and upward displacements of ANS, Point A, and prosthion, and outward displacement of the zygomatic process of the maxilla and the maxillary process of the zygomatic bone. They concluded that, the site of miniplate placement should be considered to obtain proper stress and displacement values in different areas with maxillary hypoplasia.

- ***De Clerck et al.*** (19) in 2012, evaluated three dimensional changes in mandibular and glenoid fossa after bone-anchored Class III intermaxillary traction. Twenty-five consecutive skeletal Class III patients between the ages of nine and thirteen years (mean age,11.10 ± 1.1 year) were treated with Class III intermaxillary elastics and bilateral miniplates. The patients had cone-beam computed tomography (CBCT) images taken before initial loading and at the end of active treatment. Three-dimensional models were generated from these images, registered on the anterior cranial base, and analyzed by using colour maps.

  Posterior displacement of the mandible at the end of treatment was observed in all subjects (posterior ramus: mean, 2.74 ± 1.36 mm; condyles: mean, 2.07 ± 1.16 mm; chin: mean, -0.13 ± 2.89 mm). Remodeling of the glenoid fossa at the anterior eminence (mean, 1.38 ± 1.03 mm) and bone resorption at the posterior wall (mean, -1.34 ± 0.6 mm) were observed in most patients.

- ***Fernandez et al.*** (29) in 2012, in a systematic review compared the effects of bone and dento-alveolar dentofacial orthopedics for Class III malocclusion. Thirty studies were selected after applying the criteria. Protraction rates differed within a range of one- to two-fold between bone-anchored and dentoalveolar therapies. All studies noted the effect of clockwise rotation on the mandible and an increase in inferior-anterior and total facial height; this was more obvious in dentoalveolar therapy than in bone-anchored orthopedics. Dental parameters like overjet increased significantly with both sets of groups, ranging from 1.7 to 7.9 mm with dentoalveolar therapy and from 2.7 to 7.6 mm with bone-anchored orthopedics.

- ***Yan et al.*** **(**20***)*** in 2013, compared the biomechanical effects in craniomaxillary complex during maxillary protraction with bone anchorage vs conventional dental anchorage. Two finite element models were developed. One simulated maxillary protraction with dental anchorage in the maxillary first molars and the other with bone anchorage in the infra-zygomatic buttresses of the maxilla. The magnitude of the applied forces was 500 gram per side, and the force directions were 0°, 10°, 20°, and 30° forward and downward relative to the occlusal plane. They observed that the finite element model of the craniomaxillary complex could displace in an almost translatory manner when the force direction was about 20° in the bone anchorage model and about 30° in the dental anchorage model. The nodes representing the sutures at the back of the maxilla showed greater stress in the bone anchorage model than in the dental anchorage model in the same force direction. It is the opposite at the front of the maxilla.

- ***Hino et al.*** (18) in 2013, evaluated the growth and treatment effects on the midface and the maxillary dentition produced by facemask therapy in association with rapid maxillary expansion (RME/FM) compared with bone-anchored maxillary protraction (BAMP). Forty-six patients with Class III malocclusion were treated with either RME/FM (n= 21) or BAMP (n =25). Three-dimensional models generated from CBCT scans, taken before and after approximately 1 year of treatment, their study showed that orthopedic changes could be obtained with both RME/FM and BAMP treatments, with protraction of the maxilla and the zygomas. Approximately half of the RME/FM patients had greater dental than skeletal changes, and a third of the RME/FM compared with 17% of the BAMP patients had a predominantly vertical maxillary displacement.

- ***Zhang et al.*** (30) in 2015, evaluated displacements prediction from 3D finite element model of maxillary protraction with and without rapid maxillary expansion in a patient with unilateral cleft palate and alveolus, deformation of the craniomaxillary complex after applied orthopaedic forces in different directions were also assessed. A three-dimensional finite element model of 1,277,568 hexahedral elements (C3D8) and 1,801,945 nodes was established based upon CT scan of a patient. A force of 4.9 N per side was directed on the anatomic height of contour on the buccal side of the first molar. The angles between the force vector and occlusal plane were −30°, −20°, −10°, 0°, 10°, 20°, and 30°. Protraction force alone led the craniomaxillary complex moved forward and counter-clockwise, accompanied with lateral constrain on the dental arch. Additional rapid maxillary expansion resulted in a more positive reaction including both larger sagittal displacement and the width of the dental arch increase.

- ***Eid et al.*** (31) in 2016, evaluated the effect of bone-anchored maxillary protraction in treatment of growing patients with Class III malocclusion. The sample of this study consisted of ten subjects. Each treated patient had four miniplates that were inserted between the lower left and right lateral incisor and canine and on the left and right infrazygomatic crest of the maxillary buttress. Class III elastics were applied between the miniplates on each side for twenty- four hours a day. The initial force was 300 g per side increased to 350 after one month and increased to 450 g per side two months later. Lateral cephalograms of each patient were evaluated at the beginning of treatment (T1), at the end of active treatment (T2). The effect of treatment was compared to the effect of growth changes in a matched untreated control group of the same malocclusion. The bone-anchored maxillary protraction approach induced a significant orthopedic maxillary advancement, and retarded the mandibular growth with improvement of facial profile. Maxillomandibular divergency was increased mainly due a counter-clockwise rotation of the maxilla.

- ***Yatabe et al.*** (32) in 2017, evaluated the mandibular and glenoid fossa (GF) changes after bone-anchored maxillary protraction (BAMP) therapy in patients with unilateral complete cleft lip and palate (UCLP). The cleft group (CG) comprised of 19 patients with mean age of 11.8 years. The noncleft group (NCG) comprised 24 patients without clefts with mean initial age of 11.7 years. Both groups had Class III malocclusion and were treated with BAMP therapy for 18 and 12 months, respectively. Cone-beam computed tomography (CBCT) scans were performed before and after treatment and superimposed on the anterior cranial fossa (ACF). Mandibular rotations and three-dimensional linear displacements of the mandible and GF were quantified.

  Immediately after active treatment, the GF was displaced posteriorly and laterally in both groups relative to the ACF. The overall GF changes in the CG were significantly smaller than in the NCG. Condylar displacement was similar in both groups, following a posterior and lateral direction. The gonial angle was displaced posteriorly, laterally, and inferiorly in both groups. The intercondylar line rotated in opposite directions in the CG and NCG groups. In the CG, most changes of the GF and mandible were symmetrical. Overall, GF and mandibular changes after BAMP therapy were similar in patients with and without clefts. The exception was the posterior remodeling of the GF that was slightly smaller in patients with UCLP.

- ***Ozdemir et al.*** (33) in 2018, studied the different skeletal advancement methods used in the treatment of maxillary retrusion patients. Computed tomography images of a young adolescent patient with maxillary retrusion were processed using three-dimensional medical image processing software to obtain a patient-specific model.

Three different treatment scenarios were envisaged for the finite element analysis. In the first scenario, rapid maxillary expansion (RME) and face mask (FM); in the second, bone-assisted maxillary advancement and RME, and in the third, hybrid hyrax and mentoplate combination methods were used. The hyrax screw was activated by 0.25mm in each model, with a force of 500g in the first scenario and 250g in the second and third scenario for each side. Von Mises stresses and the initial displacements were evaluated when different maxillary protraction methods were applied. They found that similar stress distributions were observed in the skull where the methods of RME/FM model and bone-assisted maxillary advancement were used. Stresses were higher than the hybrid hyrax and mentoplate combination method. When the displacement values were compared, anterior movement was found in the maxilla in the bone-supported model to include the middle face, while anterior movement of maxilla was detected on the Le Fort 1 level with the hybrid hyrax and mentoplate combination method. Dentoalveolar anterior movement was detected in the RME/FM model. It was observed that the bone-assisted maxillary advancement method provides more skeletal efficiency than the RME/FM and the hybrid hyrax and mentoplate combination methods.

- ***Hevele et al.*** (34) in 2018, evaluated the failure rate and associated factors through a retrospective study of 218 patients. A total of 218 patients (112 males and 106 females) with average 11.4 years, treated by 38 orthodontists, received four miniplates (total 872 miniplates) from 2008 to 2016 at three maxillofacial centers in two countries. Factors affecting the success and failure of the miniplates were retrospectively examined and skeletal changes on cephalometric radiographs examined for 52 patients. Elastic traction was performed for 22.9 months, on average. The miniplate survival rate was 93.6%. 25.7% of the patients suffered failure of one of the miniplates. Postoperative antibiotics and placement of the neck of the miniplate in the attached gingiva significantly improved the success rate. Miniplate failure was six times higher in the maxilla and occurred more in younger patients. Self-drilling screws were significantly better than self-tapping screws for fixing the miniplate. In conclusion, bone-anchored maxillary protraction on four miniplates is an effective method for correcting a Class III relationship, but has less skeletal effect than previously reported in the literature.

- ***Eom et al.*** (35***)*** in 2018, analyzed initial displacement and stress distribution of the maxillofacial complex during dentoskeletal maxillary protraction with various appliance designs placed on the palatal region by using three-dimensional finite element analysis. Six models of maxillary protraction were developed: conventional facemask (Type A), facemask with dentoskeletal hybrid anchorage (Type B), facemask with a palatal plate (Type C), intraoral traction using a Class III palatal plate (Type D), facemask with a palatal plate combined with rapid maxillary expansion (RME; Type E), and Class III palatal plate intraoral traction with RME (Type F). In Types A, B, C, and D, maxillary protraction alone was performed, whereas in Types E and F, transverse expansion was performed simultaneously with maxillary protraction. Type C displayed the greatest amount of anterior dentoskeletal displacement in the sagittal plane. Types A and B resulted in similar amounts of anterior displacement of all the maxillofacial landmarks. Type D showed little movement, but Type E with expansion and the palatal plate displayed a larger range of movement of the maxillofacial landmarks in all directions. The palatal plate served as an effective skeletal anchor for use with the facemask in maxillary protraction. In contrast, the intraoral use of Class III palatal plates showed minimal skeletal and dental effects in maxillary protraction. In addition, palatal expansion with the protraction force showed minimal effect on the forward movement of the maxillary complex.

- ***Jayan et al.*** (36) in 2019, evaluated displacement and stress distribution in maxillofacial complex following maxillary protraction with conventional and modified facemask using finite element analysis. Cone beam computerized tomography images are used to generate two finite element models. A force of 1500 gram was applied at 30 degrees in a downward and forward direction to the maxillary occlusal plane in the first model and at a distance of 15 mm and parallel to the maxillary occlusal plane in the second model. Stress generated in the frontomaxillary, pterygomaxillary, zygomaticomaxillary, zygomaticofrontal and zygomaticotemporal sutures and the displacement of the frontal process of the maxilla, Prosthion, point A and FA point of the first molar were studied in both models. In the modified face mask, maximum stresses were generated in the zygomaticotemporal suture and frontomaxillary sutures. In the conventional facemask, maximum stresses were generated in the pterygomaxillary and zygomaticomaxillary sutures. In the modified facemask, landmarks Prosthion, point A and FA point of the first molar showed greater movement in the anterior direction and in the transverse direction. In the vertical direction, the magnitude of displacement of the frontal process of the maxilla, prosthion, point A and FA point of the first molar was more in the conventional facemask. The modified facemask demonstrated lesser magnitude of maxillary rotation in a counter-clockwise direction and more anteroposterior movement as compared to the conventional facemask.

- ***Khan et al.*** (37) in 2020, measured the stress distributions on the temporomandibular joint (TMJ) due to the face mask appliance using different levels of forces and different angulations using finite element analysis. Three-dimensional finite element model of the craniofacial complex was constructed from a cone-beam computed tomography (CBCT) scan of a patient, with the help of the Mimics software. The forces were applied on the hooks and the anchorage was taken from the chin and the forehead. Four different force directions were applied—0, 10, 20, and 30° from the occlusal plane with each having three different force levels, 800 g, 1000 g, and 1200 g (combined force on both sides). The stress distribution of TMJ was analyzed. The results indicated that the maxillary protraction appliance had a reactionary force on TMJ. Maximum stress was observed with 1200 g load and at the 0° angulation condition and the minimum stress was observed for 800 g load and at an angulation of 30°. On the articular disk, condylar cartilage, glenoid fossa, and condyle, stresses increased with increase in load. However, with an increase in angulation for the given load, the stresses reduced gradually.

- ***Rai et al.*** (38) in 2021, evaluated the biomechanical effects on maxillomandibular complex of skeletally anchored Class III elastics with varying angulations using the 3D finite element analysis. Two 3-dimensional analytical models were developed using the from sequential computed tomography images taken from a Skeletal Class III subject. The models were meshed into 465,091 tetrahedral elements and 101,247 nodes. Intraoral mechanics for skeletally anchored maxillary protraction (I-SAMP) were applied on two models i.e. A and B (without and with maxillary expansion respectively) between miniplates on maxilla and mandible on both right and left sides with three different angulations of forces—10°, 20° and 30°. Although the craniomaxillary complex in both the models (A and B) displaced forward while demonstrating rotations in opposite directions, the displacements and rotations decreased gradually with the increase of the angle of load application from 10° to 30°. The mandible rotated clockwise in both the simulations, but the displacement of mandibular surface landmarks was higher in Simulation A. However, the antero-inferior displacement of the glenoid fossa was higher in Simulation B than in A. Significant displacement of maxillofacial sutures and structures was witnessed with I-SAMP with maxillary expansion.

- ***Bhad et al.*** (22) in 2021, evaluated the stress distribution on maxilla, mandible, and glenoid fossa after application of Class III intermaxillary anteroposterior orthopedic forces of 150, 250, and 400 gm applied to a three-dimensional (3D) model of the young human dry skull. A 3D finite element model was developed from the computed tomography images of a growing boy (age, 13 years). ANSYS software used to simulate Class III force of progressively increasing intensity over maxilla, mandible, and glenoid fossa to quantify the biomechanical reaction with two components, direction and stress. Detailed changes were quantified in the maxillofacial sutures, dentition, mandible, and glenoid fossa with bone-anchored maxillary protraction (BAMP) to analyze their effects. As the force increases from 150, 250 to 400 g, stresses are increased on all structures associated except maxillary central incisor which showed a decrease in the stresses. Stress generated at the circum-maxillary sutures was minimal. As with any other Class III force, stresses were distributed on whole of condyle, capsular ligament, and minimal at glenoid fossa.

# MATERIALS AND METHODS

## Setting and Location

The study was conducted in the Department of Dentistry, All India Institute of Medical Sciences Jodhpur in collaboration with Department of Mechanical Engineering, Indian Institute of Technology Jodhpur. Ethical approval was obtained from the Institutional Ethics Committee, AIIMS Jodhpur (AIIMS/IEC/2021/3303), Rajasthan, India. An informed consent was signed by the child's father to use computed tomography (CT) images and magnetic resonance image (MRI) after clarifying the aims and purpose of this research.

## Source of Data

Pre-treatment CT scan of skull and MRI scan image of temporomandibular joint of a growing patient presenting with Class III skeletal malocclusion with maxillary deficiency was taken. The patient underwent orthodontic treatment.

## Study Design

This is an in-vitro three-dimensional finite element analysis study evaluating the stress distribution pattern on a finite element model (FEM).

## Sample Selection Criteria

**Inclusion Criteria: -**

a. Growing patient with age range between 11 to 13 years
b. Skeletal Class III malocclusion with: -
    i. ANB angle -4 degree or less;
    ii. wits appraisal -2 mm or less;
    iii. Frankfort mandibular plane angle 25 degree or less.

**Exclusion Criteria: -**

a. Asymmetric skeletal structures
b. Fracture or discontinuity in maxilla or mandible
c. Presence of any pathological lesion in maxillofacial region

## METHODOLOGY

After taking approval from Institutional Ethics Committee (IEC), pre-treatment computed tomography (CT) scan images of skull and magnetic resonance imaging (MRI) scan of temporomandibular joint of a patient, presented with Class III malocclusion were taken based on the inclusion and exclusion criteria.

## ACQUISITION AND STANDARDIZATION OF SCAN

Helicoidal, multi-slice CT scan acquisition was performed with a Somaton Definition Flash 128-slice Siemens CT scanner (Siemens, Xangai, China) with a voxel size of $200mm^3$, slice thickness of 1mm at 120 kV, 230 mA. The scan was obtained with the bite in maximum intercuspation. The scanned images were saved in DICOM (Digital Imaging and Communications in Medicine) file format.

MRI scan of temporomandibular joint was performed with high intensity 3-Tesla magnet (GE 3T Discovery MR750w, Siemens, Xangai, China) and in a 3-in dual surface coil. Slice thickness of the scanned image was 2mm and images were captured at 0.5 mm interval. Scanning was done in closed and open mouth position keeping the patient in supine position. The scanned images were saved in DICOM file format.

The analytical three-dimensional FEM model of the cranio-maxillary complex was generated from the CT and MRI scan images of the patient by using multiple software.

## SOFTWARE USED FOR PRESENT STUDY

1. MIMICS (Materialise Interactive Medical Image Control System) 21.0; Materialise, Leuven, Belgium
2. 3-Matic 11.0; Materialise, Leuven, Belgium
3. SolidWorks 2021 SP2.0; Dassault Systems, Concord, Mass
4. ANSYS Workbench 2021R1; Canonsburg, Pennsylvania

## AN OVERVIEW ABOUT FINITE ELEMENT METHOD

Finite element method is known as the efficient and most accurate method to get the solution in the field of engineering industry. In this method, analysis of a complex region defining a continuum is discretized into simple geometric shapes called finite elements. The material properties and the governing relationship are considered over these elements and expressed in terms of unknown values at element corners. An assembly process, duly considering the loading and constrains, result in a set of equations. Solution of these equations gives us the approximate behavior of the continuum.

The advent of the mini-computers has made the technology to improve drastically and has covered a wide area in engineering industries as well. Here in this case the computers obtain the solution, as they are faster and accurate.

The solution of the FEM is an advanced computer technique of structural stress analysis was developed in early 1960's to solve the problems of aerospace industry. The term 'finite element' was coined by Argyris and Clough in 1960. Its use has been extended to solve problems in heat transfer, fluid flow, electromagnetic mass transport, in medicine and other branches of health sciences.

The solutions obtained are nearer to actual solution. Nowadays the numerical method has made its mark in all engineering industries as it is efficient, economical, reliable and faster in providing the solution. Some of the analysis packages in the market are ANSYS, NASTRAN, PRO-E, ABACUS, IDEAS, NISA, WECAN, CATIA, etc.

The Accuracy of the Finite element solution depends on

i. The discretization, which is characterized by the finite element mesh and the choice of elements.
ii. Type of element (lower order, higher order)
iii. Shape of the element (triangular, quadrilateral, tetrahedron, hexahedron etc.)
iv. Geometry (simple, complex)
v. Refinement of the mesh.
vi. Application of the load.
vii. Skill
viii. Software

FEM is a technique for obtaining a solution to a complex mechanical problem by dividing the problem domain into a collection of smaller and simpler domains (elements) in which the variables of the field can be interpolated with the use of shape and other function. The elements are connected at specific location called nodal points or nodes. The boundary conditions and loading configurations are numerically defined as displacements and forces, respectively in boundary nodes.

Every element is assigned one or more parameters that define its material behaviour. The computer program calculates the stiffness characteristics of each element and assembles the element mesh through mutual forces and displacements in each node. The computer time needed depends progressively on the number of elements applied and on the element type.

**BASIC STEPS INVOLVED IN THE CONSTRUCTION OF FINITE ELEMENT MODELS IN GENERAL**

**A. PRE-PROCESSING STAGE**

a) Construction of geometric model
b) Discretization into finite elements
c) Assigning material properties
d) Defining the boundary conditions

**B. PROCESSING OR SOLUTION STAGE**

e) Application of forces

**C. POST PROCESSING STAGE**

f) Analysis and interpretation of results

**1. PRE-PROCESSING STAGE**

a) **Construction of a geometric model**

The purpose of the geometric modelling phase is to represent a geometry in terms of points (grids), line surfaces (patches) and volume (hyper patches).The first requirement for the analysis is the geometric model. These can be drafted or created either in the analysis software itself or the model can be drafted from any computer assisted designing software and can be imported to the analysis software.

The software used for the geometric modelling was MIMICS 21.0, 3-Matic 11.0 and SolidWorks 2021 SP 2.0.

b) **Discretization process**

Discretization is a process of dividing the domain/component into number of elements. For this, an assumption is made that the elements are interconnected by nodes. The main idea behind the discretization process is to improve the accuracy of the results. This is because if the entire component is divided into number of elements, then the stress distribution in each element will be nearer to the actual results and thereby we get accurate plot of the stress distribution in a component.

c) **Assigning material properties**

Each structure was then assigned a specific material property. The mechanical properties --Young's modulus and Poisson's ratio are defined to the component. This is done to feed the values for calculation of the solution. By using these material properties, the solutions are obtained. The material properties used in this study have been taken from previous finite element studies. (20,39)

d) **Defining the boundary condition**

The boundary conditions here mean that whether the domain/structure/component perform a static or dynamic action. The boundary condition is selected based upon the mode of analysis such as structural, dynamic, thermal, fluid, etc.

## 2. PROCESSING/ SOLUTION STAGE

e) **Application of load**

The discretized domain is subjected to known loads. The application of loads depends upon the geometry of components and the application of the component. The load is applied either on the nodes, lines or area.

Types of Loads are as follows: -

For Structural Problems: Forces, Moments, Pressure, Torque, Etc.
For Thermal Problems: Gravity, Radiation, Convection, Temperature, Etc.

**3. POST PROCESSING STAGE**

f) **Analysis and interpretation of results**

The sequential application of the above steps leads to a system of algebraic equations where the nodal displacements are unknown. These equations are solved by frontal solver technique present in the ANSYS software. The results can be obtained instantaneously and are most accurate. Stress nephrogram and displacement nephrogram can be generated in this software.

**STEPS INVOLVED IN THE CONSTRUCTION OF 3D FEM MODEL IN THE PRESENT STUDY**

1. **Pre-processing stage**

**A. Construction of three-dimensional model of skull**

The DICOM data were exported in a three-dimensional image processing software MIMICS 21.0; Materialise, Leuven, Belgium. The images were three dimensionally reconstructed with threshold values between the range of 226 to 3071 Hounsfield unit (HU).

By thresholding, the segmentation object would include only those pixels that were within the Hounsfield Unit or grey value range. Based on the HU values, hard tissue structures were detected from all the pixels of CT images (Figure 1).

A green coloured ‘segmentation mask’ was generated containing the hard tissues from the pixels falling within the range of 226 HU to 3071 HU. Segmentation mask is a collection of pixels of interest that constitute an object. From this mask bone and teeth were separated out by the following methods:

a) Defining the boundary of hard tissue mask

A rectangular box of adequate width and length, was drawn on the magnified coronal view of the initial green coloured hard tissue mask. All the hard tissue structures were within the box in all the coronal section images.

In the coronal section, at the position 199.5059, all the pixels were erased from the initial hard tissue mask that were within the rectangular box to determine the anterior boundary of the skull model (Figure 2).

At the coronal position of 67.5820, all the pixels within the box were erased by the same method. That determined the posterior boundary of the skull model (Figure 3).

In the axial section, a rectangular box of adequate width and length were drawn, keeping all the hard tissue structures within the boundary of the box. At the axial position 160.3, all the pixels were erased by the same method. This determined the upper most extension of the geometric skull model (Figure 4).

In the axial section at the slice level 14.0, all the pixels from the green mask were erased by the same method (Figure 5). That defined the lower most extension of the skull model.

Thereby upper boundary of CT scan slices containing the region of interest, ranges from axial section 160.3 (above the level of frontal sinus) to 14.0 (below the level of lower border of chin). Anteriorly it is extended from coronal slice position 186.5449 (at the tip of nasal bone) to slice position 69.4336 (at the at the level of mid-section of foramen magnum). The resulting mask contained the part of the maxillofacial skeleton which is extended posteriorly up to the mid-section of foramen magnum, mandible, hyoid bone and cervical vertebrae (C1 to C3).

b) <u>Separating the maxillofacial bones and mandible from rest of the parts</u>

'Region growing tool' splits the segmentation created by thresholding, into several objects and removes floating pixels. It calculated all the structures in continuity from the initial hard tissue mask. Thereby hyoid bone was separated from the rest of the part as it was not in continuity with mandible. It created secondary mask.

A rectangular box of adequate dimension was drawn on the magnified views of the coronal images containing cervical vertebrae below the level of foramen magnum. All the pixels containing vertebrae from C1 to C3, were erased manually from every sagittal slices.

The final segmented mask contains the maxillofacial bones up to the posterior extent of midsection of foramen magnum and whole mandible.

c) <u>Separation of teeth from hard tissue structures</u>

By thresholding (Hounsfield Unit values of 1380 to 3071) from the previous hard tissue mask, only tooth structures were detected in the scanned images. By 'region grow' operation a new mask was generated containing the teeth structures only (Figure 6).

By 'multiple-slice edit' tool all the non-anatomic cavities and holes were filled for all the pixels of axial images to avoid generation of any sharp edges and angles within the skull model.

Both the mask containing maxillofacial bones and teeth, were assembled to generate the final segmentation mask. By region growing operation all the artefacts and floating pixels were removed. All the sharp edges of the resulting mask were made smooth to generate a well-formed finite element model. The 3D model generated from this final mask was exported in Stereolithography (STL) file format (Figure 7).

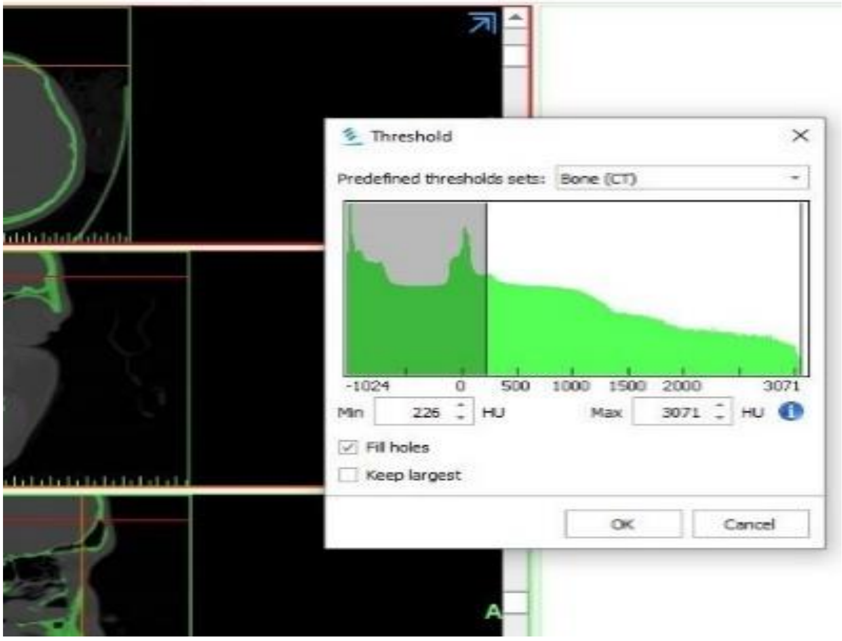


**Fig 1- Green mask indicating hard tissue structures obtained from CT scan of skull**

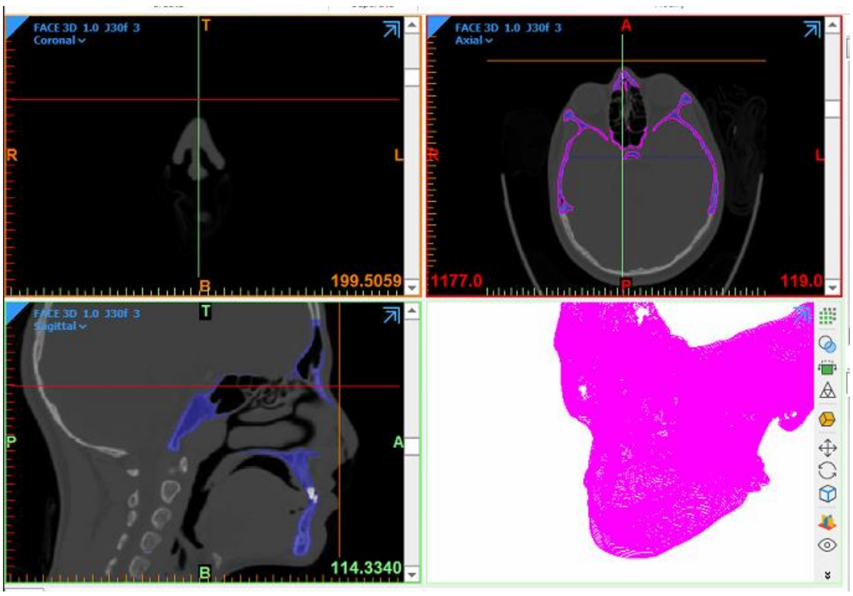


**Fig 2- Coronal (199.5059) and sagittal (114.3340) sections depicting anterior boundary of the constructed skull model**

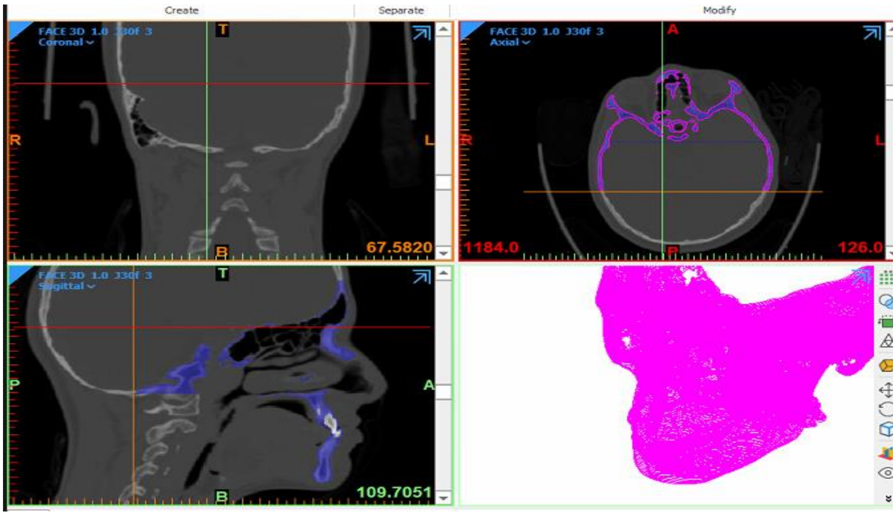


**Fig 3- Coronal (67.5820) and sagittal (109.7051) sections showing posterior border of the constructed skull model**

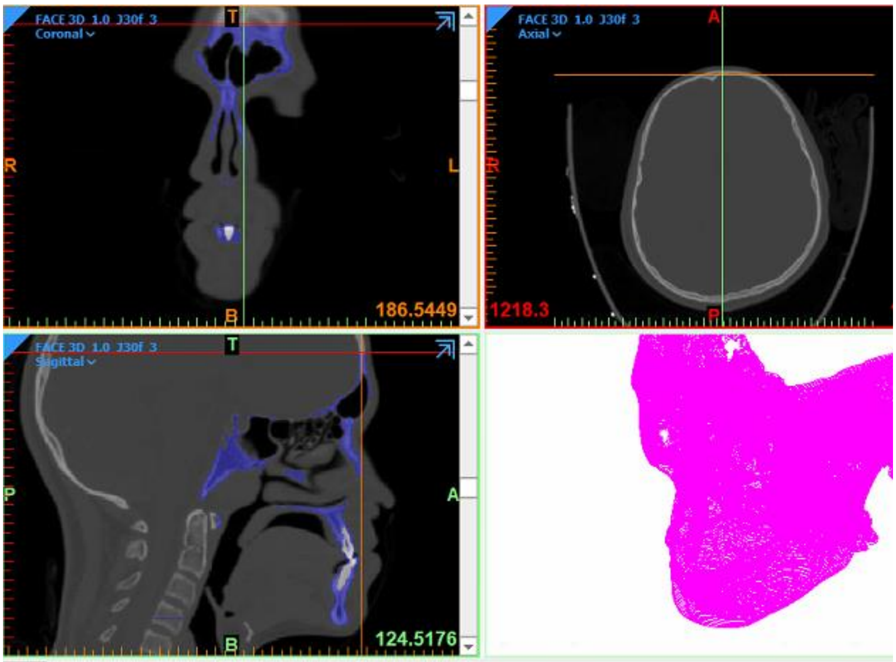


**Fig 4- Axial (160.3) and sagittal (124.5176) sections depicting the upper boundary of the constructed skull model**

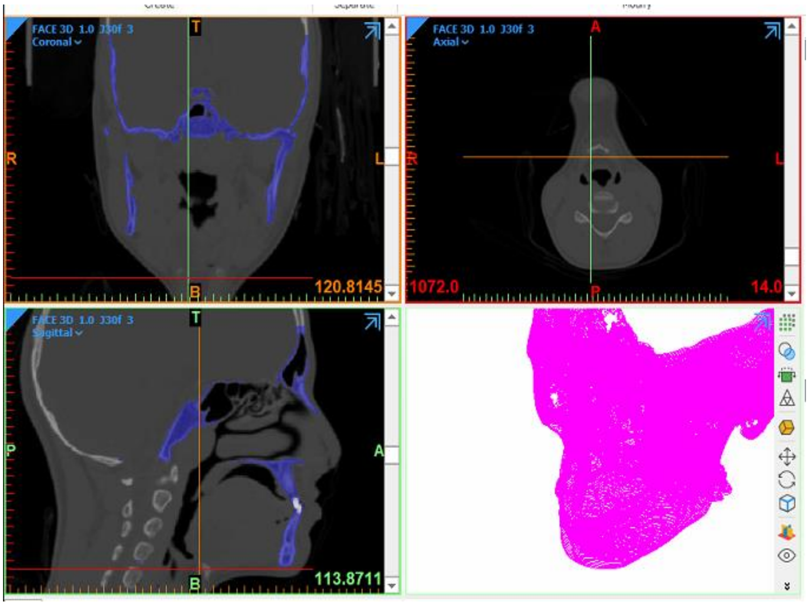


**Fig 5- Axial (14.0) and sagittal (113.8711) sections depicting lower boundary of the constructed skull model**

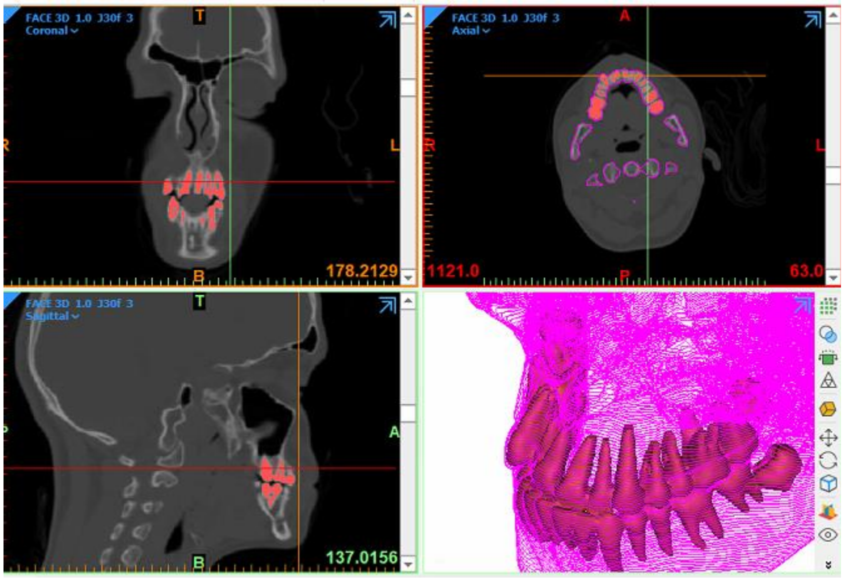


**Fig 6- Segmentation of the teeth from hard tissue structures**

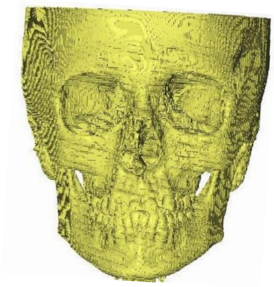

**Fig 7- Three-dimensional constructed model of bone and teeth generated from CT scan images of the skull**

**B. Construction of three-dimensional model of right temporomandibular soft-tissue structures from MRI scan images**

From the scanned DICOM data, fifteen axial slices were selected corresponding to right temporomandibular joint structures, ranging from axial slice position -75.5276 to slice position -44.7754 (Figure 8). Those slices were exported into MIMICS 21.0 software; Materialise, Leuven, Belgium.

From the MRI images right temporomandibular joint articular disc and surrounding soft tissue structures were detected out from rest of the structures by thresholding using Hounsfield unit values (HU 342-1541) of the soft tissue structures (Figure 9) initial segmentation mask was formed.

a. Defining the boundary of the soft tissue model

A rectangular box of adequate length and width was drawn that incorporated all the structures of interest in all the axial sections. From the axial section 26.4000 all the pixels from that initial segmentation mask, were erased corresponding to coronal section level 90.0096. It defined the uppermost boundary of the soft tissue (Figure 10).

In the axial slice section 11.0000, all the pixels from the initial segmentation mask were erased corresponding to the coronal section 90.0096 (Figure 11). It defined the lower most boundary of the soft tissue model.

Our region of interest extended coronally from axial section 26.4000 (at the level of upper border of right articular disc); apically to axial section 11.0000 (at the level of right condylar neck).

b. Separating the soft tissue structures

Manually all the unnecessary pixels, from each axial slice within the upper and lower boundary, had been removed.

By 'region grow tool' the area between the upper and lower boundary, was calculated. This final soft tissue mask contained all the necessary soft tissue structures (articular disc and muscle fibers) corresponding to the right temporomandibular joint. From the segmented-out mask, three-dimensional geometric model of right condylar soft tissue structure was calculated.

The calculated 3D model was exported in Stereolithography (STL) file format to 3-Matic 11.0 software (Materialise, Leuven, Belgium).

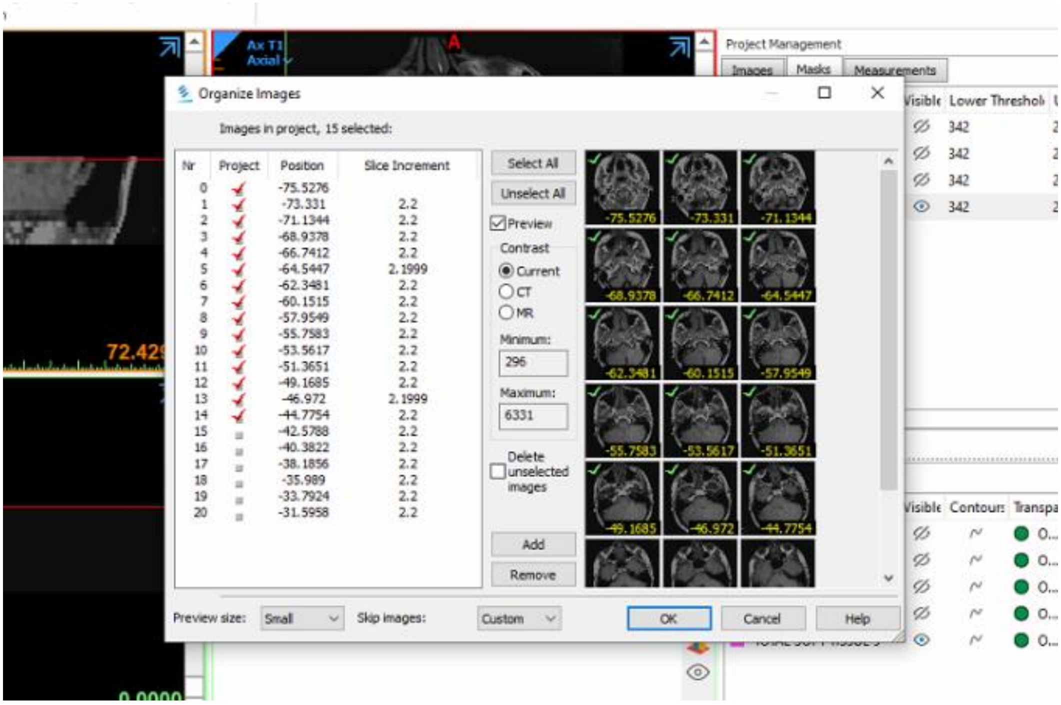


**Fig 8- Fifteen slices selected from MRI scan data, ranging from axial slice position -75.5276 to -44.7754 to construct the right temporomandibular soft tissue structures**

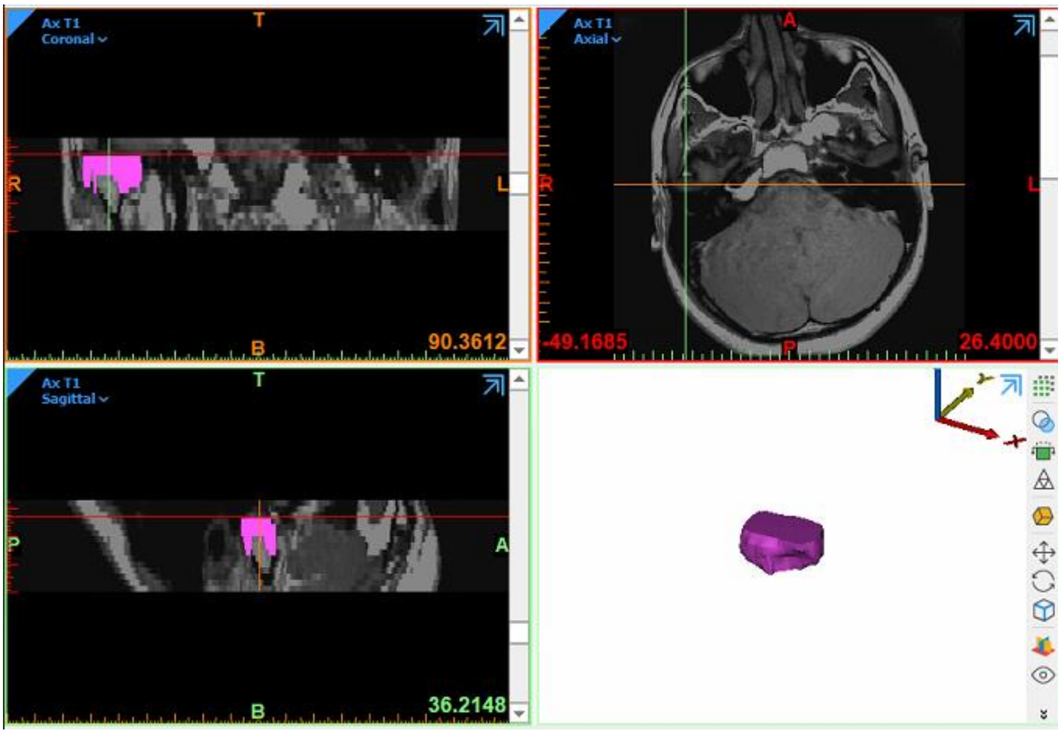


**Fig 9- Coronal (90.3632), axial (26.4000) and sagittal (36.2148) sections depicting the upper boundary of right temporomandibular soft tissue structures**

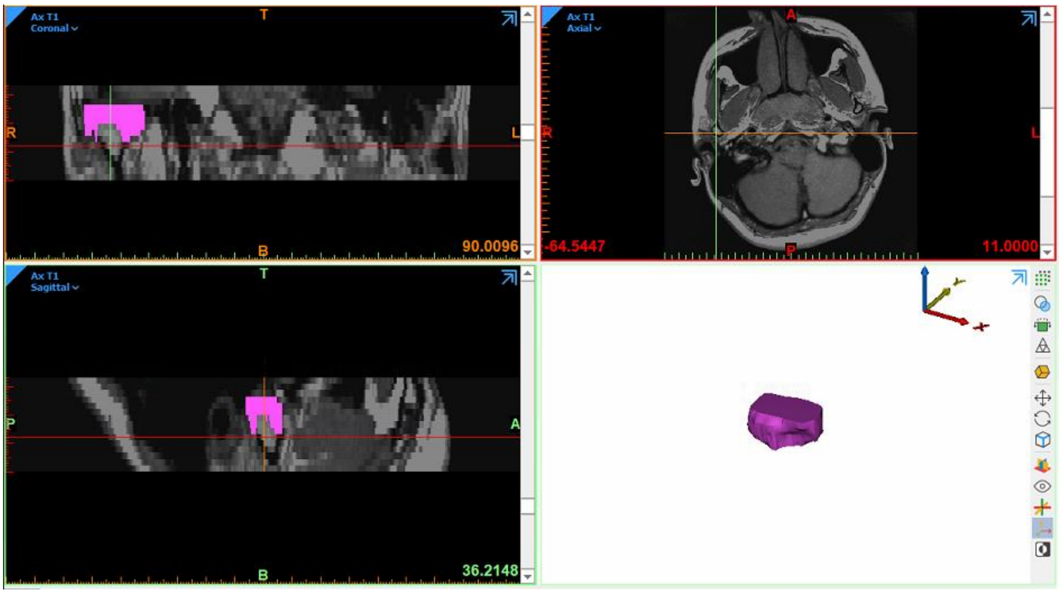


**Fig 10- Coronal (90.0095), axial (11.0000) and sagittal (36.2148) sections depicting the lower boundary of the right temporomandibular soft tissue**

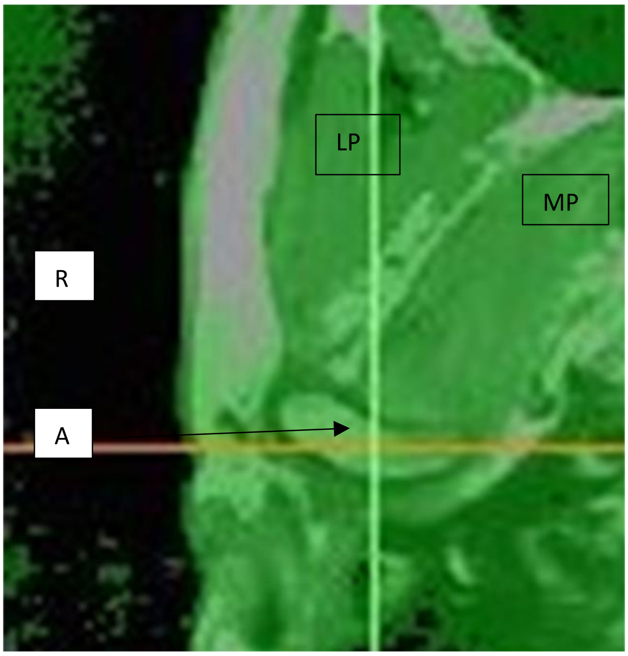


**Fig 11- Axial section showing right temporomandibular articular disc (A), lateral (LP) and medial pterygoid (MP) muscles indicated by green mask. R= right side**

## C. Anchor plate and screw designing

In a 3D computer-aided design (CAD) software (SolidWorks 2021 SP2.0, Dassault Systems) three-dimensional model of Y-type anchor plate (thickness,0.8mm; length,10.5 mm; width,2mm; hole diameter,2mm; distance between the centers of holes,6.5mm; angulation between the holes 60 degree; Skeletal Anchorage System, Sugawara, Japan), I-shaped anchor plate (thickness,0.8mm; length,10.5 mm; width,2mm; hole diameter,2mm; distance between the centers of holes,6.5mm; Skeletal Anchorage System, Sugawara, Japan) and screws (2mmX8mm) were designed and files were exported in Stereolithography (STL)file format (Figure 12).

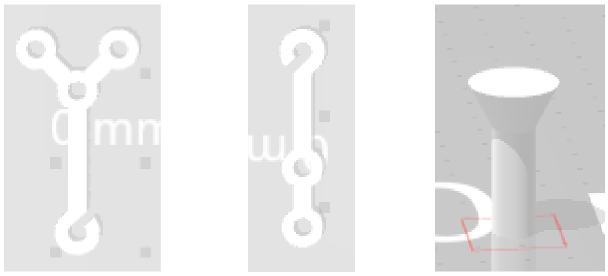

**Fig 12- Three-dimensional STL model of Y shaped anchor plate, I shaped plate and mini-screw designed in SolidWorks 2021 SP2.0**

## D. Assembling all the stl models into finite element model

Surface STL of plate was formed of 970 triangles, occupying surface area of 842.6059 mm$^2$ and volume of 261.12mm$^3$. In 3-matic, two Y-shaped anchor plates and six associated screws in the right and left infra-zygomatic crest region and two I-shaped anchor plates and four associated screws, in the mandibular para-symphysis area between mandibular permanent lateral incisor and mandibular permanent canine on the right and left side, were fixed respectively by surface projection method according to the anatomic contour. Wrap operation was done between the plates and screws to fill any gap between them by ‘Wrap’ tool.

Surface STL of soft tissue structures of right temporomandibular joint was formed of 392 triangles, 198 points, occupying surface area of 1049.6230 mm$^2$ and volume of 2104.4099 mm$^3$.

Right temporomandibular soft tissue structures were superimposed on right condylar head and aligned with condylar head by projection method.

In 3-Matic, three-dimensional geometric model (STL) of cranio-maxillary bones, right temporomandibular joint soft tissue structures, anchor plates and screws were meshed into tri-angular surface mesh model by 'Adaptive remesh' tool, keeping the 'non-manifold assembly' option toogled off.

After remeshing all the structures, node continuity was formulated between all the three-dimensional mesh structures by making intersection based non-manifold assembly among them. Resulting finite element model was made of 2,83,059 surface triangles.

After assembling, the following surface sets were generated: -

i. External surface of the skull
ii. External surface of right temporomandibular soft tissue
iii. External surface of right Y-shaped anchor plate
iv. External surface of left Y-shaped anchor plate
v. External surface of right I-shaped anchor plate
vi. External surface of left I-shaped anchor plate
vii. External surfaces of screws
viii. Intersection between right upper anchor plate holes and corresponding screws
ix. Intersection between left upper anchor plate holes and corresponding screws
x. Intersection between right lower anchor plate holes and corresponding screws
xi. Intersection between left lower anchor plate holes and corresponding screws
xii. Intersection between right temporomandibular soft tissue and right condylar head

Further adaptive remeshing of all the surface sets were done keeping the largest triangle edge length 5.000 and non-manifold option toogled on. Assembled model was inspected for presence of any intersecting triangle, bad contour, overlapping triangle, noise shell. Twelve intersecting triangles were detected at the intersection area in the right temporomandibular joint area. Manually these intersecting triangles were deleted and new triangles were drawn.

The assembled model was inspected for element quality. Following threshold were made to inspect element quality-

a. Ansys element quality ≥ 0.0100
b. Minimum face angle ≥ 5.0000
c. Maximum face angle ≤170.0000

All the values were within threshold limit. This assembled model was further broken down into parts containing three entities- skull with teeth, right temporomandibular soft tissue, and four wrapped plates and screws. Three-dimensional volumetric model was generated for each part from surface mesh model. The three-dimensional volumetric finite element model consisted of 1,07,529 tetrahedral (Tet 10) elements and 1,80,161 nodes (Table 1).

**Table 1. Elements and nodes details of each structure**

| **Body** | **Elements** | **Nodes** |
|---|---|---|
| Skull model | 105,561 | 175,879 |
| Right temporomandibular soft tissue | 1845 | 1001 |
| Right upper anchor plate and screws | 206 | 521 |
| Left upper anchor plate and screws | 287 | 710 |
| Right lower anchor plate and screws | 201 | 513 |
| Left lower anchor plate and screws | 273 | 693 |

Aspect ratio for each part was ≤100. ANSYS element quality was checked for each part. All the parts showed values within threshold level. Volumetric mesh and surface mesh were exported in cdb. file format for each part. Three cdb. files were exported in to ANSYS. Files containing skull, plates and screws and temporomandibular soft tissue structures were 36.2 MB, 493 KB and 387 KB respectively in size. The final three-dimensional finite element model was imported in a solver program (ANSYS Workbench 2021R1) (Figure 13).

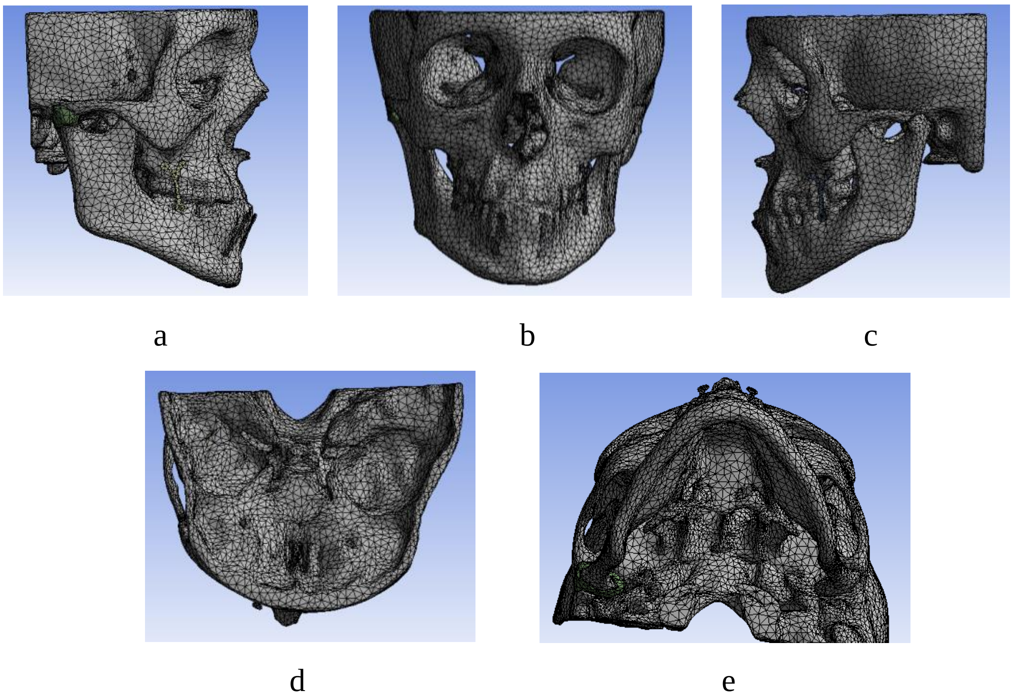


**Fig 13-Final assembled model a. right lateral view; b. frontal view; c. left lateral view; d. upper view; e. bottom view**

Material properties of various objects were assigned in the respective structures based on the data of previous studies (20, 39) (Table 2). All the materials used in this study were considered isotropic and linearly elastic.

**Table 2. Young's modulus and Poisson's ratio for the respective structures in the present study** (20,39)

| Material | Young's modulus (MPa) | Poisson's ratio |
|---|---|---|
| Cortical bone | $1.37 \times 10^4$ | 0.30 |
| Cancellous bone | $7.9 \times 10^3$ | 0.30 |
| Sutures | 7 | 0.40 |
| Anchor plate | $1.05 \times 10^5$ | 0.33 |
| Mini-screw | $1.05 \times 10^5$ | 0.33 |
| Tooth | $2.07 \times 10^4$ | 0.30 |
| Articular disc | 10 | 0.40 |

Nodes were selected along the circum-maxillary sutures (zygomaticomaxillary, zygomaticofrontal, zygomaticotemporal, nasomaxillary, nasofrontal, pterygomaxillary, fronto maxillary, midpalatal, internasal) along the condylar head and along the right temporomandibular soft tissue structures to calculate the Von mises stress and displacement of structures in all three planes of space (Fig 14 to Figure 19).

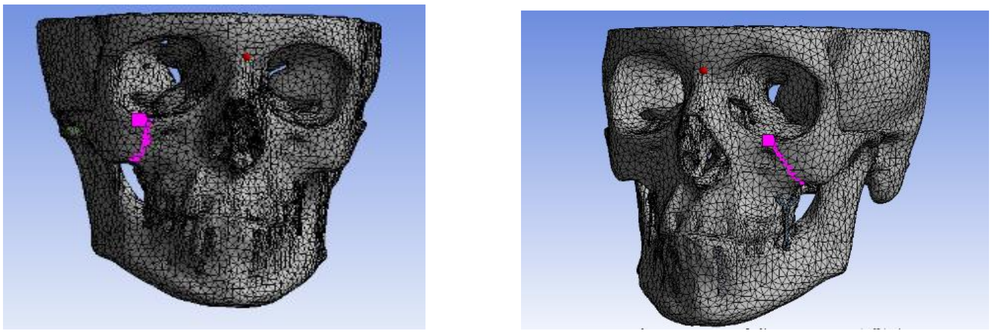

**Fig14- Nodes selected along right and left zygomatico-maxillary sutures**

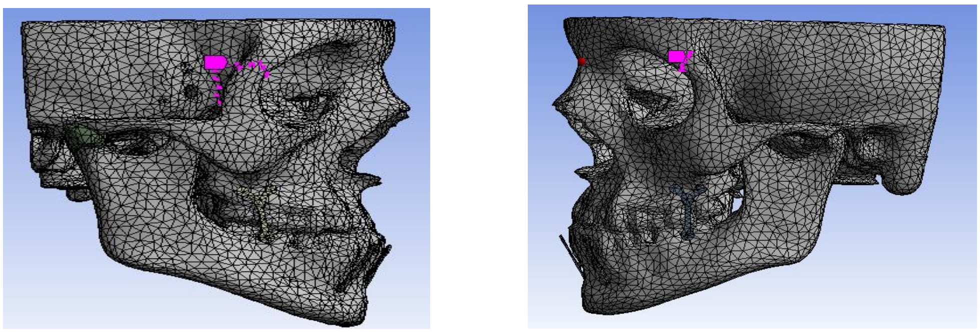

**Fig 15- Nodes selected along right and left zygomatico-frontal sutures**

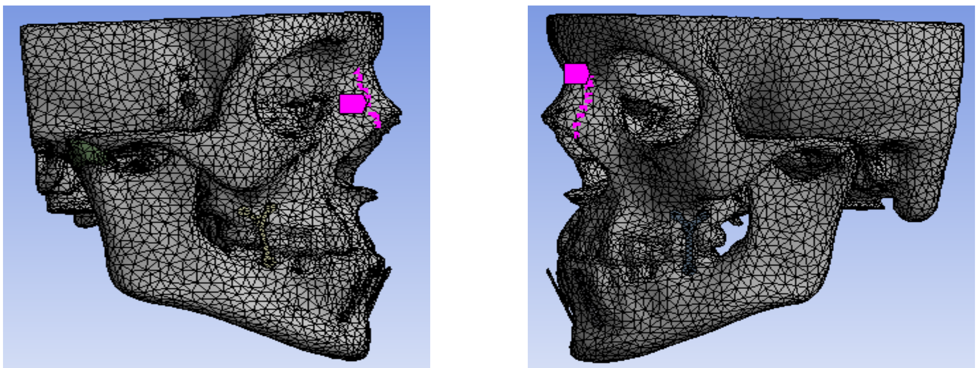

**Fig 16- Nodes selected along right and left naso-maxillary sutures**

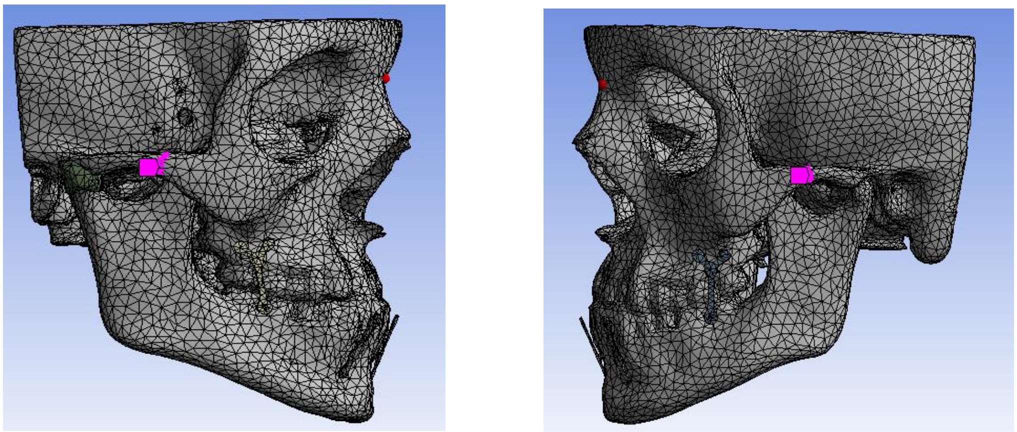

**Fig 17- Nodes selected along right and left zygomaticotemporal sutures**

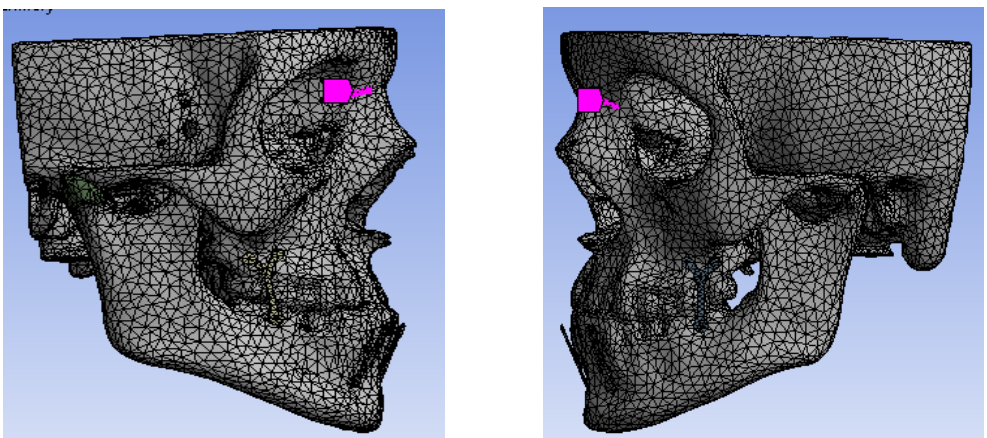

**Fig 18- Nodes selected along right and left fronto maxillary sutures**

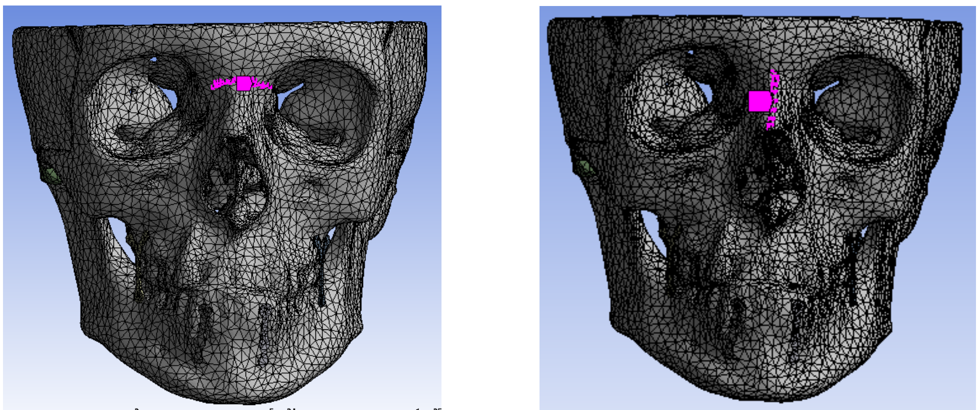

**Fig 19- Nodes selected along nasofrontal and internasal sutures**

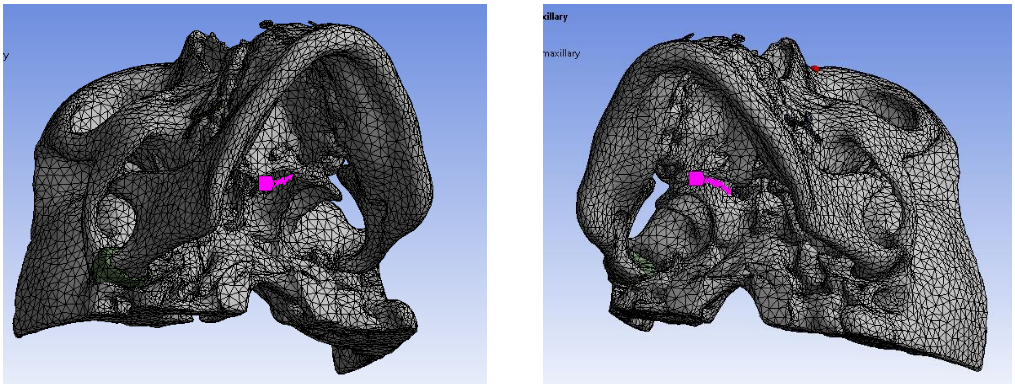

**Fig 20- Nodes selected along right and left pterygomaxillary sutures**

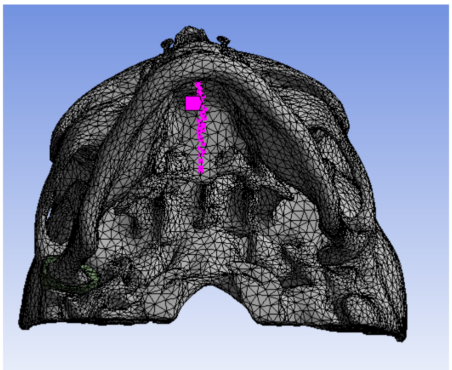

**Fig 21- Nodes selected along midpalatal suture**

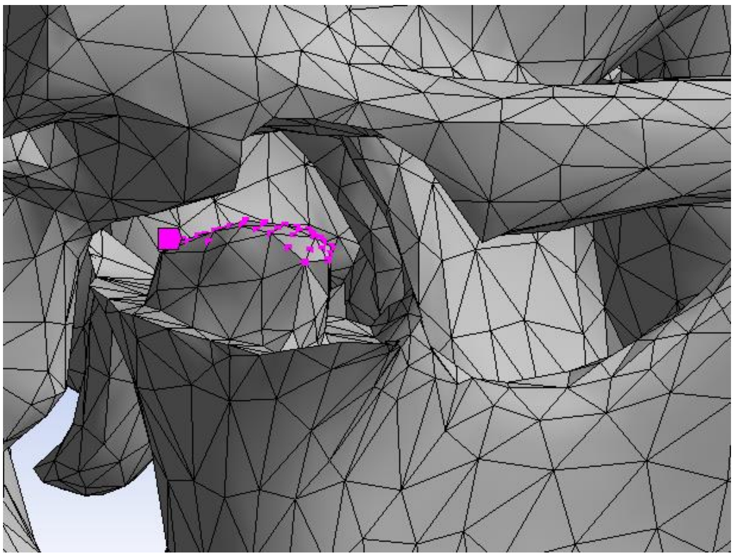

**Fig 22 - Nodes selected along right condylar head**

Single node was selected at the point of force application on each anchor plate and corresponding co-ordinate system was drawn which is 10 degrees ,20 degrees and 30 degrees to the occlusal plane in sagittal plane.

Zero-displacement, Zero-rotation boundary condition was imposed on the structures around the foramen magnum, upper and posterior border of the finite element model (Fig 20).

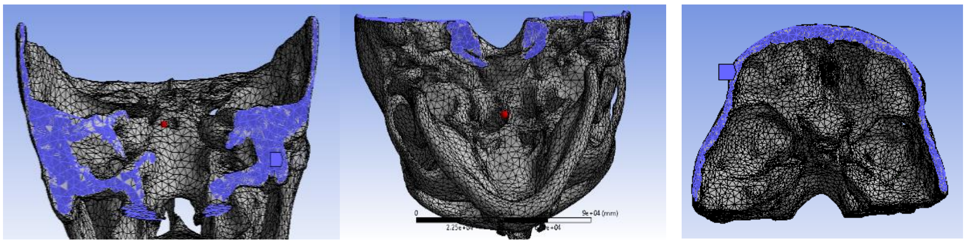

**Fig 23- Zero-moment, zero-rotation, zero displacement boundary condition imposed along the posterior surface, upper border and around the foramen magnum**

2. **Processing stage (analysis and solution of problem)**

Nodes were selected on anchor plates and 150 gm, 250gm, 400 gm of Class III force were applied sequentially at 10 degrees, 20 degree and 30 degrees angulation to the occlusal plane on selected nodes to evaluate the Von mises stress generation pattern and displacement of various structures (Figure 24 to 32).

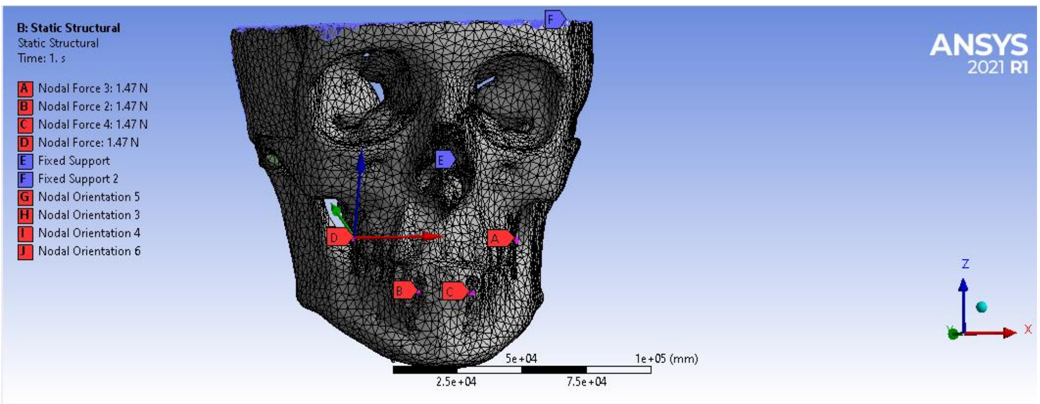


**Fig 24- Application of 150-gram intermaxillary Class III orthopedic force at selected nodes on the anchor plates at an angle of 10° to the occlusal plane**

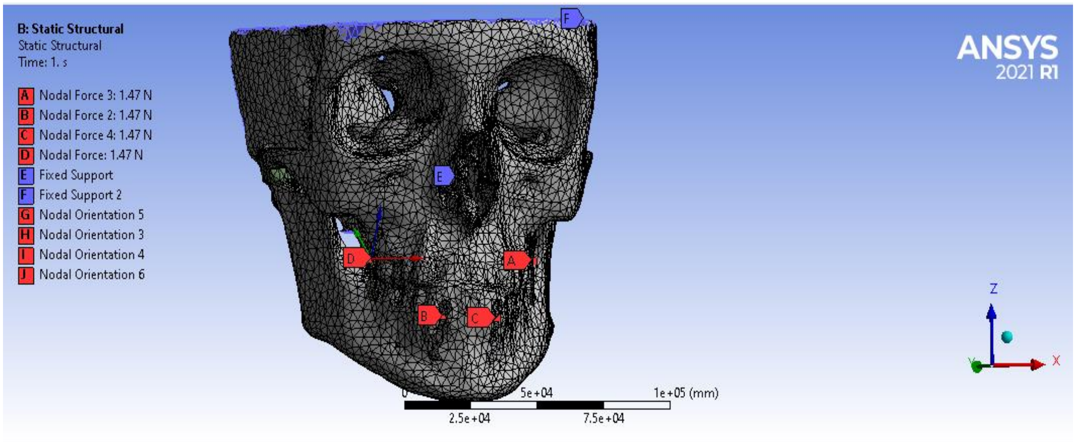


**Fig 25- Application of 150-gram intermaxillary Class III orthopedic force at selected nodes on the anchor plates at an angle of 20° to the occlusal plane**

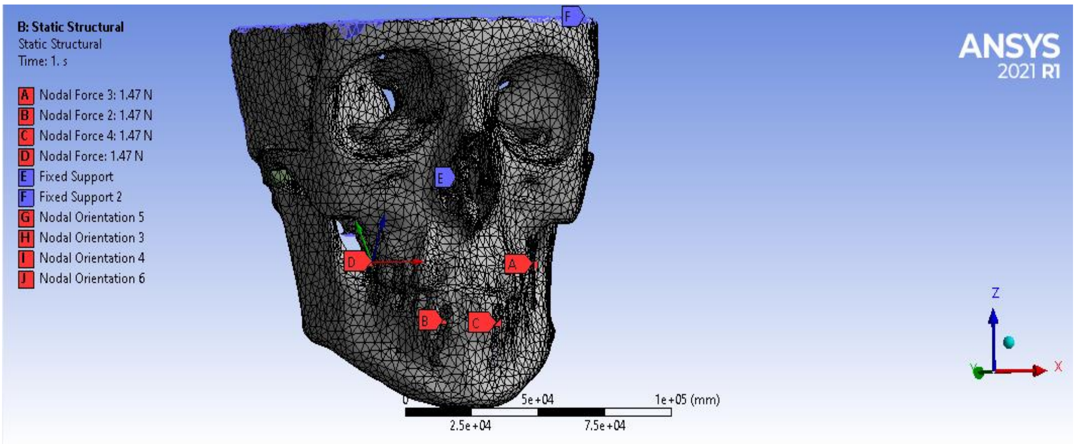


**Fig 26- Application of 150-gram intermaxillary Class III orthopedic force at selected nodes on the anchor plates at an angle of 30° to the occlusal plane**

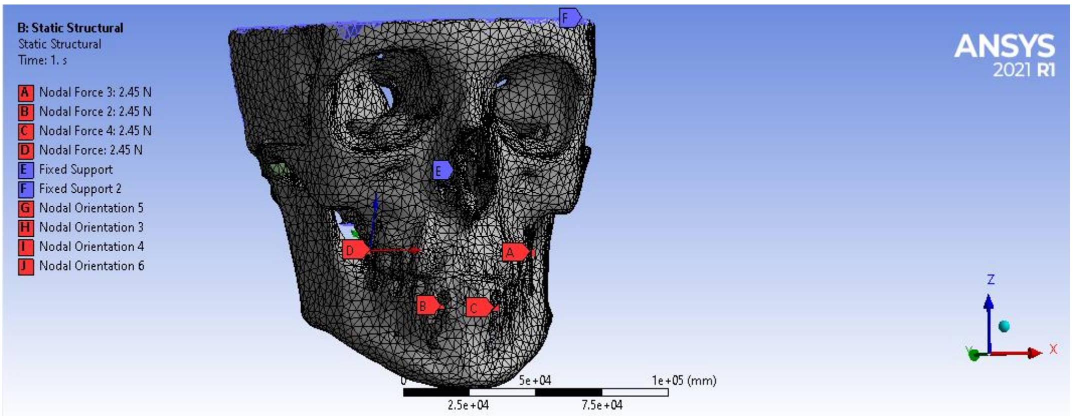


**Fig 27- Application of 250-gram intermaxillary Class III orthopedic force at selected nodes on the anchor plates at an angle of 10° to the occlusal plane**

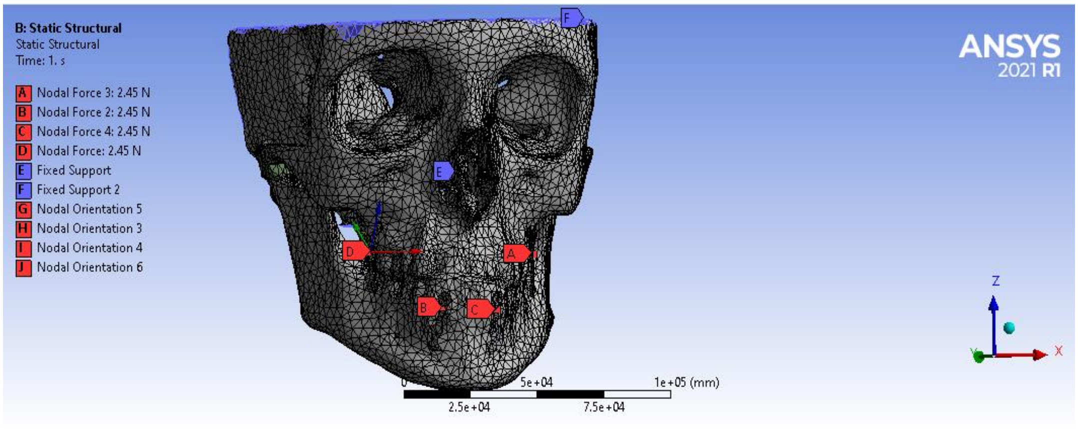


**Fig 28- Application of 250-gram intermaxillary Class III orthopedic force at selected nodes on the anchor plates at an angle of 20° to the occlusal plane**

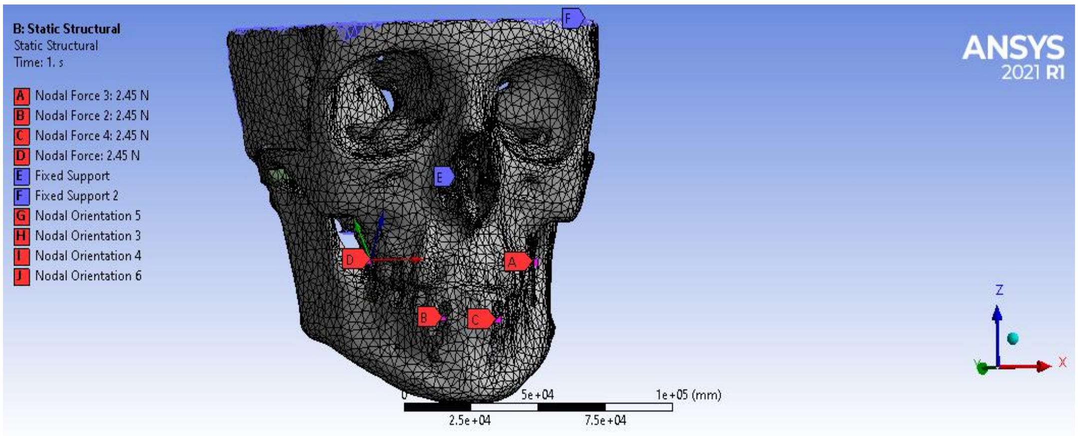


**Fig 29- Application of 250-gram intermaxillary Class III orthopedic force at selected nodes on the anchor plates at an angle of 30° to the occlusal plane**

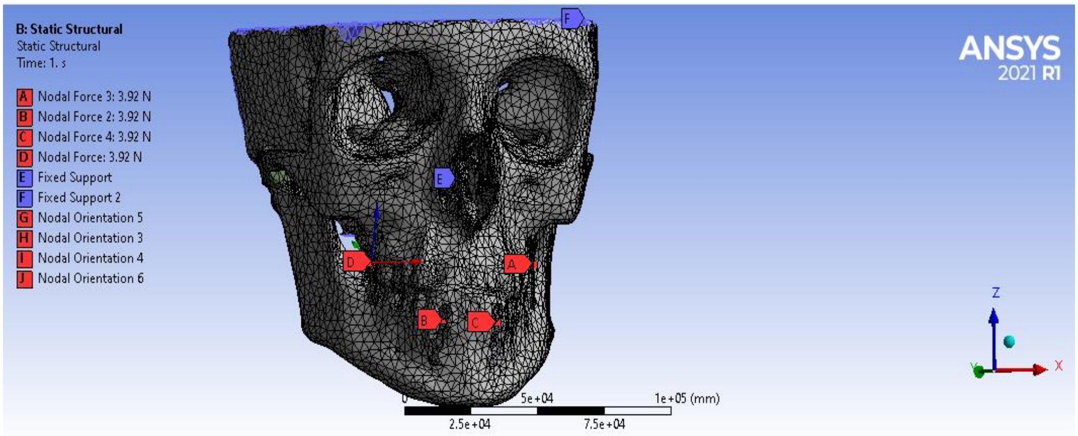


**Fig 30- Application of 400-gram intermaxillary Class III orthopedic force at selected nodes on the anchor plates at an angle of 10° to the occlusal plane**

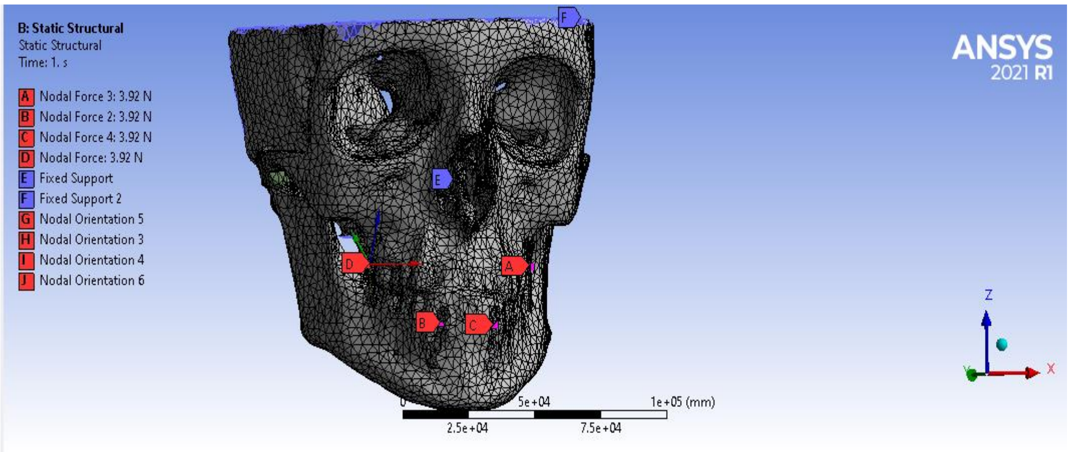


**Fig 31- Application of 400-gram intermaxillary Class III orthopedic force at selected nodes on the anchor plates at an angle of 20° to the occlusal plane**

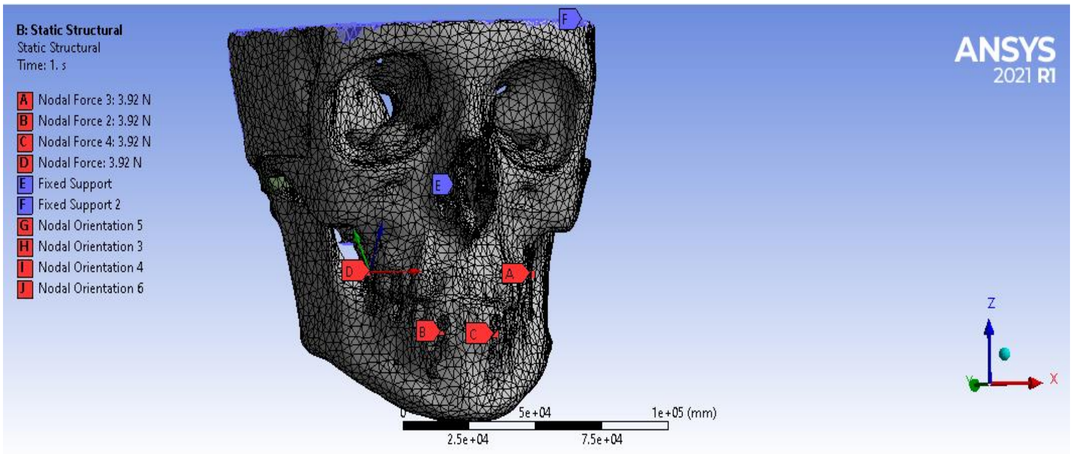


**Fig 32- Application of 400-gram intermaxillary Class III orthopedic force at selected nodes on the anchor plates at an angle of 30° to the occlusal plane**

## 3. POST-PROCESSING STAGE

Von Mises stress values on selected nodes and geometry; displacement of various nodes and surface landmarks in antero-posterior and vertical dimension, after application of 150gm, 250gm and 400 gm force sequentially at 10 degrees, 20 degree and 30 degrees angulation to the occlusal plane, were analysed and expressed in a graphical manner in all three planes of space. Utilizing the software, nodal and element solutions were plotted, areas of high stress concentration was detected. Stress and displacement values were exported in Microsoft excel for analysis.

## WORKFLOW

CT scan of skull and MRI of temporomandibular joint of a patient having skeletal Class III malocclusion (DICOM image format)

↓

DICOM images exported into MIMICS 21.0 software

↓

Segmentation of the cranio-maxillary structures from the CT scan data and segmentation of the right temporomandibular soft tissue structures from MRI data and generation of 3D surface STL model of skull and temporomandibular soft tissue structures

↓

Designing of anchor plate and screw (3D STL model) in SolidWorks 2021 SP2.0 software

↓

STL of skull, temporomandibular soft tissue structures, anchor plate and screws exported into 3-Matic 11.0 software, followed by adaptive remeshing of all the structures

↓

Assembling of TMJ soft tissues, anchor plates and screws into the skull STL

↓

Generation of 3D volumetric finite element model from assembled surface STL consisting 1,07,529 tetrahedral elements and 1,80,161 nodes

↓

Splitting the assembled model into three entities: - skull model, plate and screw model, temporomandibular soft tissue model

Splitting the assembled model into three entities: - skull model, plate and screw model, temporomandibular soft tissue model

↓

Exported into ANSYS 2021R1 software

↓

Assigning material properties and boundary conditions

↓

Application of 150,250 and 400 gm load at selected nodes on anchor plates at 10°, 20°, and 30° angulations to the occlusal plane

↓

Static structural analysis

↓

Interpretation of results

# RESULTS

Intermaxillary protraction forces of 150 gm, 250 gm, and 400 gm were applied bilaterally at selected nodes on the upper and lower anchor plates at an angle of 10°, 20°, and 30° to the occlusal plane and Von Mises stress values were calculated in circum-maxillary sutures, condylar head, articular disc and displacement of surface landmarks such as ANS, PNS, pogonion and condylion were recorded.

**Table 3. Maximum Von Mises stress values (MPa) in the circum-maxillary sutures on the application of 150 gm protraction force at an angle of 10°, 20°, and 30° to the occlusal plane.**

| Circum-maxillary sutures | Maximum Von Mises stress values (MPa) | | |
|---|---|---|---|
| | **10° angle** | **20° angle** | **30° angle** |
| 1. Pterygomaxillary | 3.15E-04 | 3.11E-04 | 3.07E-04 |
| 2. Zygomaticotemporal | 8.08E-04 | 7.99E-04 | 7.90E-04 |
| 3. Zygomaticomaxillary | 5.04E-04 | 5.02E-04 | 4.92E-04 |
| 4. Zygomaticofrontal | 4.50E-04 | 4.31E-04 | 4.10E-04 |
| 5. Frontomaxillary | 7.52E-05 | 7.27E-05 | 6.82E-05 |
| 6. Frontonasal | 5.78E-05 | 5.04E-05 | 4.52E-05 |
| 7. Midpalatal | 1.92E-04 | 1.75E-04 | 1.55E-04 |
| 8. Nasomaxillary | 1.14E-04 | 8.29E-05 | 5.44E-05 |
| 9. Internasal | 9.21E-05 | 7.80E-05 | 6.98E-05 |

Maximum Von Mises stress values (MPa) were measured along the corresponding nodes of right-sided circum-maxillary and midline sutures. On application of 150 gm forces, the highest amount of Von Mises stress was observed in zygomaticotemporal followed by zygomaticomaxillary, zygomaticofrontal, pterygomaxillary, midpalatal, nasomaxillary, internasal, frontomaxillary and frontonasal sutures in descending order. As the angulation of force increased from 10° to 30°, Von Mises stress value decreased in all the sutures (Table 3, Figure 33). Overall stress nephrogram also observed after application of force (Figure 34 to 36)

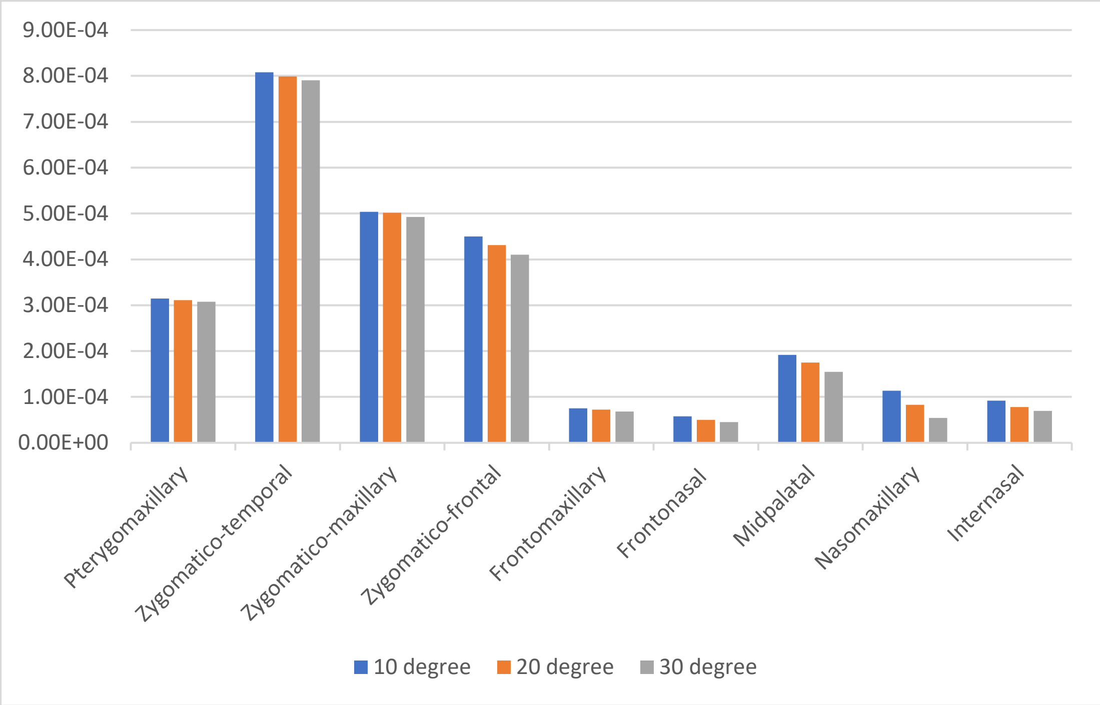


**Figure 33- Plot of comparison of maximum Von Mises stress values (MPa) at circum-maxillary sutures after application of 150 gm of Class III protraction force at different angulations to the occlusal plane.**

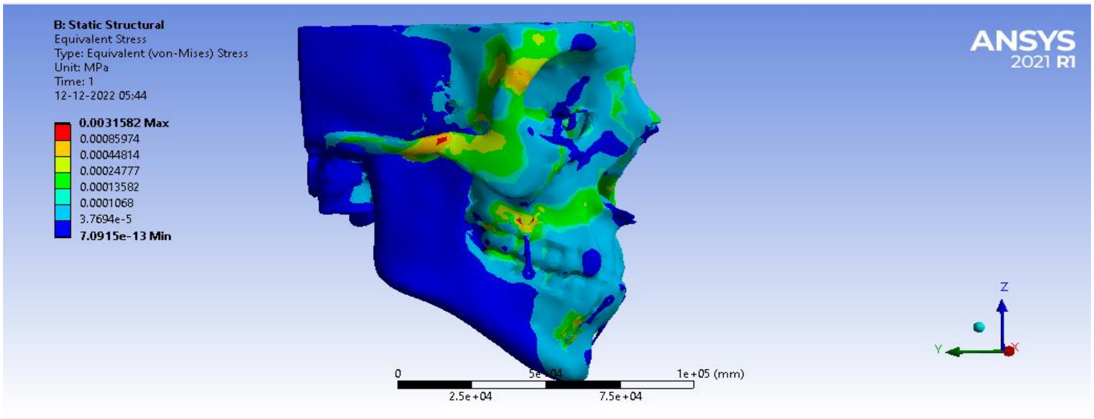


**Figure 34- Von Mises stress distribution after application of 150 gm of force at an angle of 10 °to the occlusal plane**

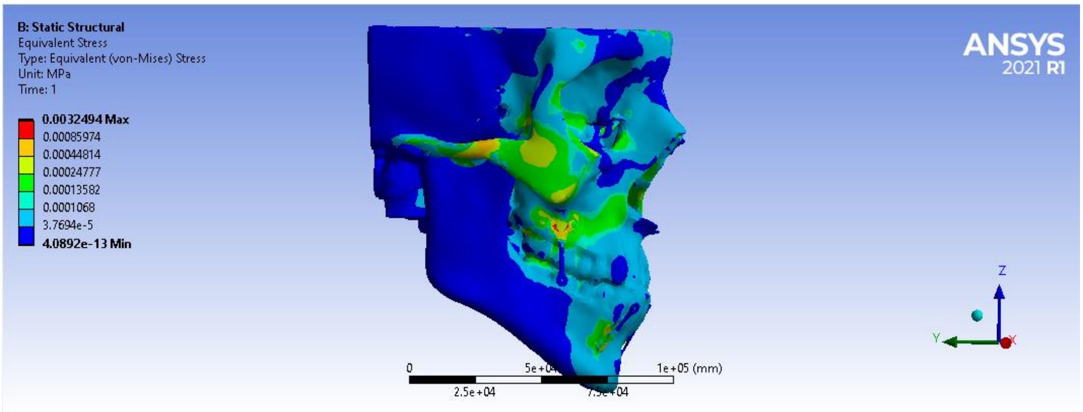


**Figure 35- Von Mises stress distribution after application of 150 gm of force at an angle of 20 °to the occlusal plane**

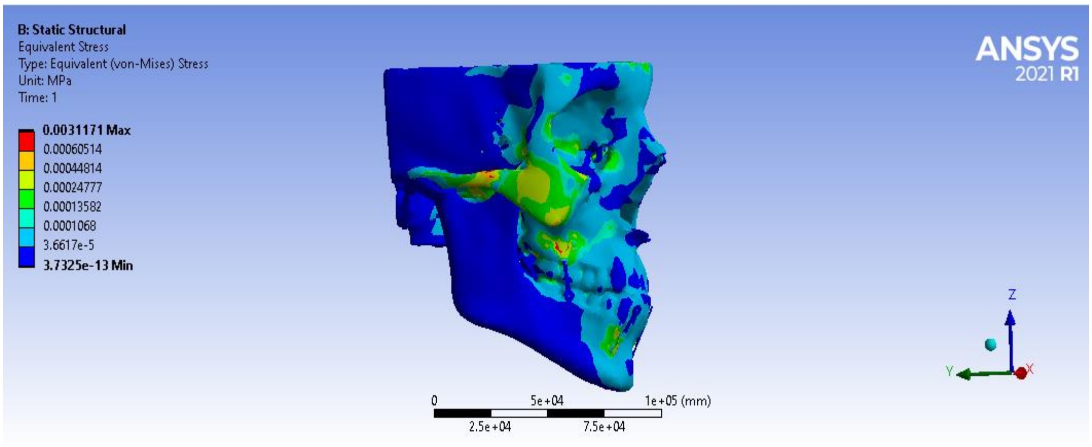


**Figure 36- Von Mises stress distribution after application of 150 gm of force at an angle of 30 °to the occlusal plane**

**Table 4. Maximum Von Mises stress values (MPa) in the circum-maxillary sutures on the application of 250 gm protraction force at an angle of 10˚, 20°, and 30° to the occlusal plane.**

| Circum-maxillary sutures | Maximum Von Mises stress values (MPa) | | |
|---|---|---|---|
| | **10° angle** | **20° angle** | **30° angle** |
| 1. Pterygomaxillary | 3.32E-04 | 3.25E-04 | 3.17E-04 |
| 2. Zygomaticotemporal | 8.21E-04 | 8.06E-04 | 7.91E-04 |
| 3. Zygomaticomaxillary | 5.11E-04 | 5.07E-04 | 5.03E-04 |
| 4. Zygomaticofrontal | 5.16E-04 | 4.84E-04 | 4.49E-04 |
| 5. Frontomaxillary | 8.17E-05 | 7.42E-05 | 7.31E-05 |
| 6. Frontonasal | 8.62E-05 | 5.20E-05 | 4.87E-05 |
| 7. Midpalatal | 2.80E-04 | 2.52E-04 | 2.18E-04 |
| 8. Nasomaxillary | 2.04E-04 | 1.48E-04 | 8.90E-05 |
| 9. Internasal | 1.38E-04 | 1.08E-04 | 8.03E-05 |

On application of forces of 250 grams on each side, Von Mises stress values increased in all the circum-maxillary sutures. At an angle of 10° to the occlusal plane, the highest amount of Von Mises stress was found in the zygomaticotemporal suture followed by zygomaticofrontal, zygomaticomaxillary, pterygomaxillary, midpalatal, nasomaxillary, internasal, frontonasal, frontomaxillary sutures. As the angulation of force increased from 10° to 30°, Von Mises stress value decreased in all sutures (Table 4, Figure 37). Overall stress nephrogram was also observed after the application of force (Figure 38 to 40)

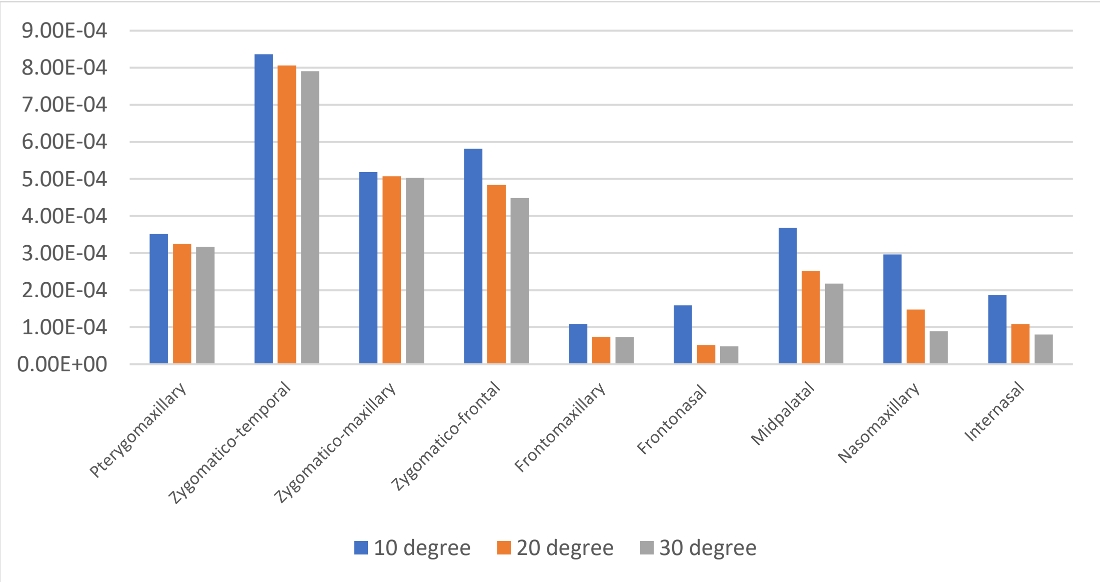


**Figure 37- Plot of comparison of maximum Von Mises stress values (MPa) at circum-maxillary sutures after application of 250 gm of Class III protraction force at different angulations to the occlusal plane.**

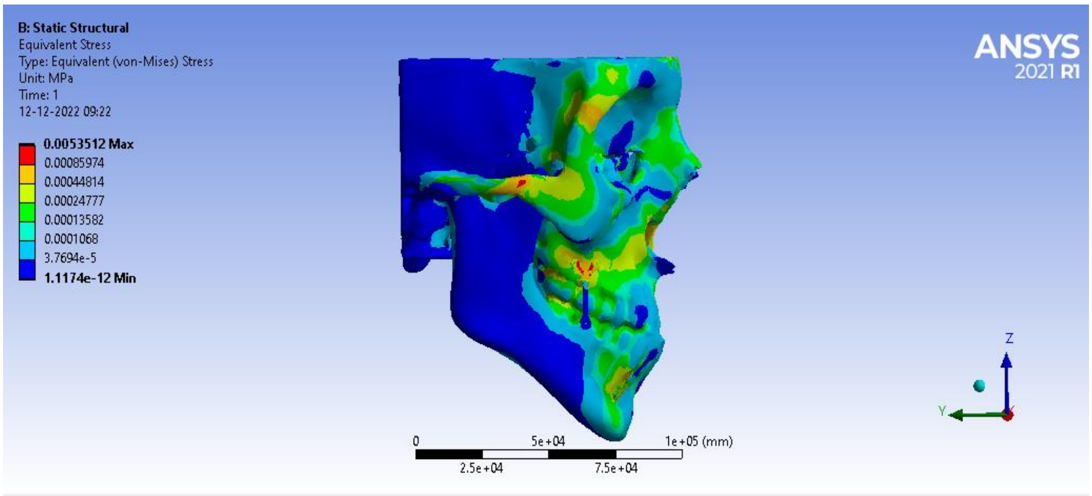


**Figure 38- Von Mises stress distribution after application of 250 gm of force at an angle of 10 °to the occlusal plane**

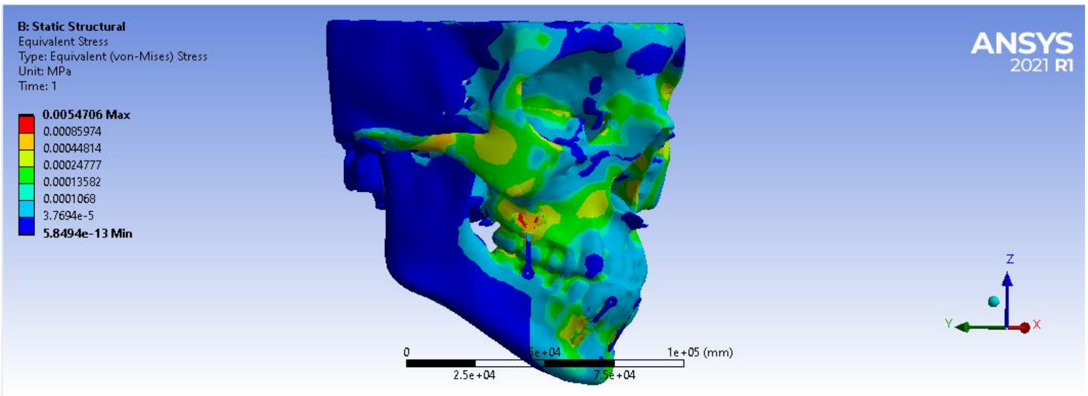


**Figure 39- Von Mises stress distribution after application of 250 gm of force at an angle of 20 °to the occlusal plane**

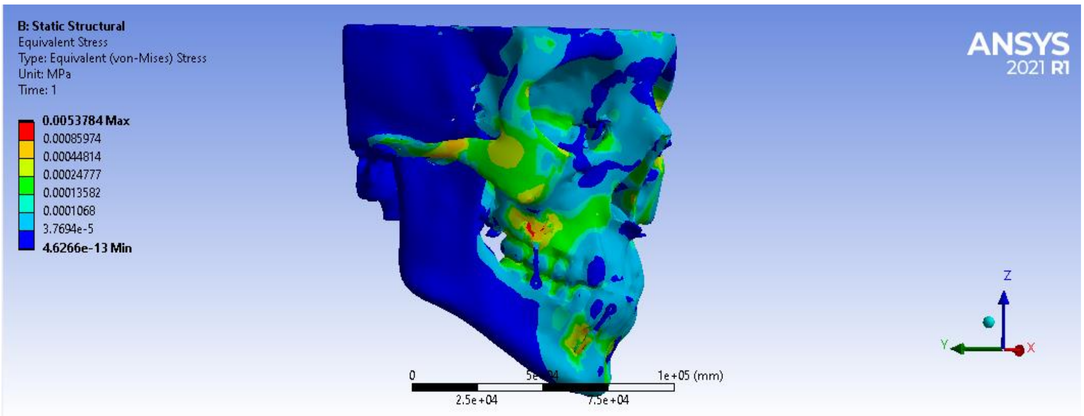


**Figure 40- Von Mises stress distribution after application of 250 gm of force at an angle of 30 °to the occlusal plane**

**Table 5. Maximum Von Mises stress values (MPa) in the circum-maxillary sutures on the application of 400 gm protraction force at an angle of 10°, 20°, and 30° to the occlusal plane.**

| Circum-maxillary sutures | Maximum Von Mises stress values (MPa) | | |
|---|---|---|---|
| | **10° angle** | **20° angle** | **30° angle** |
| 1. Pterygomaxillary | 3.52E-04 | 3.41E-04 | 3.29E-04 |
| 2. Zygomaticotemporal | 8.36E-04 | 8.14E-04 | 7.92E-04 |
| 3. Zygomaticomaxillary | 5.19E-04 | 5.13E-04 | 5.07E-04 |
| 4. Zygomaticofrontal | 5.82E-04 | 5.38E-04 | 4.88E-04 |
| 5. Frontomaxillary | 1.09E-04 | 8.32E-05 | 7.32E-05 |
| 6. Frontonasal | 1.59E-04 | 1.02E-04 | 4.94E-05 |
| 7. Midpalatal | 3.68E-04 | 3.29E-04 | 2.82E-04 |
| 8. Nasomaxillary | 2.96E-04 | 2.17E-04 | 1.31E-04 |
| 9. Internasal | 1.87E-04 | 1.44E-04 | 9.83E-05 |

On application of forces of 400 gm, maximum Von Mises stress values also increased for all the circum-maxillary sutures. At 10° angulation of the applied force, the highest amount of stress was found in the zygomaticotemporal suture followed by zygomaticofrontal, zygomaticomaxillary, midpalatal, pterygomaxillary, nasomaxillary, internasal, frontonasal and fronto maxillary sutures. As the angulation of force increased from 10° to 30°, the Von Mises stress value decreased in all the sutures. With the increase in the amount of Class III protraction force, maximum Von Mises stress values were increased in all the circum-maxillary sutures. With an increase in the angulation of the force, maximum Von Mises stress values were reduced in all the circum-maxillary sutures irrespective of the amount of force application (Table 6, Figure 41). Overall stress nephrogram was also observed after the application of force (Figure 42 to 44).

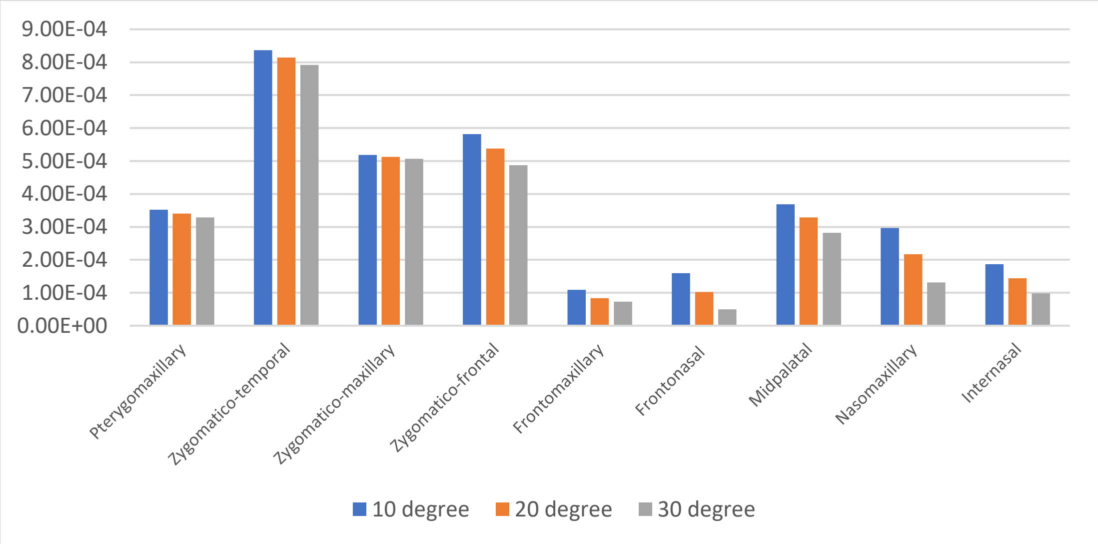


**Figure 41. The plot of comparison of maximum Von Mises stress values (MPa) at circum-maxillary sutures after application of 400 gm of Class III protraction force at different angulations to the occlusal plane.**

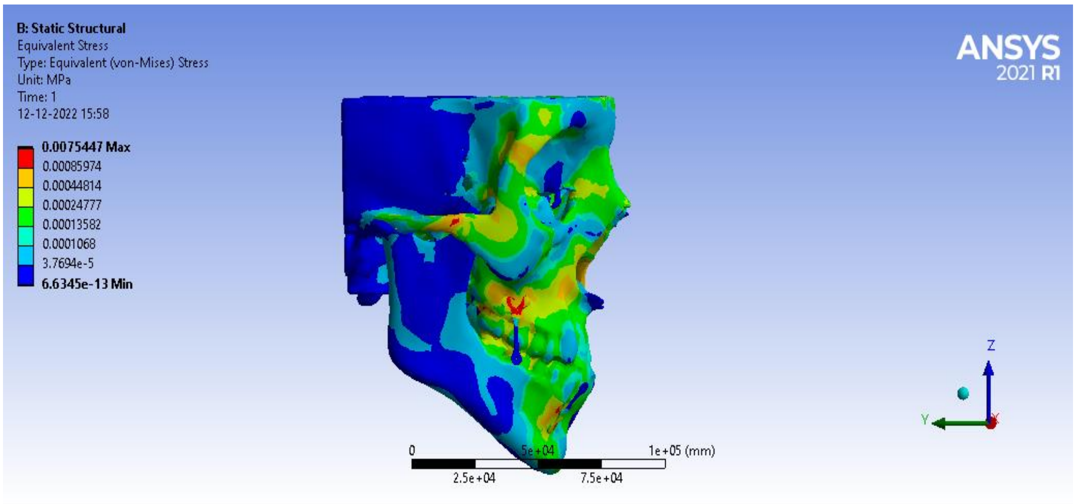


**Figure 42- Von Mises stress distribution after application of 400 gm of force at an angle of 10 °to the occlusal plane**

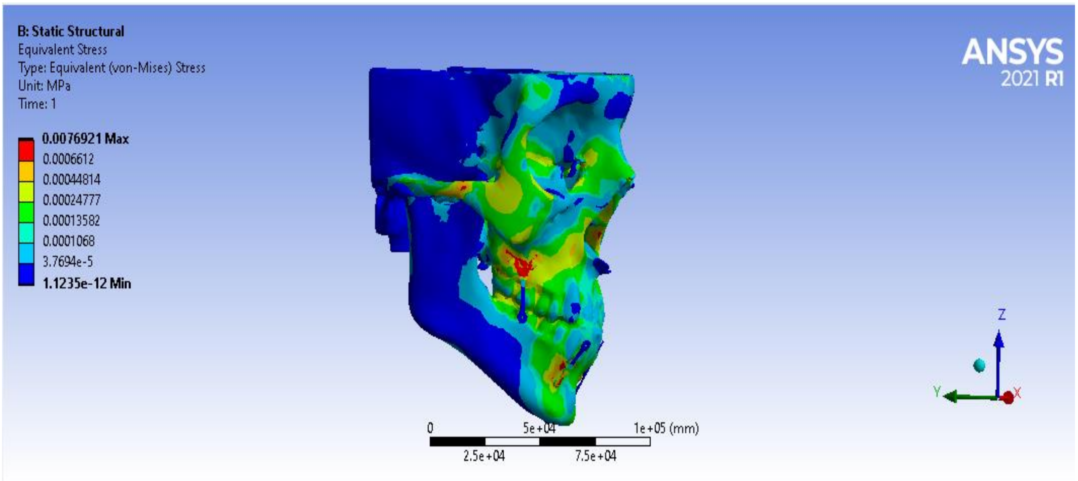


**Figure 43- Von Mises stress distribution after application of 400 gm of force at an angle of 20 °to the occlusal plane**

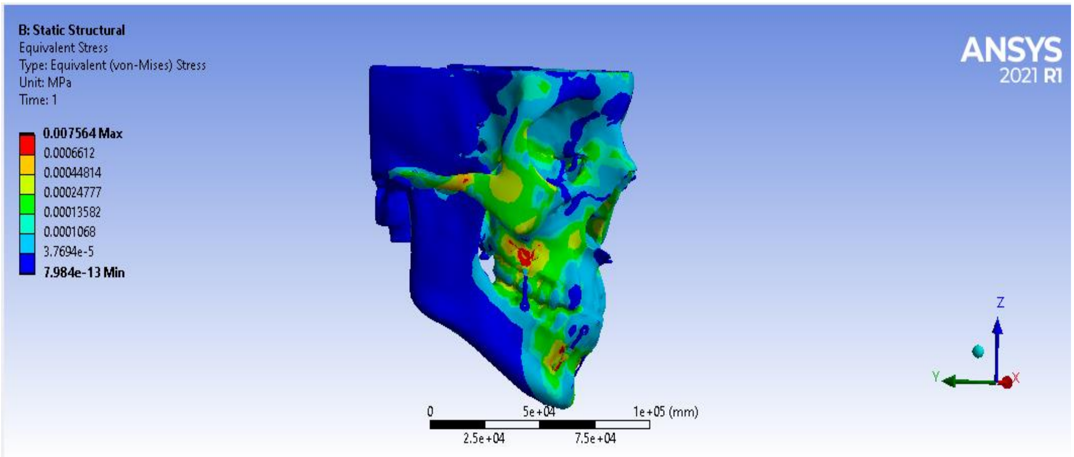


**Figure 44- Von Mises stress distribution after application of 400 gm of force at an angle of 30 °to the occlusal plane**

**Table 6. Maximum Von Mises stress values (MPa) in the right condylar head on the application of 150 gm, 250 gm, and 400 gm protraction force at an angle of 10°, 20°, and 30° to the occlusal plane.**

| Amount of Class III intermaxillary force | Maximum Von Mises stress values (MPa) | | |
|---|---|---|---|
| | 10° angle | 20° angle | 30° angle |
| **150 gm** | 5.47E-06 | 4.28E-06 | 2.97E-06 |
| **250 gm** | 9.11E-06 | 7.14E-06 | 4.95E-06 |
| **400 gm** | 1.46E-05 | 1.14E-05 | 7.92E-06 |

Maximum Von Mises stress values (MPa) were recorded along the corresponding nodes of the right-sided condylar head. Von mises stress values increased with the increase in force values from 150 to 400 gm at all angulations. However, at each force value, as the angulation increased from 10° to 30°, a decrease in Von Mises stress was observed (Table 6, Figure 45).

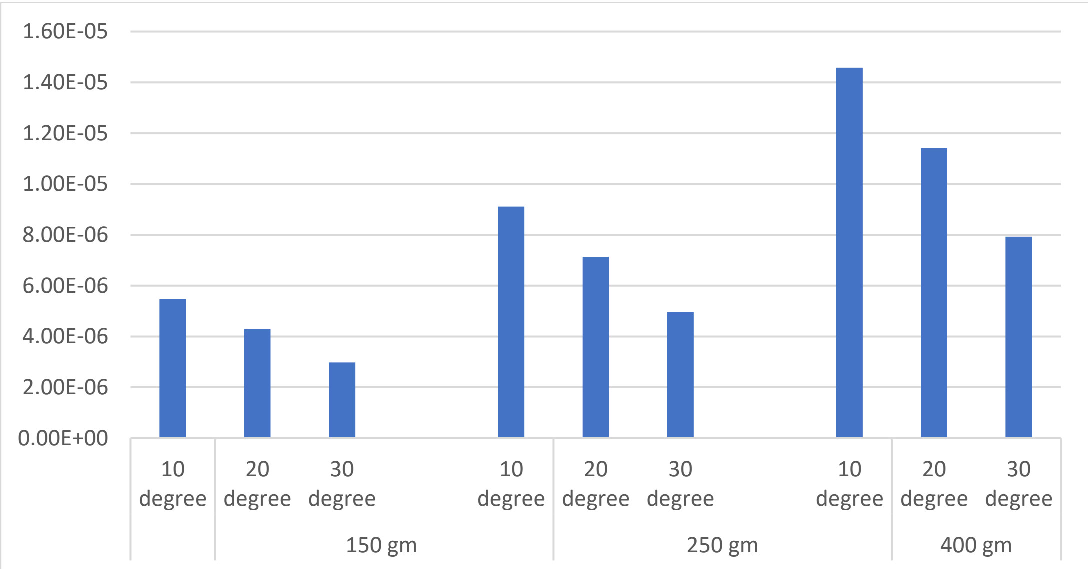


**Figure 45. The plot of comparison of maximum Von Mises stress values (MPa)at the right condylar head after application of 150, 200, and 400 grams of Class III protraction force at different angulations to the occlusal plane.**

**Table 7. Maximum Von Mises stress values (MPa) in the articular disc on the application of 150 gm, 250 gm, and 400 gm protraction force at an angle of 10°, 20°, and 30° to the occlusal plane.**

| Amount of Class III intermaxillary force | Maximum Von Mises stress values (MPa) | | |
|---|---|---|---|
| | 10° angle | 20° angle | 30° angle |
| **150 gm** | 6.02E-07 | 4.75E-07 | 3.35E-07 |
| **250 gm** | 1.00E-06 | 7.92E-07 | 5.58E-07 |
| **400 gm** | 1.61E-06 | 1.27E-06 | 8.93E-07 |

Maximum Von Mises stress values were recorded along the corresponding nodes of the articular disc of the right-sided temporomandibular joint. After application of 150 gm, 250 gm, and 400 gm Class III intermaxillary force at an angulation of 10°, 20°, and 30° to the occlusal plane, the highest amount of maximum Von Mises stress was observed at the lateral border of the articular disc for all the combinations of force. The amount of Von Mises stress increased with a sequential increase in the amount of applied force. With the increase in the angulation of Class III force relative to the occlusal plane, Von Mises stress values decreased in a regular pattern. The highest amount of Von Mises stress was found when 400 gm force was applied at 10° to the occlusal plane. The lowest value of Von Mises stress was observed during 150gm force application at an angle of 30° to the occlusal plane (Table 7, Figures 46 to 55).

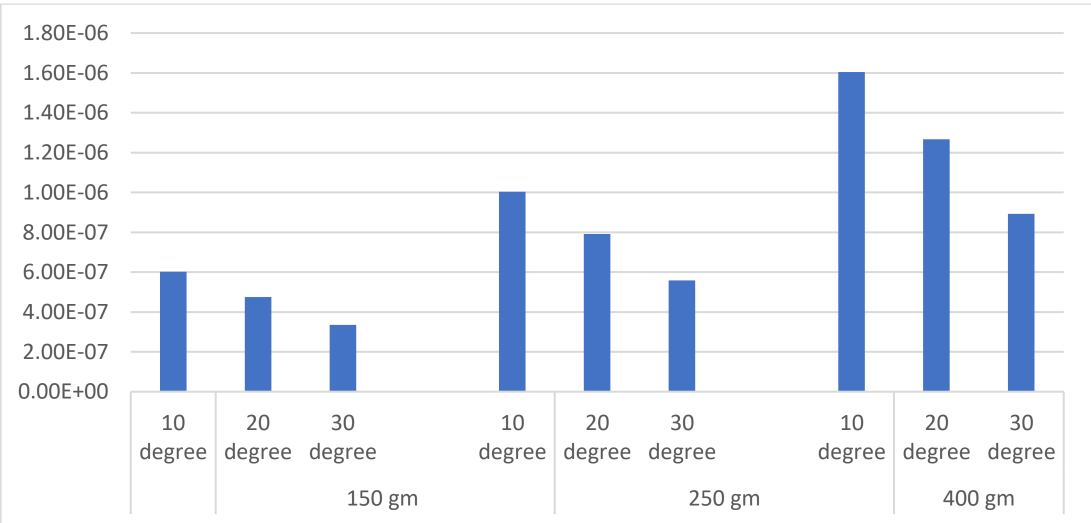


**Figure 46. The plot of comparison of maximum Von Mises stress values (MPa) at the articular disc of the right temporomandibular joint after application of 150, 200, and 400 grams of Class III protraction force at different angulations to the occlusal plane.**

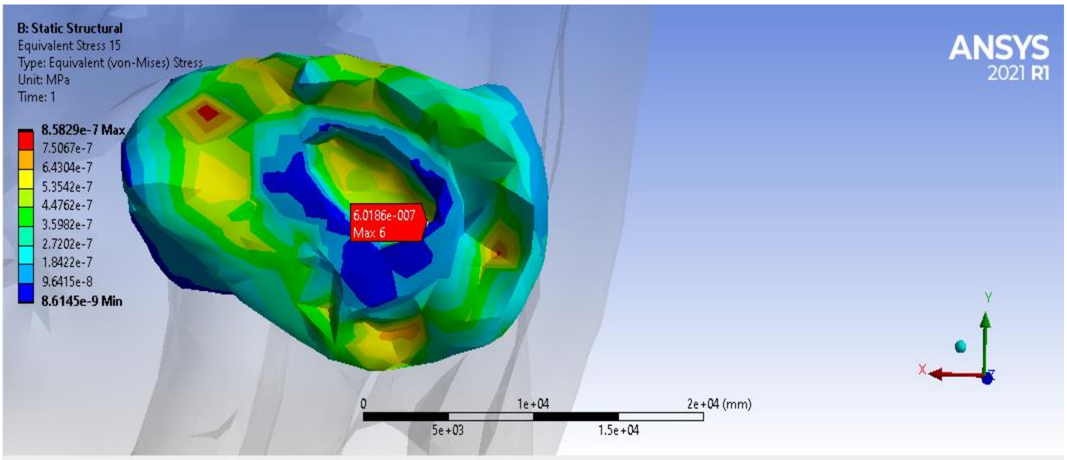


**Figure 47- Von Mises stress distribution at articular disc after application of 150 gm of force at an angle of 10 °to the occlusal plane**

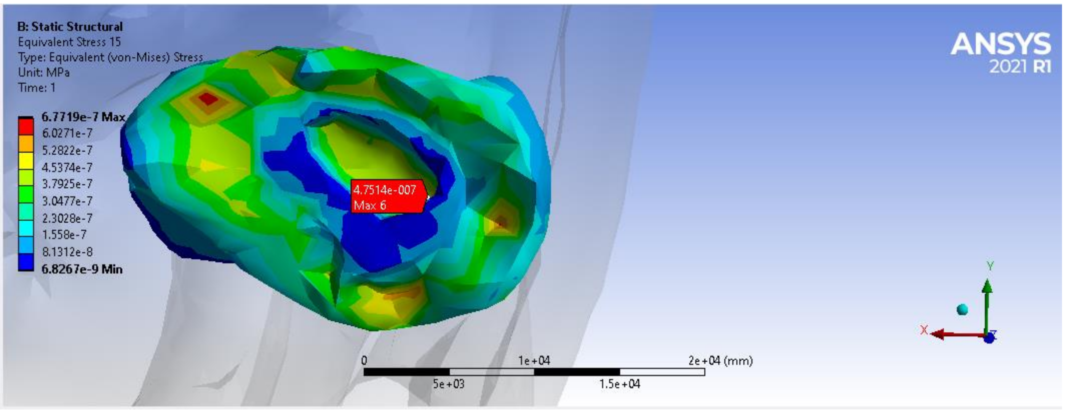


**Figure 48- Von Mises stress distribution at articular disc after application of 150 gm of force at an angle of 20 °to the occlusal plane**

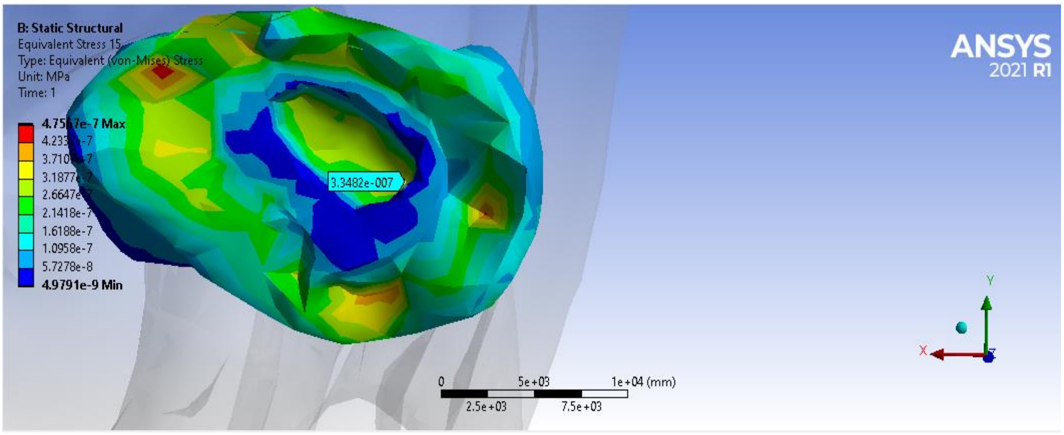


**Figure 49- Von Mises stress distribution at articular disc after application of 150 gm of force at an angle of 30 °to the occlusal plane**

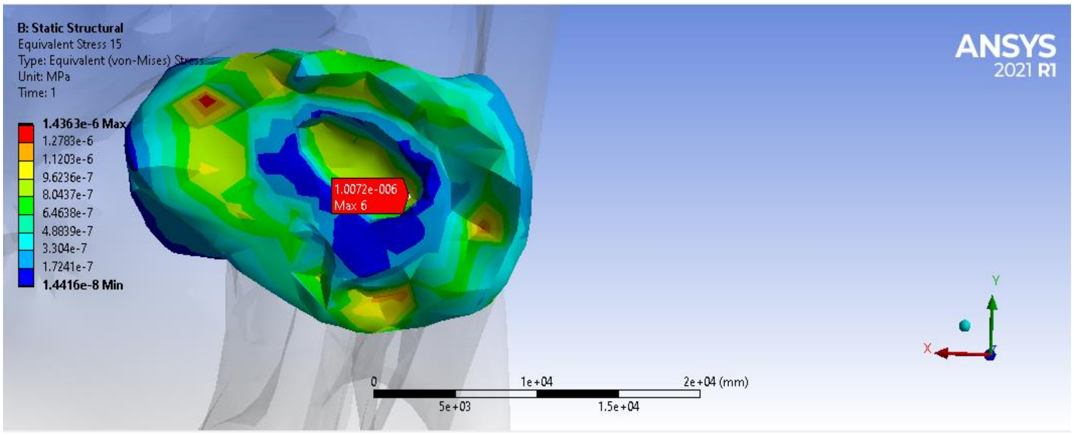


**Figure 50- Von Mises stress distribution at articular disc after application of 250 gm of force at an angle of 10 °to the occlusal plane**

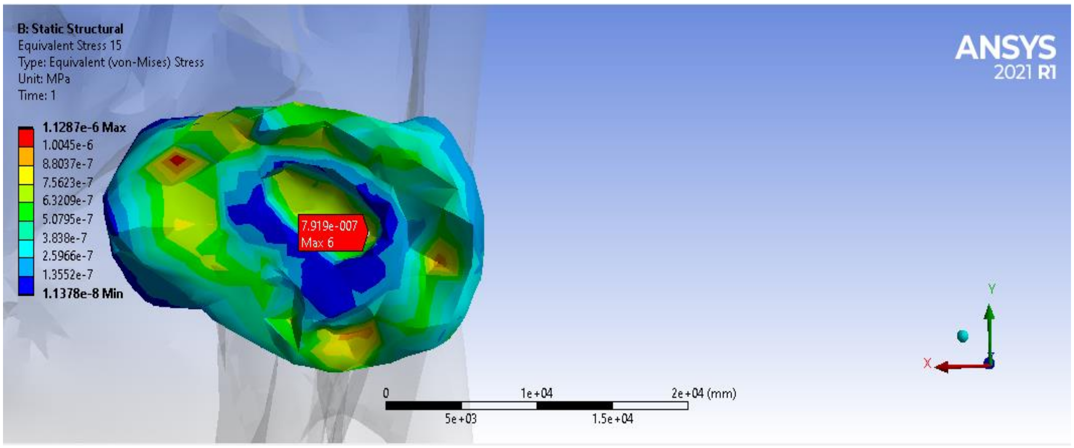


**Figure 51- Von Mises stress distribution at articular disc after application of 250 gm of force at an angle of 20 °to the occlusal plane**

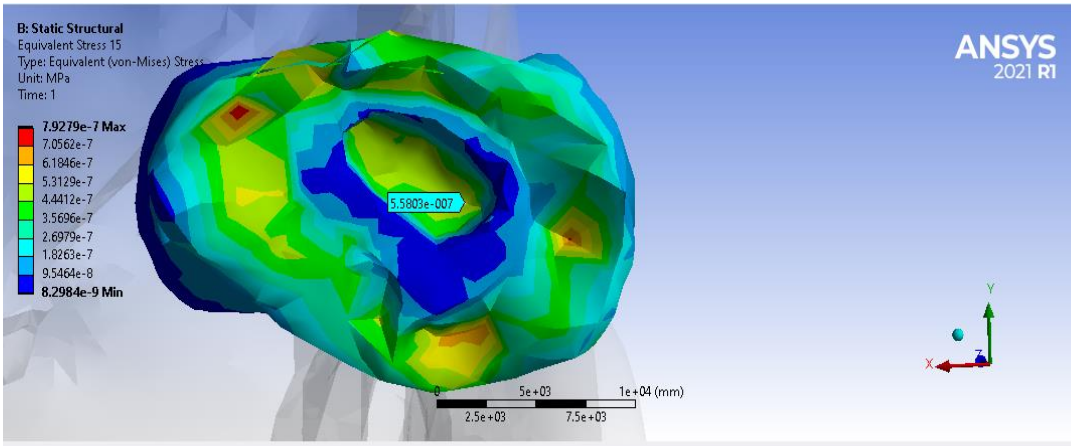


**Figure 52- Von Mises stress distribution at articular disc after application of 250 gm of force at an angle of 30 °to the occlusal plane**

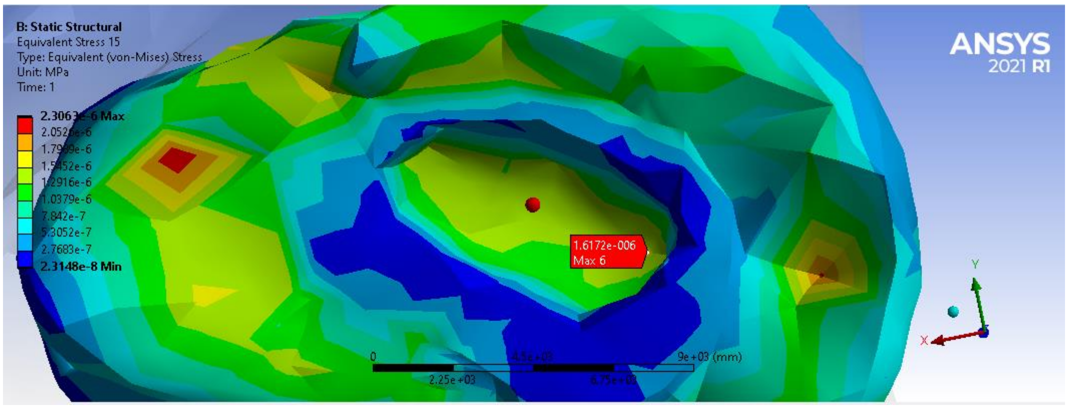


**Figure 53- Von Mises stress distribution at articular disc after application of 400 gm of force at an angle of 10 °to the occlusal plane**

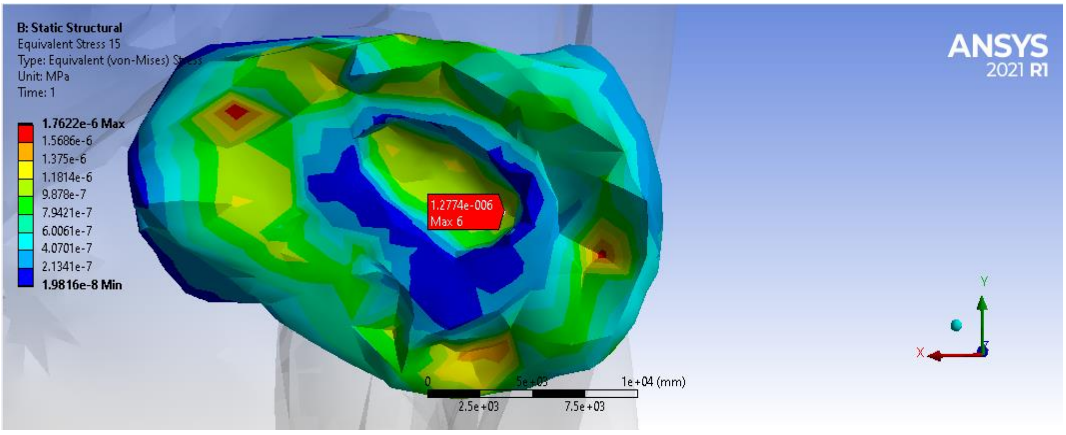


**Figure 54- Von Mises stress distribution at articular disc after application of 400 gm of force at an angle of 20 °to the occlusal plane**

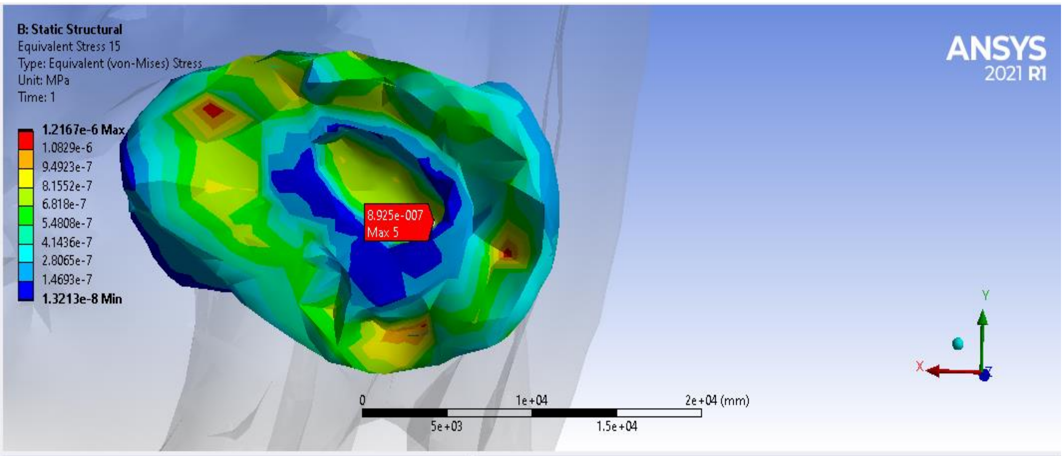


**Figure 55- Von Mises stress distribution at articular disc after application of 400 gm of force at an angle of 30 °to the occlusal plane**

**Table 8. Comparison of displacement (mm) of ANS, PNS, pogonion, and condylion in anteroposterior (Y) and vertical (Z) dimensions after application of 150 gm force at various angulations to the occlusal plane**

| Landmarks | Dimension | 10-degree | 20-degree | 30-degree |
|---|---|---|---|---|
| ANS | Y (mm) | -7.24E-05 | -5.81E-05 | -4.21E-05 |
| | Z (mm) | -1.78E-04 | -1.32E-04 | -8.23E-05 |
| PNS | Y (mm) | -5.89E-05 | -4.74E-05 | -3.44E-05 |
| | Z (mm) | -8.74E-05 | -7.48E-05 | -5.98E-05 |
| Pogonion | Y(mm) | 4.15E-04 | 3.22E-04 | 2.19E-04 |
| | Z (mm) | -1.59E-04 | -1.11E-04 | -5.99E-05 |
| Condylion | Y (mm) | -1.43E-05 | -5.73E-06 | 3.05E-06 |
| | Z (mm) | 2.81E-04 | 2.21E-04 | 1.55E-04 |

Y- anteroposterior displacement; Z- vertical displacement
- forward - downward
+ backward + upward

ANS showed forward and downward displacement. With an increase in angulation of applied force, forward and downward displacement of ANS was reduced sequentially.

PNS also showed forward and downward displacement, but the amount of displacement was less as compared to ANS.

Pogonion point showed backward and downward displacement. The amount of displacement was reduced with an increase in the angle of the force application.

Condylion showed forward and upward movement at 10° and 20° of angulation. But when angulation of force was increased to 30° to the occlusal plane, condylion showed backward and upward displacement. The amount of upward displacement also reduced with an increase in angulation of force application. The highest amount of displacement in the anteroposterior dimension was found at the pogonion point irrespective of angulation of applied force. Condylion showed the highest amount of vertical displacement irrespective of angulations of applied force (Table 8). Deformation of various surface structures was also observed in the displacement nephrogram after the application of 150 gm of force (Figure 56 to 58).

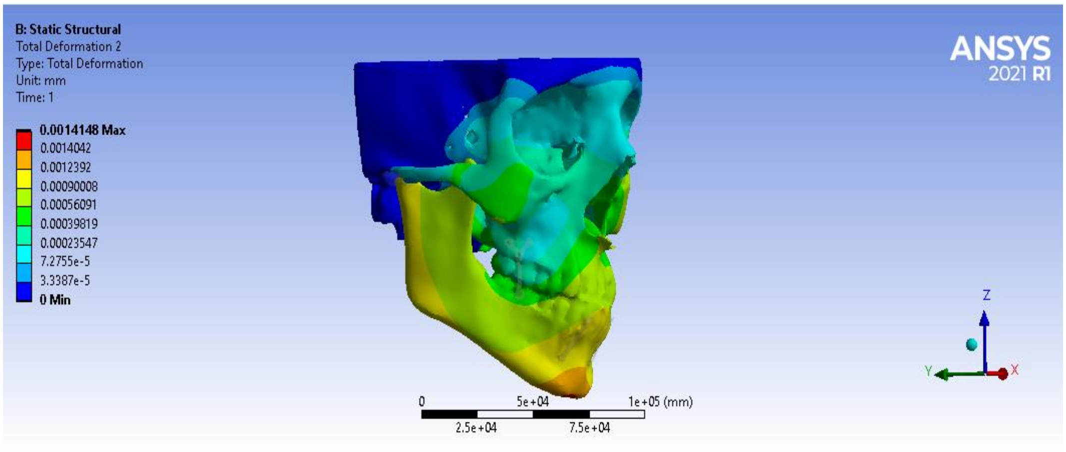


**Fig 56- Pattern of displacement of various surface structures after application of 150 gm of force at 10° to the occlusal plane**

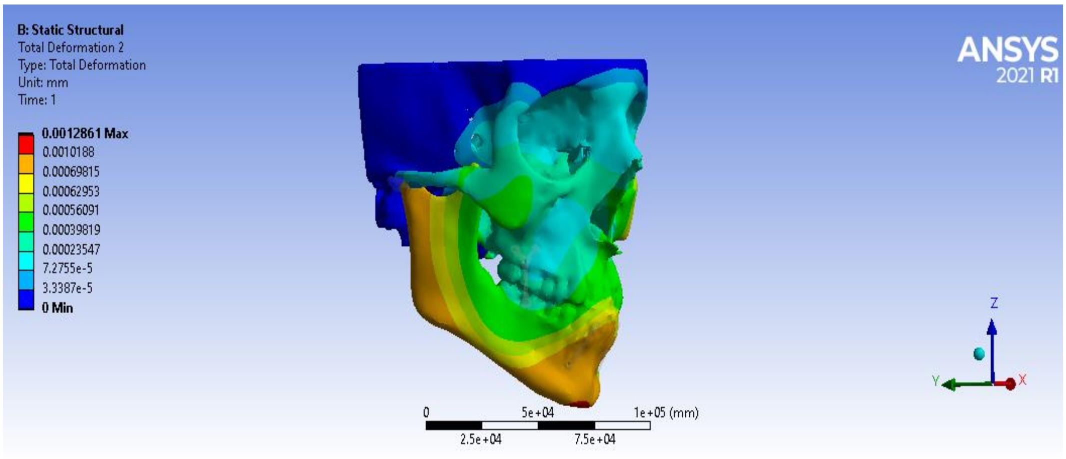


**Fig 57- Pattern of displacement of various surface structures after application of 150 gm of force at 20° to the occlusal plane**

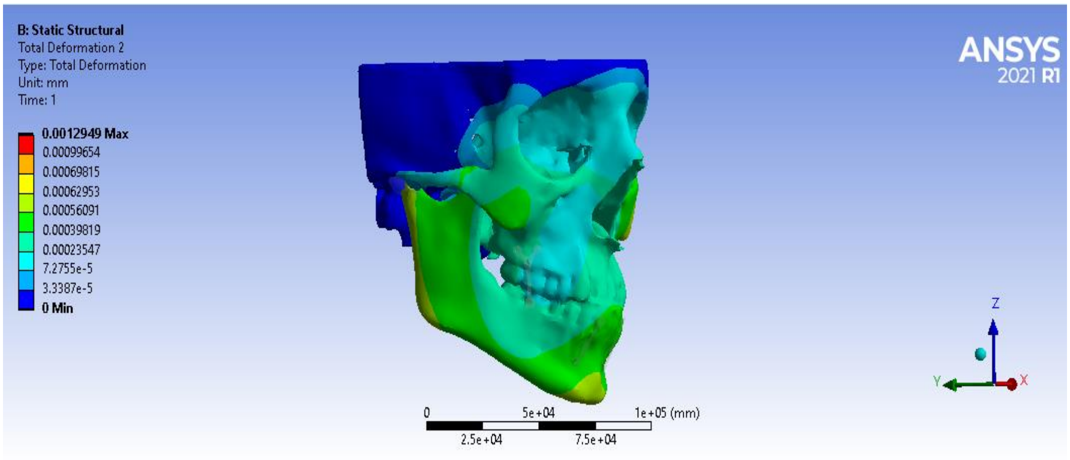


**Fig 58- Pattern of displacement of various surface structures after application of 150 gm of force at 30° to the occlusal plane**

**Table 9. Comparison of displacement (mm) of ANS, PNS, pogonion, and condylion in anteroposterior (Y) and vertical (Z) dimensions after application of 250 gm force at various angulations to the occlusal plane**

| Landmarks | Dimension | 10-degree | 20-degree | 30-degree |
|---|---|---|---|---|
| ANS | Y (mm) | -1.21E-04 | -9.69E-05 | -7.01E-05 |
| | Z (mm) | -2.96E-04 | -2.20E-04 | -1.37E-04 |
| PNS | Y (mm) | -9.82E-05 | -7.90E-05 | -5.73E-05 |
| | Z (mm) | -1.46E-04 | -1.25E-04 | -9.97E-05 |
| Pogonion | Y (mm) | 6.92E-04 | 5.36E-04 | 3.65E-04 |
| | Z (mm) | -2.65E-04 | -1.85E-04 | -9.98E-05 |
| Condylion | Y (mm) | -2.39E-05 | -9.54E-06 | 5.08E-06 |
| | Z (mm) | 4.68E-04 | 3.69E-04 | 2.59E-04 |

Y- anteroposterior displacement; Z- vertical displacement
- forward - downward
+ backward + upward

When 250 gm of force was applied, ANS showed forward and downward displacement. With the increase in angulation of applied force, the amount of forward and downward displacement was reduced gradually.

PNS showed forward and downward displacement, however, the amount of displacement is quantitatively less than in ANS.

Pogonion point showed backward and downward displacement and the amount of displacement was reduced with the increase in the angle of force application both anteroposteriorly and vertically.

Condylion showed forward and upward movement at 10° and 20° of angulation. But when angulation was increased to 30°, condylion showed backward and upward displacement. The amount of upward displacement also reduced with the increase in angulation.

The highest amount of anteroposterior and vertical displacement was shown by pogonion and condylion respectively at all the angulations (Table 9). Deformation of various surface structures was also observed in the displacement nephrogram after the application of 250 gm of force (Figure 59 to 61).

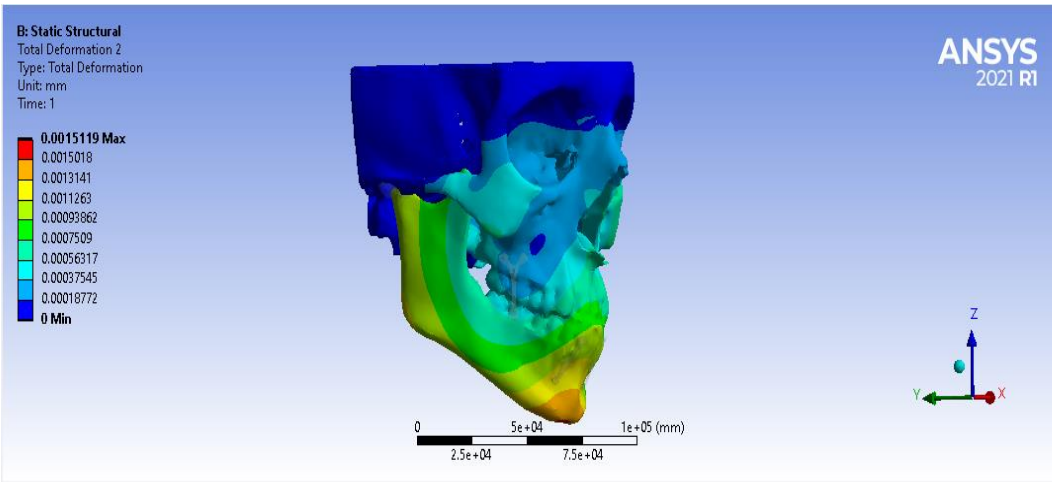


**Fig 59- Pattern of displacement (mm) of various surface structures after application of 250 gm of force at 10° to the occlusal plane**

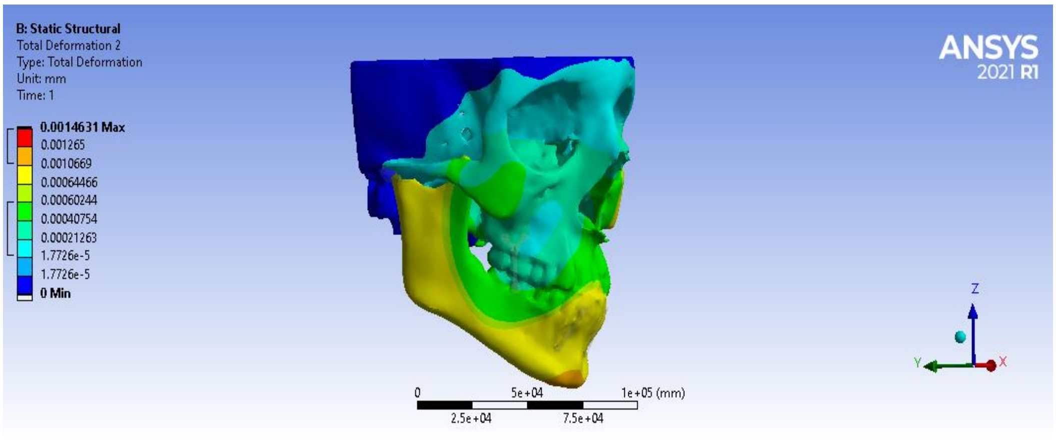


**Fig 60- Pattern of displacement (mm) of various surface structures after application of 250 gm of force at 20° to the occlusal plane**

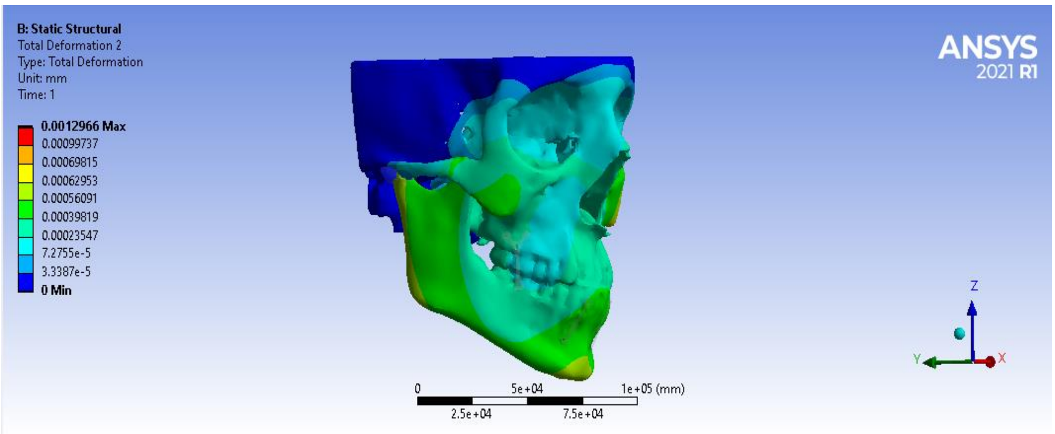


**Fig 61- Pattern of displacement (mm) of various surface structures after application of 250 gm of force at 30° to the occlusal plane**

**Table 10. Comparison of displacement (mm) of ANS, PNS, pogonion, and condylion in anteroposterior (Y) and vertical (Z) dimensions after application of 400 gm force at various angulations to the occlusal plane.**

| Landmarks | Dimension | 10-degree | 20-degree | 30-degree |
|---|---|---|---|---|
| ANS | Y (mm) | -1.93E-04 | -1.55E-04 | -1.12E-04 |
| | Z (mm) | -4.74E-04 | -3.52E-04 | -2.20E-04 |
| PNS | Y (mm) | -1.57E-04 | -1.26E-04 | -9.16E-05 |
| | Z (mm) | -2.33E-04 | -1.99E-04 | -1.60E-04 |
| Pogonion | Y (mm) | 1.11E-03 | 8.58E-04 | 5.84E-04 |
| | Z (mm) | -4.24E-04 | -2.96E-04 | -1.60E-04 |
| Condylion | Y (mm) | -3.82E-05 | -1.53E-05 | 8.13E-06 |
| | Z (mm) | 7.49E-04 | 5.90E-04 | 4.14E-04 |

Y- anteroposterior displacement, Z- vertical displacement
- forward - downward
+backward + upward

When 400 gm of force was applied, ANS showed forward and downward displacement. With the increase in angulation of applied force, a gradual reduction in the amount of displacement of ANS was observed both anteroposteriorly and vertically.

PNS showed forward and downward displacement, however, the amount of displacement is quantitatively less than at ANS.

Pogonion point showed backward and downward displacement and the amount of displacement was reduced with an increase the in the angle of force application both anteroposteriorly and vertically.

Condylion showed forward and upward movement at 10 and 20 degrees of angulation. But when angulation was increased to 30°, condylion showed backward and upward displacement. The amount of upward displacement also reduced with an increase in angulation. The highest amount of anteroposterior and vertical displacement was shown by pogonion and condylion respectively, irrespective of the angle of Class III force application (Table 10). Deformation of various surface structures was also observed in the displacement nephrogram after the application of 400 gm of force (Figure 62 to 64).

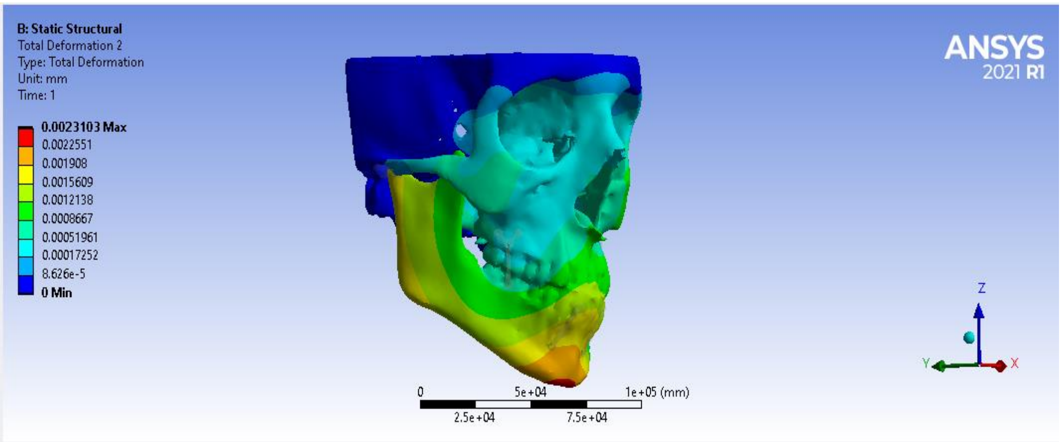


**Fig 62- Pattern of displacement (mm) of various surface structures after application of 400 gm of force at 10° to the occlusal plane**

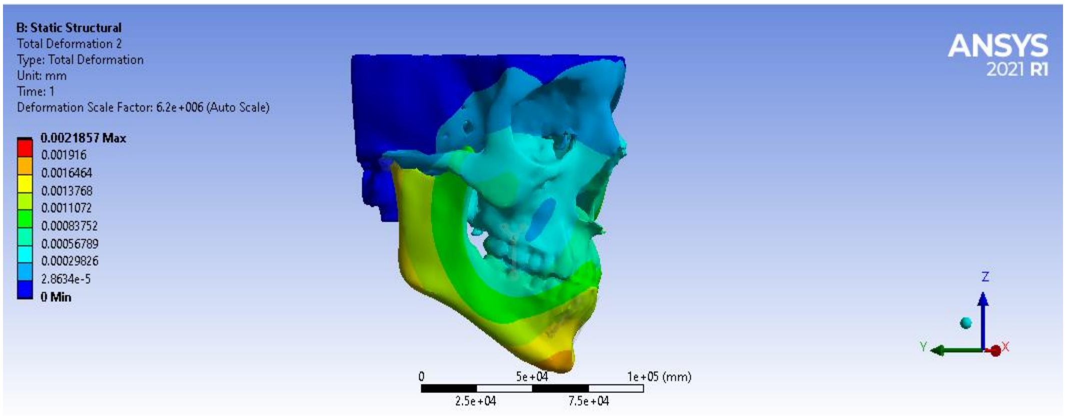


**Fig 63- Pattern of displacement (mm) of various surface structures after application of 400 gm of force at 20° to the occlusal plane**

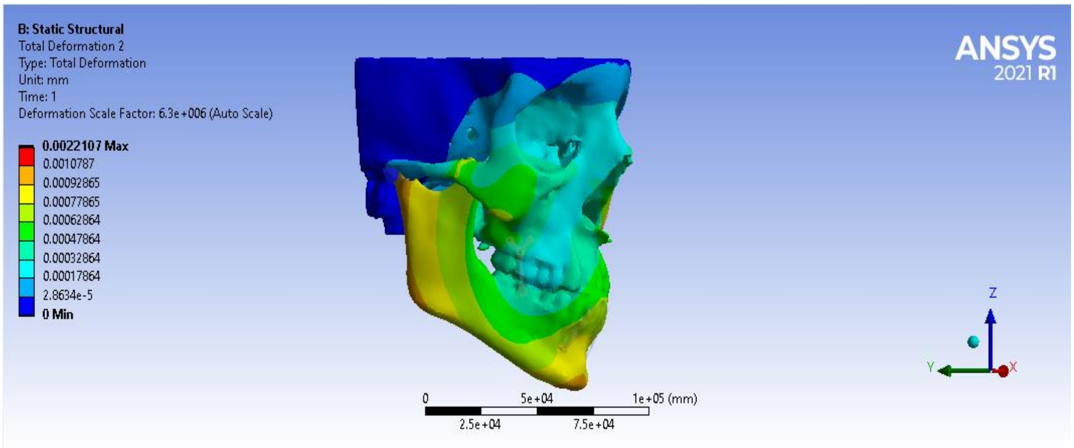


**Fig 64- Pattern of displacement (mm) of various surface structures after application of 400 gm of force at 30° to the occlusal plane**

# DISCUSSION

Finite element method is considered one of the best non-invasive, analytical research adjuncts for better understanding and visualization of the biomechanical response to various loading conditions. In complex geometry like the craniofacial skeleton and temporomandibular joint, the finite element method closely approximates original loading situations under specific boundary conditions (44). Complex three-dimensional problems in an irregular geometry, would not be able to solve by any other non-invasive approach in a less time frame. Though quantitatively the result is valid for only a single specific finite element model, qualitatively it can follow the same response if the same situation is simulated in multiple finite element models having different sizes and spatial orientations of similar structures. That indicates the validity and acceptance of finite element analysis in biomedical research (22). Multiple loading situations can be simulated in the same model, making it a more reliable approach to compare biomechanical responses under different amounts of force levels and varying degrees of force angulations.

Over a decade, bone-anchored maxillary protraction (BAMP) has become one of the promising orthopedic protocols for treating skeletal Class III malocclusion in growing patients. Evidence-based studies had shown that BAMP offered superior skeletal effects and minimal dental compensations over conventional treatment approaches like facemask with rapid maxillary expansion (FM/RME) or chincup. De Clerck et al. (16) recorded 4 mm of forward skeletal and soft tissue advancement of maxillary structures in patients treated by protraction technique. Cevidanes et al. (27) found 2.5 mm of more sagittal advancement of maxilla in BAMP protocol compared to facemask with rapid palatal expansion approach. Hino et al. (18) in a comparative study between BAMP vs. FM/RME, found 3.7 mm of advancement of both maxilla and zygoma in BAMP group, suggesting movement of maxilla and zygoma as a single unit under Class III protraction force. Contribution of circum-maxillary sutural expansion and associated skeletal growth, under the continuous, low amount of intermaxillary Class III protraction force was thought to be the sole factor in correcting skeletal malocclusion and improving facial profile. De Clerck et al. (19) also observed the mandibular restraining effect and associated bony remodeling of the condylar head and glenoid fossa, from cone beam computed tomography (CBCT) images of patients undergoing the BAMP approach.

Yatabe et al. (32) found a similar response of the glenoid fossa and condyle in unilateral complete cleft lip and palate patients undergoing BAMP protocol. Thereby, they notified that the mandibular contribution along with the sutural growth of the maxilla could be the explanation for the favorable orthopedic effect of the BAMP approach.

In BAMP protocol, angulation of Class III intermaxillary orthopedic force changes with the height of the hook on the anchor plate, where elastics are engaged (38). According to Tanne et al. (24) differences in the direction and magnitude of applied load can produce different patterns of stress distribution and displacement in maxillofacial structures.

Multiple finite element studies had evaluated the biomechanical response of BAMP protocol in craniomaxillary skeleton (22,38). However, to the best of our knowledge, no study has evaluated the biomechanical responses of circum-maxillary sutures, mandibular condyle, and temporomandibular soft tissue structures under different amounts and angulations of force applications. Therefore, this study was designed to evaluate the biomechanical effects at circum-maxillary sutures, condylar head, and articular disc under different loading situations.

**Overall stress distribution over the maxillofacial skeleton and circummaxillary sutures**

In the present study, the highest amount of Von Mises stress value was found at the base of the zygoma and anterolateral surface of the chin, where the anchor plates were fixed to the bone. This finding is similar to the observation by Lee and Beak (21). This finding could be due to effective transmission of intermaxillary Class III force, from the anchor plate to the maxillofacial skeleton, irrespective of the amount and direction of the applied force.

In the present study, the maximum Von Mises stress values were greater in the zygomaticotemporal, zygomaticomaxillary, zygomaticofrontal, pterygomaxillary, and midpalatal sutures in comparison to the frontomaxillary, frontonasal, and internasal sutures. This finding is similar to the finite element studies by Rai et al. (38) and Lee and Baek (21). They suggested that stress distribution more likely followed the zygomatic and pterygomaxillary buttresses in the maxillofacial skeleton irrespective of the amount and forward and downward inclination of the line of action of applied force with respect to the occlusal plane. The higher amount of Von Mises stress at these sutures was due to the placement of the upper miniplate at the base of the zygoma.

The presence of higher amount of maximum Von Mises stress at the zygomaticotemporal, zygomaticomaxillary, and pterygomaxillary sutures could contribute to the greater amount of sutural separation and resulting osteoblastic activity contributing towards the advancement of the maxilla and associated bones. This finding of our study is consistent with the results of a previous clinical study by Hino et al. (18) where significant amount of advancement of maxilla and zygoma was found. Zygomaticotemporal suture, in particular showed maximum stresses amongst the other sutures which could be due to lesser surface area of the zygomaticotemporal suture, resulting in more amount of stress distribution over a small surface area. However, Lee and Beak (21) found highest amount of Von Mises stress at superior part of pterygomaxillary suture. The difference could be due to different special orientation of sutures in relation to the line of action of force. Several experimental studies reported that zygomaticomaxillary sutures offered major resistance to orthopedic protraction force (40, 41) and showed similar or more complex interdigitations compared to other circummaxillary sutures (42).

In a study conducted by Angileiri et al. (43) it was found that compared to facemask with RME protocol, BAMP showed its efficacy even at higher maturation stages of circummaxillary sutures. This might be explained by the findings from the present study that BAMP protocol effectively transferred orthopedic protraction force into the zygomaticomaxillary sutures, as higher amount of Von mises stress was observed in zygomaticomaxillary sutures irrespective of amount and inclination of the applied force. That suggested its usefulness to produce significant orthopedic maxillary advancement even at higher age groups (11-14 years) or higher maturational stages of circummaxillary sutures.

Another important finding in the present study was that with the increase in the amount of applied force, the maximum Von Mises stress values increased for all the sutures at all angulations. This finding is in accordance with the FEM study by Bhad et al. (22) who also reported increase in Von Mises stress values at zygomaticotemporal, zygomaticofrontal, frontonasal and zygomaticomaxillary suture when Class III orthopedic force was increased from 150, 250 to 400 gm. The reason for presence of greater amount of stress with increase force levels could be attributed to the effect that greater amount of force gets distributed over the craniomaxillary sutures which in turn leads to greater amount of Von Mises stress at the sutures.

**Effect of change in angulation of the applied force**

In the present study, it was observed that with the increase in angulation for the applied force, Von Mises stress values were reduced for all the sutures. In a finite element study by Rai et al. (38) also reported similar decrease in stresses with increase in angulations. As the angulation of applied force increased to 30° to the occlusal plane, the horizontal component of force vector was reduced. It leads to lesser amount of Von Mises stress distribution at the circum- maxillary sutures. This might explain greater contribution of horizontal component of force for forward maxillary advancement at decreased angulations.

In the present study, with the increase in angulation of the applied force, greater amount of reduction in Von Mises stress values were found in zygomaticofrontal, frontonasal, nasomaxillary and internasal suture. This suggests that as the direction of force gets more downward, relatively small amount of force gets distributed towards midline. This finding was in contrast with the study conducted by Yan et al. (20) where increase in stress values were found in pterygopalatine suture. This might be due to anatomic variation or differences in special configuration of circummaxillary sutures in relation to the line of action of applied force.

The findings in the present study suggests that minimum downward and forward angulation of the applied force relative to the occlusal plane causes most effective stress distribution at the circummaxillary sutures at a particular amount of force, which could cause most favorable advancement of maxillary complex.

**Stress distribution in the condylar head and articular disc at the temporomandibular joint**

In the present study, at 150 gm of applied force, in the mandible, Von Mises stress values were distributed mostly at the condylar head and posterior part of sigmoid notch. When the applied force amount was increased to 250 gm, greater amount of Von Mises stress was observed in the condylar head, neck of the condyle and upper part of the posterior border of the ramus of the mandible. At 400 gm of applied force, greater amount of Von Mises stress was found at the upper part of the posterior border of ramus, condylar neck and throughout the coronoid notch as evident from the stress nephrogram. This finding could be due to transmission of force trajectory along the posterior border of the ramus of the mandible.

The greater amount of Von Mises stress distribution along the posterior border of the ramus and condyle could create compressive stress at this area. This might lead to remodeling resorption along the posterior border of ramus and condyle. Similar bone resorption at the posterior wall of glenoid fossa was observed in a clinical study by De Clerck et al (19).

In the present study, the highest amount of Von Mises stress was found in the anterolateral surface of the condylar head which increased with amount of applied force. This finding is in accordance with the finite element study conducted by Bhad et al. (22) who also reported increase in Von Mises stress values when the Class III orthopedic force was increased from 150 gm to 400 gm. The higher stresses on the condylar head could be explained by the greater amount of force transmission along the stress trajectory of mandible, terminating at the condylar head.

In the present study, one important finding was that, Von Mises stress values reduced gradually at the condylar head, with the increase in force angulations. This finding was similar to that of a finite element analysis by Khan et al. (37) in which the biomechanical effect of facemask on the temporomandibular joint was evaluated on application of 800, 1000, and 1200 gm of protraction force at an angle of 0°, 10°, 20° and 30° to the occlusal plane. It can be assumed that at increased angulation such as 30° angle Class III protraction force tended to be more parallel to the long axis (condylion-pogonion line) of the mandible. The stresses were more uniformly distributed along the long axis of the mandible at this angulation of applied force, thereby producing lesser amount of Von Mises stress at the condylar head. As the angulation of force (upward and backwardly directed at the lower plate) was decreased to 10°, the force was directed more in the backward direction, which might have caused the higher amount of Von Mises stress along the posterior stress trajectory of the mandible. This finding could not be compared with any other finite element study evaluating the stress distribution pattern at mandibular condyle and articular disc following BAMP protocol. To the best of our knowledge, there was no study evaluating the biomechanical effects of BAMP protocol on mandibular condyle and articular disc at different amount and direction of applied force.

In the present study, highest amount of maximum Von Mises stress at the articular disc was found on the inferior surface at the anterolateral part of articular disc. This might be due to transmission of stress from the corresponding areas of condylar head, irrespective of the amount and direction of the applied force. Von Mises stress values at the articular disc were almost ten-times less than the values at the condylar head, for each combination of amount and direction of applied force. This finding could be attributed to the shock absorbing effect of the articular disc.

Another significant finding in the present study was Von Mises stress at the condylar head and adjoining articular disc was of much lower magnitude as compared to. This might because of distant positioning of the temporomandibular joint from the point of force application at the anterolateral surface of chin. As low level of stress was distributed in the temporomandibular joint, this might contribute towards reduced discomfort in the temporomandibular joint and thereby increased patient compliance towards BAMP protocol in comparison to facemask or chin cup orthopedic therapy.

**Displacement of ANS and PNS**

In the present study, ANS and PNS showed forward and downward displacement under the application of intermaxillary Class III protraction force, which correlated well with the forward and downward maxillary growth as described by Moss (48). ANS showed more amount of forward and downward displacement than PNS, as it was located away from the center of rotation of the skull model. According to Melsen (46) the palatine bone between the facial skeleton and cranial base acts as a buffer. This might be the reason for the differences in the amount of displacement of ANS and PNS under the same force.

In the present study, it was found that the palatal plane demonstrated clockwise rotation. With the increase in force angulation, the clockwise rotational tendency reduced. This finding correlates well with the clinical observation by De Clerck et al. (26) in which a significant but small (around 1°) amount of clockwise rotation of the palatal plane was found in noted in patients treated with the BAMP protocol. The above findings could be explained by the position of the center of resistance of the skull model which might be located posterior and inferior to the line of action of the applied force. In contrast with the present study, Nguyen et al. (28) found a minute degree of counter-clockwise rotation of the maxilla in patients treated with BAMP protocol. On the contrary, Yan et al. (20) found that at 0° to 10° angle to the occlusal plane, the maxilla showed counter-clockwise rotation, at 20°, no rotational tendency and at 30° angulation, the maxillary complex showed a clockwise rotation of the palatal plane. The variation in findings of this present study from these studies might be due to different positional relationships between the center of resistance of the maxillofacial complex and the line of action of force.

Increase in angulation of applied force resulted in reduction of amount of ANS and PNS displacement. This finding was similar to the observation made by Rai et al. (38). Reduction in Von Mises stress values in all the circummaxillary sutures with the increase in angulation of applied force, might have resulted in lesser displacement of the maxilla.

**Displacement of pogonion and condylion**

The findings in the present study showed that pogonion was displaced in backward and downward directions irrespective of the amount of force and angulation whereas condylion point displaced in forward and upward directions at 10°, 20° angle, and backward and upward direction at 30° angulation of applied force. These observations indicated the clockwise rotation of the mandible.

This finding in the present study was in agreement with a systematic review by Fernandez et al. (29) where they compared the effects of bone-anchored maxillary protraction with dentoalveolar anchored maxillary protraction and concluded that all the thirty studies reported similar findings like clockwise mandibular rotation and thereby increase in anterior facial height in those patients treated either by modified facemask therapy or followed BAMP protocol. In the present study, the backward and downward displacement of pogonion was also consistent with the previous clinical study by De Clerck et al. (19) who observed 0.13 ±2.89 mm of posterior displacement of the chin.

In the present study, it was found that, with the increase in angulation of applied force, pogonion and condylion reduced their displacement both in sagittal and anteroposterior dimensions. It indicated reduced clockwise rotational tendency of the mandible with the increase in force angulation. This finding is similar to the study conducted by Rai et al. (38) in which 250 gm of Class III intermaxillary force was applied at an angle of 10°, 20°, and 30° to the occlusal plane and found that when angulation of the applied force increased from 10° to 20°, backward and downward displacement of pogonion and backward and upward displacement condylion was reduced whereas at 30° angle only the downward displacement of pogonion was further reduced reduced. This might be due to decreasing the distance between the center of rotation of the mandible and applied force, with increasing its angulation. The center of rotation might be located at the condylar neck above the line of action of force.

The upward and forward condylar displacement at 10° and 20° of force angulation as found in the present study could be correlated with the previous clinical study by De Clerck et al. (26) who assessed the upward and forward growth of condyle in patients treated by BAMP protocol and observed significant increase in the ramal height in upward and forward dimension, which was contributed by upward and forward condylar growth.

In the present study, at 30° angulation, condylion showed backward and upward displacement. This finding is in accordance with the clinical study by De Clerck et al. (19) who found significant changes at the temporomandibular joint. Around 1.3 mm of bone formation was detected at the anterior eminence of the glenoid fossa while similar amount of bone resorption was detected at the posterior wall of the fossa. The findings in the present study might explain the glenoid fossa remodeling effect by the BAMP protocol. The backward displacement of the condylion at 30° angulation might be caused by line of action of applied force at the lower miniplate passing through the center of resistance of the mandible. These findings also indicated the mandibular restraining effect of the BAMP protocol.

In the present study, maximum amount of displacement was found in pogonion in comparison to ANS, PNS and condylion point. This observation correlates well with the finding of Bhad et al. (22) who found major contribution in correcting skeletal discrepancy was offered by the mandibular posterior displacement rather than forward maxillary advancement.

Overall, the current FEM model at various forces and angulation demonstrated a positive effect of the BAMP protocol in correcting the skeletal Class III malocclusion in growing patients

## Strengths and limitations of this study

To the best of our knowledge there was no finite element study evaluating the biomechanical effects of bone anchored maxillary protraction on the temporomandibular joint structures which includes condylar head and articular disc in relation to the varying amount and direction of Class III intermaxillary orthopedic force. In this present study, the effects of the growth of the maxillofacial skeleton and overlying soft tissues on the skull were not considered. Osteoblastic, osteoclastic, and fibroblastic activity at the sutures could not be evaluated through finite element analysis. Thereby, the findings in our study may differ from clinical outcome.

# CONCLUSIONS

The following conclusions can be drawn from the present FEM study:

1. Maximum Von Mises stresses were detected at zygomaticotemporal, zygomaticomaxillary and pterygomaxillary sutures at all angulations.
2. As the angulations of the applied force increased from 10 to 30 degree Von Mises stress value decreased. Hence it might be suggested that during orthopedic correction, the force angulation should be kept minimum as possible in relation to the occlusal plane.
3. Von Mises stress values reduced in condylar head and articular disc with increase in angulation from 10 to 30 degree.
4. With increase in angulation from 10 to 30 degree of the applied force, there is reduction in displacement of ANS, PNS, pogonion and condylion.
5. Bone anchored maxillary protraction causes posterior displacement of mandible, thereby BAMP has mandibular restraining effect in accordance with maxillary advancement.

# SUMMARY

**Objectives:** To analyze the stress distribution pattern in the circum-maxillary sutures, mandibular condyle and articular disc and displacement of various surface landmarks during bone anchored maxillary protraction procedure using finite element analysis.

**Materials and Methods:** CT scan of skull and MRI images of temporomandibular joint was taken of a 12 years old male patient having skeletal Class III malocclusion according to inclusion and exclusion criteria. DICOM images were exported in Mimics 21.0 and 3D geometric model of skull and temporomandibular joint was generated. STL model of miniplates were formed in Solidworks 2021 SP2.0. 3D geometric models of skull, temporomandibular soft tissue and miniplates with associated screws were assembled in 3-Matic. Three-dimensional volumetric model was generated and exported into ANSYS 2021R1.150gm, 250gm, and 400 gm of intermaxillary Class III orthopedic force at an angulation of 10°, 20° and 30° angle to the occlusal plane, was applied on the selected nodes at the upper and lower miniplates bilaterally. Maximum Von Mises stress values were recorded in all the circummaxillary sutures, condylar head and articular disc. Displacement of ANS, PNS, pogonion and condylion was recorded in anteroposterior and vertical dimension.

**Results:** Highest amount of maximum Von Mises Stress value was found in zygomaticotemporal suture followed by zygomaticomaxillary, zygomaticofrontal and pterygomaxillary sutures. Von Mises stress values increased in all the sutures with the increase in force value from 150gm to 400 gm. Von Mises stress values were found to be decreased with increase in force angulation from 10° to 30° to the occlusal plane. Maximum Von Mises stress values were highest at the anterolateral surface of condylar head and adjoining articular disc. Stress values were increased in the condylar head and articular disc with increase in the amount of force and reduced with the increase in angulation of Class III orthopedic force. Forward and downward displacement of ANS and PNS was observed irrespective of amount of force and angulation. With the increase in angulation from 10° to 30°, forward and downward displacement of ANS and PNS was reduced. Pogonion displaced in backward and downward direction in all the angulations, whereas condylion displaced backward and upward direction at 10°

and 20° angulations but at 30° showed upward and backward displacement. Amount of displacement reduced with the increase in angulation of applied force.

**Conclusion:** Bone-anchored maxillary protraction is an effective treatment approach that shows both forward advancements of the maxilla and backward displacement of the mandible. During orthopedic correction, the force angulation should be kept minimum as possible in relation to the occlusal plane.

# BIBLIOGRAPHY


1. Hardy D, Cubas Y, Orellana M. Prevalence of angle class III malocclusion: A systematic review and meta-analysis. Open Journal of Epidemiology 2012;2:75-82.
2. Baik HS. Clinical results of the maxillary protraction in Korean children. Am J Orthod Dentofacial Orthop 1995;108:583-92.
3. Singh SP, Kumar V, Narboo P. Prevalence of malocclusion among children and adolescents in various school of Leh Region. Imedpub J 2015;1(2):1-6.
4. Kaur H, Pavithra US, Abraham R. Prevalence of malocclusion among adolescents in South Indian population. J Int Soc Prev Community Dent 2013;3(2):97-102.
5. Narayanan RK, Jeseem MT, Kumar TA. Prevalence of malocclusion among 10-12-year-old school children in Kozhikode district, Kerala: An epidemiological study. Int J Clin Pediatr Dent 2016;9(1):50-5.
6. Guyer EC, Ellis EE, McNamara JA, Behrents RG. Components of class III malocclusion in juveniles and adolescents. Angle Orthod 1986;56:7-30.
7. Ellis E, McNamara JA. Components of adult Class III malocclusion. J Oral Maxillofac Surg 1984;42:295-305.
8. Chang HP, Kinoshita Z, Kawamoto T. Craniofacial pattern of Class III deciduous dentition. Angle Orthod 1992;62:139-44.
9. Kim JH, Viana MA, Graber TM, Omerza FF, BeGole EA. The effectiveness of protraction face mask therapy: a meta-analysis. Am J Orthod Dentofacial Orthop 1999;115:675-85.
10. Sung SJ, Baik HS. Assessment of skeletal and dental changes by maxillary protraction. Am J Orthod Dentofacial Orthop 1998;114(5):492-502.
11. Hagg U, Tse A, Bendeus M, Rabie AB. Long-term follow-up of early treatment with reverse headgear. Eur J Orthod 2003;25:95-102.
12. Baccetti T, Franchi L, McNamara JA Jr. Treatment and posttreatment craniofacial changes after rapid maxillary expansion and facemask therapy. Am J Orthod Dentofacial Orthop 2000;118:404-13.
13. Westwood PV, McNamara JA, Baccetti T, Franchi L, Sarver DM. Long-term effects of Class III treatment with rapid maxillary expansion and facemask therapy followed by fixed appliances. Am J Orthod Dentofacial Orthop 2003;123(3):306-20.

14. Baccetti T, Franchi L, McNamara JA. Cephalometric variables predicting the long-term success or failure of combined rapid maxillary expansion and facial mask therapy. Am J Orthod Dentofacial Orthop 2004;126:16-22.
15. Wells AP, Sarver DM, Proffit WR. Long-term efficacy of reverse pull headgear therapy. Angle Orthod 2006;76:915-22.
16. De Clerck HJ, Cornelis MA, Cevidanes LH, Heymann GC, Tulloch CJ. Orthopedic traction of the maxilla with miniplates: a new perspective for treatment of midface deficiency. J Oral Maxillofac Surg 2009;672:123-9.
17. Heymann GC, Cevidanes L, Cornelis M, De Clerck HJ, Tulloch JF. Three-dimensional analysis of maxillary protraction with intermaxillary elastics to miniplates. Am J Orthod Dentofacial Orthop 2010;137:274-84.
18. Hino CT, Cevidanes LH, Nguyen TT, De Clerck HJ, Franchi L, McNamara JA. Three-dimensional analysis of maxillary changes associated with facemask and rapid maxillary expansion compared with bone anchored maxillary protraction. Am J Orthod Dentofacial Orthop 2013;144:705-14.
19. De Clerck H, Nguyen T, Paula LK, Cevidanes L. Three-dimensional assessment of mandibular and glenoid fossa changes after bone-anchored Class III intermaxillary traction. Am J Orthod Dentofacial Orthop 2012;142(1):25-31.
20. Yan X, He W, Lin T, Liu J, Bai X, Yan G et al. Three-dimensional finite element analysis of the craniomaxillary complex during maxillary protraction with bone anchorage vs conventional dental anchorage. Am J Orthod Dentofacial Orthop 2013;143:197-205.
21. Lee NK, Baek SH. Stress and displacement between maxillary protraction with miniplates placed at the infrazygomatic crest and the lateral nasal wall: a 3-dimensional finite element analysis. Am J Orthod Dentofacial Orthop 2012; 141:345-51.
22. Bhad WA, Dhage AS, Baheti NR, Chavan SJ, Mehta NS. Evaluation of stress distribution in maxilla, mandible, and glenoid fossa after Class III intermaxillary traction: A three-dimensional finite element analysis study. Int J Orthod Rehabil 2021;12:91-7.
23. Tanaka E, Rodrigo DP, Tanaka M, Kawaguchi A, Shibazaki T, Tanne K. Stress analysis in the TMJ during jaw opening by use of a three-dimensional finite element model based on magnetic resonance images. Int J Oral Maxillofac Surg 2001;30:421-30.

24. Tanne K, Hiraga J, Kakiuchi K, Yamagata Y, Sakuda M. Biomechanical effect of anteriorly directed extraoral forces on the craniofacial complex: a study using the finite element method. Am J Orthod Dentofacial Orthop 1989;95(3):200-7.
25. Gautam P, Valiathan A, Adhikari R. Skeletal response to maxillary protraction with and without maxillary expansion: a finite element study. Am J Orthod Dentofacial Orthop 2009;135(6):723-8.
26. De Clerck H, Cevidanes L, Baccetti T. Dentofacial effects of bone-anchored maxillary protraction: a controlled study of consecutively treated Class III patients. Am J Orthod Dentofacial Orthop 2010;138(5):577-81.
27. Cevidanes L, Baccetti T, Franchi L, McNamara JA, De Clerck H. Comparison of two protocols for maxillary protraction: bone anchors versus face mask with rapid maxillary expansion. Angle Orthod 2010;80(5):799-806.
28. Nguyen T, Cevidanes L, Cornelis MA, Heymann G, Paula LK, De Clerck H. Three-dimensional assessment of maxillary changes associated with bone anchored maxillary protraction. Am J Orthod Dentofacial Orthop 2011;140(6):790-8.
29. Fernández MM, Linares IA, Vico RM, Mendoza A, Reina SE. Bone- and dentoalveolar-anchored dentofacial orthopedics for Class III malocclusion: new approaches, similar objectives? a systematic review. Angle Orthod 2013;83(3):540-52.
30. Zhang D, Zheng L, Wang Q, Lu L, Ma J. Displacements prediction from 3D finite element model of maxillary protraction with and without rapid maxillary expansion in a patient with unilateral cleft palate and alveolus. Biomed Eng Online 2015;14:80.
31. Eid OM, Ramadan AA, Nadim MA, Hamed TA. Maxillary protraction using orthodontic miniplates in correction of Class III malocclusion during growth. J World Fed Orthod 2016;5:100-6.
32. Yatabe M, Garib D, Faco R, Clerck H, Souki B, Janson G et al. Mandibular and glenoid fossa changes after bone-anchored maxillary protraction therapy in patients with UCLP: A 3-D preliminary assessment. Angle Orthod 2017;87(3):423-31.
33. Ozdemir S, Goymen M. A finite element analysis of the effects of different skeletal protraction and expansion methods used in class III malocclusion treatment. Medicine Science 2018;165:898-904.

34. Hevele VJ, Nout E, Claeys T, Meyns J, Scheerlinck J, Politis C. Bone-anchored maxillary protraction to correct a class III skeletal relationship: A multicenter retrospective analysis of 218 patients. J Craniomaxillofac Surg 2018;46(10):1800-6.
35. Eom J, Bayome M, Park JH, Lim HJ, Kook YA, Han SH. Displacement and stress distribution of the maxillofacial complex during maxillary protraction using palatal plates: A three-dimensional finite element analysis. Korean J Orthod 2018;48(5):304-15.
36. Jayan R, Ani SG, Peter E. Study of displacement and stress distribution in maxillofacial complex following maxillary protraction with conventional and modified facemask: A finite element analysis. EC Dental Science 2019;18.9: 2005-19.
37. Nasir YMD, Shivamurthy PG, Sabrish S. A 3D finite element analysis of stress on temporomandibular joint due to maxillary protraction appliances with varied force levels and angulations. World J Dent 2020;11(2):128-33.
38. Rai P, Garg D, Tripathi T, Kanase A, Ganesh G. Biomechanical effects of skeletally anchored Class III elastics on the maxillofacial complex: a 3D finite element analysis. Prog Orthod 2021;22(1):36.
39. Gupta A, Kohli VS, Hazarey PV, Kharbanda OP, Gunjal A. Stress distribution in the temporomandibular joint after mandibular protraction: a 3-dimensional finite element method study. Part 1. Am J Orthod Dentofacial Orthop 2009;135(6):737-48.
40. Yu HS, Baik HS, Sung SJ, Kim KD, Cho YS. Three-dimensional finite-element analysis of maxillary protraction with and without rapid palatal expansion. Eur J Orthod 2007;29(2):118-25.
41. Tanne K, Sakuda M. Biomechanical and clinical changes of the craniofacial complex from orthopedic maxillary protraction. Angle Orthod 1991;61(2):145-52.
42. Kambara T. Dentofacial changes produced by extraoral forward force in the Macaca irus. Am J Orthod 1977;71(3):249-77.
43. Angelieri F, Ruellas AC, Yatabe MS, Cevidanes LHS, Franchi L, Hino TC et al. Zygomaticomaxillary suture maturation: Part II-The influence of sutural maturation on the response to maxillary protraction. Orthod Craniofac Res 2017;20(3):152-63.

44. Romanyk DL, Vafaeian B, Addison O, Adeeb S. The use of finite element analysis in dentistry and orthodontics: Critical points for model development and interpreting results. Semin Orthod 2020;26(3):162-73.
45. Moss ML. The functional matrix hypothesis revisited. 1. The role of mechanotransduction. Am J Orthod Dentofacial Orthop 1997;112(1):8-11.
46. Melsen B. Palatal growth studied on human autopsy material. A histologic microradiographic study. Am J Orthod 1975;68(1):42-54.

# ANNEXURES

## Annexure I: Institutional Ethical Clearance Certificate

अखिल भारतीय आयुर्विज्ञान संस्थान, जोधपुर
**All India Institute of Medical Sciences, Jodhpur**
संस्थागत नैतिकता समिति
**Institutional Ethics Committee**

**No. AIIMS/IEC/2021/** 3468 **Date: 12/03/2021**

**ETHICAL CLEARANCE CERTIFICATE**

Certificate Reference Number: **AIIMS/IEC/2021/3303**

Project title: **"Stress distribution in the maxillofacial skeleton and the temporomandibular joint following bone anchored maxillary protraction: A three-dimensional finite element method study"**

| | |
|---|---|
| Nature of Project: | **Research Project Submitted for Expedited Review** |
| Submitted as: | **M.D.S. Dissertation** |
| Student Name: | **Dr. Supratim Kundu** |
| Guide: | **Dr. Vinay Kumar Chugh** |
| Co-Guide: | **Dr. Ankur Gupta & Dr. Pravin Kumar** |

Institutional Ethics Committee after thorough consideration accorded its approval on above project.

The investigator may therefore commence the research from the date of this certificate, using the reference number indicated above.

Please note that the AIIMS IEC must be informed immediately of:

- Any material change in the conditions or undertakings mentioned in the document.
- Any material breaches of ethical undertakings or events that impact upon the ethical conduct of the research.

The Principal Investigator must report to the AIIMS IEC in the prescribed format, where applicable, bi-annually, and at the end of the project, in respect of ethical compliance.

AIIMS IEC retains the right to withdraw or amend this if:

- Any unethical principle or practices are revealed or suspected
- Relevant information has been withheld or misrepresented

AIIMS IEC shall have an access to any information or data at any time during the course or after completion of the project.

Please Note that this approval will be rectified whenever it is possible to hold a meeting in person of the Institutional Ethics Committee. It is possible that the PI may be asked to give more clarifications or the Institutional Ethics Committee may withhold the project. The Institutional Ethics Committee is adopting this procedure due to COVID-19 (Corona Virus) situation.

If the Institutional Ethics Committee does not get back to you, this means your project has been cleared by the IEC.

On behalf of Ethics Committee, I wish you success in your research.

**Dr. Praveen Sharma**
Member Secretary

Member secretary
Institutional Ethics Committee
AIIMS,Jodhpur

Basni Phase-2, Jodhpur, Rajasthan-342005; **Website:** www.aiimsjodhpur.edu.in; **Phone:** 0291-2740741 Extn. 3109
**E-mail** : ethicscommittee@aiimsjodhpur.edu.in; ethicscommitteeaiimsjdh@gmail.com

**Annexure II: Patient Information Leaflet (English)**

**All India Institute of Medical Sciences, Jodhpur**
**Department of Dentistry**
**Patient Information Leaflet**

You are being invited to willing fully participate in the study entitled

**"STRESS DISTRIBUTION IN THE MAXILLOFACIAL SKELETON AND THE TEMPOROMANDIBULAR JOINT FOLLOWING BONE ANCHORED MAXILLARY PROTRACTION: A THREE-DIMENSIONAL FINITE ELEMENT METHOD STUDY"**

You have been requested to volunteer for a research study since you have undergone fixed orthodontic treatment. Class III malocclusion is one of the reason for which patient seeks orthodontic treatment. Bone anchored maxillary protraction (BAMP) is one of the treatment options for correction of Class III malocclusion in growing patients. BAMP may have effect on maxilla, mandible and temporomandibular joint. Since there is less literature describing the stress pattern generation in maxilla, mandible and temporomandibular joint during BAMP procedure, this study is aimed to analyze stress pattern generation on finite element model obtained from computerized tomography of skull and magnetic resonance imaging of temporomandibular joint.

**Confidentiality**

Your medical records and identity will be treated as confidential documents. They will only be revealed to other doctors/scientists/monitors/auditors of the study if required. The results of the study may be published in a scientific journal but you will not be identified by name.

**Ethics committee approval has been obtained for the study.**

**Your participation and rights**

Your participation in the study is fully voluntary and you may withdraw from the study anytime without having to give reasons for the same. In any case, you will receive the appropriate treatment for your condition. You will not be paid any amount for the participation in the study. You will have to pay for the routine investigations that will be done.

Contact Person: for further queries-

**Dr. SUPRATIM KUNDU**
Post Graduate student,
Orthodontics and Dentofacial Orthopaedics,
Department of Dentistry,
AIIMS, Jodhpur.
Mobile No: - 8902690889
Email ID: supratimkundupiku@gmail.com

## Annexure III: Patient Information Leaflet (Hindi)

**अखिल भारतीय आयुर्विज्ञान संस्थान, जोधपुर**
**दंत चिकित्सा विभाग**
**<u>रोगी सूचना पत्र</u>**

आपको अध्ययन में पूरी तरह भाग लेने के लिए आमंत्रित किया जा रहा है

शीर्षक: **"STRESS DISTRIBUTION IN THE MAXILLOFACIAL SKELETON AND THE TEMPOROMANDIBULAR JOINT FOLLOWING BONE ANCHORED MAXILLARY PROTRACTION: A THREE-DIMENSIONAL FINITE ELEMENT METHOD STUDY"**

आपसे शोध अध्ययन के लिए स्वयंसेवक बनने का अनुरोध कर रहा है क्योंकि आप फिक्स्ड ऑर्थोडॉन्टिक ट्रीटमेंट करवा रहे है ।

**गोपनीयता**

आपके मेडिकल रिकॉर्ड और पहचान को गोपनीय दस्तावेज माना जाएगा। यदि आवश्यक हो तो वे केवल अध्ययन के अन्य डॉक्टरों / वैज्ञानिकों / मॉनीटर / लेखा परीक्षकों को ही प्रकट किए जाएंगे। अध्ययन के परिणाम वैज्ञानिक पत्रिका में प्रकाशित किए जा सकते हैं लेकिन आपको नाम से पहचाना नहीं जाएगा। अध्ययन के लिए नैतिकता समिति की मंजूरी प्राप्त की गई है।

आपकी भागीदारी और अधिकारअध्ययन में आपकी भागीदारी पूरी तरह से स्वैच्छिक है और आप इसके कारणों के बिना किसी भी समय अध्ययन से वापस ले सकते हैं। किसी भी मामले में, आपको अपनी स्थिति के लिए उचित उपचार प्राप्त होगा। अध्ययन में भागीदारी के लिए आपको कोई राशि नहीं दी जाएगी। आपको नियमित जांच के लिए भुगतान करना होगा जो किया जाएगा।

संपर्क व्यक्ति: आगे के प्रश्नों के लिए-

**डॉ. सुप्रतिम कुंडू**
पोस्ट ग्रजुएट छात्र
ऑर्थोडोंटिक्स और डेंटोफेशियल ऑर्थोपेडिक्स
दंत चिकित्सा विभाग
एम्स, जोधपुर
मोबाइल नंबर: -8902690889
ईमेल आईडी: supratimkundupiku@gmail.com

## Annexure IV: Informed Consent Form (English)

**All India Institute of Medical Sciences, Jodhpur**

**Department of Dentistry**

**<u>Informed Consent Form</u>**

Subject: **"STRESS DISTRIBUTION IN THE MAXILLOFACIAL SKELETON AND THE TEMPOROMANDIBULAR JOINT FOLLOWING BONE ANCHORED MAXILLARY PROTRACTION: A THREE-DIMENSIONAL FINITE ELEMENT METHOD STUDY"**

Patient OPD No: ________________________________________

I, ______________________________S/o or D/o__________________________

R/o _________________________give my full, free, voluntary consent to be a part of the study "STRESS DISTRIBUTION IN THE MAXILLOFACIAL SKELETON AND THE TEMPOROMANDIBULAR JOINT FOLLOWING BONE ANCHORED MAXILLARY PROTRACTION: A THREE-DIMENSIONAL FINITE ELEMENT METHOD STUDY"

The procedure and nature of which has been explained to me in my own language to my full satisfaction. I confirm that I have had the opportunity to ask questions. I give my permission for the use of orthodontic records, including photographs, computed tomography (CT) scan of skull and magnetic resonance imaging (MRI) scan of temporomandibular joint made in the process of examinations and treatment for the purposes of research, education, or publication in professional journals.

I understand that my participation is voluntary and I am aware of my right to opt out of the study at any time without giving any reason.

I understand that the information collected about me and any of my medical records may be looked at by responsible individual from AIIMS Jodhpur or from regulatory authorities. I give permission for these individuals to have access to my records.

Date: _____________ __________________________________

Place: ____________ Signature/Left thumb impression

(Patient) (Caregiver)

This to certify that the above consent has been obtained in my presence.

Date________________ Place: ________________

Signature of Principal Investigator

1. Witness 1 2. Witness 2

Name: _____________________ Name: _____________________

## Annexure V: Informed Consent Form (Hindi)

**अखिल भारतीय आयुर्विज्ञान संस्थान, जोधपुर**
**दंत चिकित्सा विभाग**
**सूचित सहमति प्रपत्र**

शीर्षक: **"STRESS DISTRIBUTION IN THE MAXILLOFACIAL SKELETON AND THE TEMPOROMANDIBULAR JOINT FOLLOWING BONE ANCHORED MAXILLARY PROTRACTION: A THREE-DIMENSIONAL FINITE ELEMENT METHOD STUDY"**

रोगी / स्वयं सेवी पहचान संख्या: ____________________

मैं,________________________पुत्र/पुत्री____________________________निवासी______________ ____________________________________स्वयं को अध्ययन का हिस्सा होने के लिए अपनी पूर्ण स्वैच्छिक सहमति देता हूँ। इस अध्ययन का शीर्षक है

**"STRESS DISTRIBUTION IN THE MAXILLOFACIAL SKELETON AND THE TEMPOROMANDIBULAR JOINT FOLLOWING BONE ANCHORED MAXILLARY PROTRACTION: A THREE-DIMENSIONAL FINITE ELEMENT METHOD STUDY"**

मेरी पूर्ण संतुष्टि के लिए मेरी खुद की भाषा में मुझे समझाया गया है।मैं इस बात की पुष्टि करता/करतीहूं कि मुझे सवाल पूछने का पूर्ण अवसर मिला है।

<u>मैं पेशेवर पत्रिकाओं में अनुसंधान, शिक्षा, या प्रकाशन के प्रयोजनों के लिए परीक्षाओं और उपचार की प्रक्रिया में किए गए फोटोग्राफ सहित ऑर्थोडोंटिक रिकॉर्ड्स के उपयोग के लिए मेरी अनुमति देता/देती हूं।</u>

मैं यह समझता/समझतीहूँ कि मेरी भागीदारी स्वैच्छिक है और बिना कोई कारण बताए किसी भी समय इस अध्ययन से स्वयं को वापस लेने के लिए मेरे अधिकार के बारे में मुझे पता है।

मैं यह समझता/समझती हूँ कि मेरे मेडिकल रिकॉर्ड की एकत्रित की गई जानकारी "अखिल भारतीय आयुर्विज्ञान संस्थान जोधपुर" यानि यामक अधिकारियों द्वारा देखी जा सकती है।मैं इन व्यक्तियों को मेरे रिकॉर्ड के उपयोग के लिए अनुमति देता/<u>देती</u> हूँ।

दिनांक: हस्ताक्षर / वाम अंगूठे का निशान

स्थान:

यह प्रमाणित किया जाता कि इस संस्करण की सहमति मेरी उपस्थिति में प्राप्त की गयी है।

दिनांक: प्रमुख अन्वेषक के हस्ताक्षर

स्थान:

| | |
|---|---|
| 1. साक्षी1 | 2. साक्षी2 |
| हस्ताक्षर: ______________ | हस्ताक्षर: _____________ |
| नाम:________________ | नाम: ______________ |

## Annexure VII: Plagiarism Certificate

## Plagiarism Certificate

Stress distribution in the maxillofacial skeleton and the temporomandibular joint following bone anchored maxillary protraction: A three-dimensional finite element method study

ORIGINALITY REPORT

8%
SIMILARITY INDEX

PRIMARY SOURCES

| | | | | |
|---|---|---|---|---|
| 1 | www.intechopen.com | Internet | 169 words | 1% |
| 2 | etd.aau.edu.et | Internet | 93 words | 1% |
| 3 | storage.googleapis.com | Internet | 83 words | 1% |
| 4 | www.ncbi.nlm.nih.gov | Internet | 74 words | 1% |
| 5 | docplayer.net | Internet | 67 words | 1% |
| 6 | medicalresearchjournal.org | Internet | 61 words | < 1% |
| 7 | qjegh.lyellcollection.org | Internet | 59 words | < 1% |
| 8 | norlx65.nordita.org | Internet | 43 words | < 1% |